Magnetostructural Correlations in Tetrahalocuprates

A thesis submitted in partial fulfilment of

The requirements for the degree of

Master of Science in Chemistry

At the

University of Canterbury

Christopher Glenn Saunders

University of Canterbury

Christchurch

New Zealand

2012

"Life is not easy for any of us. But what of that? We must have perseverance and above all confidence in ourselves. We must believe that we are gifted for something, and that this thing, at whatever cost, must be attained."

Marie Curie (1867-1934)

Acknowledgements

First and foremost I would like to greatly thank my supervisors Dr Jan Wikaira and Dr Chris Fitchett for giving up such a great deal of their time to help me through this project, often answering many, sometimes slightly retarded questions. My thanks to the current and previous members of Team Fitchett; Robbie, Jayne, Marie, Antony, Emma, Paul, and the Steel group for their support and frequent witty banter.

I would also like to thank all the fantastic members of the academic staff who have helped and taught me so much during my time here in both my post grad and under graduate years.

My work would have not been possible without the help of the amazing technical staff; especially Dr Matt Polson for helping with the annoying Xray crystallography issues no one else wanted to deal with.

A special thanks to all my amazing friends who have provided support, encouragement and expressing an interest in my work even though they have no chemistry backround and do a lot of smiling and nodding.

Finally, to my parents, Denis and Marion, my sisters, Kathryn and Rachel, and all the rest of my family for the endless love and support which has got me through the tough few years it has been with many large magnitude earthquakes throwing many many spanners in the works.

Contents

Abbreviations

2A5SP – 2-amino-5-substituted-pyridine

5A2SP – 5-amino-2-substituted-pyridine

M = Methyl

TMCAP – 2-amino-5-trifluoromethylpyridine

DMPY - dimethylpyridine

Abstract

This thesis describes the preparation and characterisation of a number of tetrahalocuprate complexes. The compounds were made by reacting the chosen organic cation with the desired copper(II) salt. Three series of tetrahalocuprates were studied; (1) 5-amino-2-substituted pyridines, (2) mixed halide tetrahalocuprates using different dimethylpyridine isomers and (3) imidazolium ions.

The structure of thirty three compounds were determined using single crystal X-ray crystallography. The compounds studied gave a wide range of different structures.

The 5-amino-2-substituted pyridines showed four distinct structural types; (1) two isolated protonated pyridines and a single tetrahalocuprate anion, (2) unexpected bromine substitution on the pyridine rings, (3) Cu_3Cl chains with two pyridines bound to each terminal copper and (4) water bridged copper chloride chains for the iodo substituted pyridine.

The mixed halide dimethylpyridine series illustrated the effects of varying the ratio of the halides in the tetrahalocuprate anions on the crystal packing of the compounds. A number of different structures for each isomer were studied.

Attempts were made using a range of different imidazolium ions to form tetrahalocuprates. These ions would not require acid protonation and are unknown in the literature in this manner.

Chapter 1

Introduction

During recent decades the study of magnetism of low-dimensional molecular systems has been of significant interest and has played an important role in the understanding of phase transitions and critical phenomena[1]. This interest has increased greatly due to the discovery of high temperature superconducting materials. High temperature superconductors have a greater degree of conducting and the benefit of not needing to be cooled to extremely low temperatures. The superconductivity is thought to be propagated through low-dimensional antiferromagnetic networks[2, 3]. Figure 1.1 shows the different types of low dimensional lattices where these antiferromagnetic networks are often propagated.

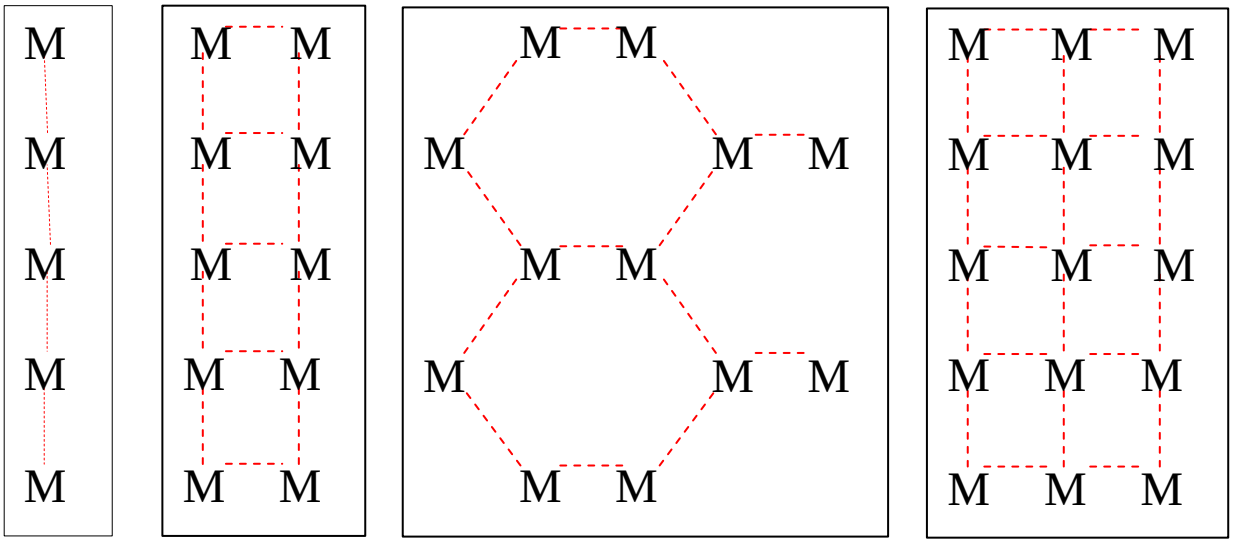

Figure 1.1 Representation of different types of low dimentional lattices, where M is a magnetic moment (metal atom or organic radical) and the dashed lines represent some kind of exchange pathway, either a bond or through space interaction. The different lattices from left to right are: uniform chain, ladder, honeycomb and 2D rectangles and squares

One theory[4] for the explanation of the superconductivity relates to holes in the generally antiferromagnetic layers of Cu(II). The high critical temperatures of the superconductors (Tc

= 130 K) is linked to the strong magnetic exchange (J/K is approximately 1500K). The Cu(II) ion has been widely used as the transition metal, M, because of its d^9 configuration and single unpaired electron, making it an S=1/2 ion. The absence of a large internal magnetic field indicated by a g-factor (orbital angular momentum) close to 2, allows the Cu(II) ion to follow an external magnetic field[5], which can be described by the isotropic Heisenburg Hamiltonian

(1)

The flexibility of the Cu(II) coordination sphere means a wide variety of structures can be formed, with only minor changes of external ligands[6]. Cu(II) compounds are particularly good for model sytsems, as there is a large amount of theoretical work in the literature[7, 8]. Continued interest in low dimensional magnetic lattices has led to a study of compounds with the general formula $A_2[MX_4]$, where A is an organic cation, M is a 2+ transition metal and X is a halide (Cl or Br)[9, 10]. The organic cation is usually a protonated base. Previous compounds have contained bases such as alkyl amines[11] or substituted pyridines[12]. A number of complexes can be found in the literature containing the tetrahalocuprate(II) moiety where the halide is either chloride or bromide.

Recent examples involving structural and/or magnetic data include; bis(3-bromopyridinium) tetrachlorocuprate(II)[13], sparteinium tetrachlorocuprate(II) monohydrate[14], bis(2-chloropyridinium)tetrachlorocuprate(II)[15], bis(2-amino-5-fluoropyridinium) tetrachlorocuprate(II)[16], bis(1-*n*-butyl-3.methylimidazolium) tetrachlorocuprate(II)[17], bis(1,3,2.benzodithiazolium) tetrachlorocuprate(II)[18], bis(2,3.dimethylpyridinium) tetrabromocuprate(II)[19], 2,5-dibromopyridinium(II)[20], bis(imidaloium) tetrachlorocuprate(II)[21], and bis(2-chloropyridinium) tetrachlorocuprate(II)[22] complexes. After significant investigation into the propagation and possible mechanisms for magnetic exchange in cuprate salts, a variety of pathways has been elucidated. One of these, which

involves magnetic exchange via non-bonding contacts between halide ions attached to a variety of metals is of particular interest in this investigation. This pathway, M-X·····X-M, is described as a double halide bridge. The sign and strength of the exchange is believed to be a function of the separation and relative orientations of the tetrahalocuprate anions[23]. If it is assumed that the strength of the magnetic exchange is dependent on both the degree of delocalization of spin density from the Cu(II) ion to the halide and the orbital overlap between the two non-bonding halide ions, then a number of variables become apparent. These factors divide into those within the tetrahalocuprate ions and those between the ions. Figure 1.2 shows the geometric parameters for describing the interaction between two CuX_4^{2-} ions,[12].

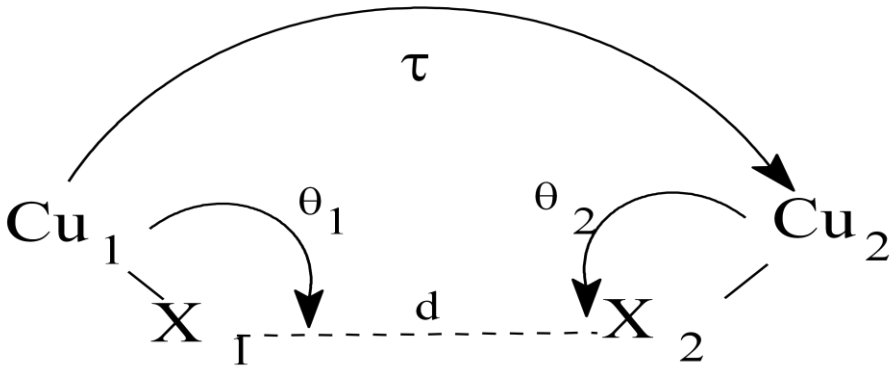

d – The distance between the Br atoms,

$_1$ – The angle Cu_1-X_1….X_2

$_2$ – The angle Cu_2-X_2….X_1

τ – The dihedral angle Cu_1–X_1 ….X_2–Cu_2

Figure 1.2 Diagram showing the geometric parameters for a double halide bridge magnetic exchange interaction

Magnetic data can be displayed in a number of ways. The different lines on each graph represent the different types of magnetism; **Ferromagnetic,** **paramagnetic,** and **Antiferromagnetic.** The plots of the most interest in this research are the antiferromagnetic systems, which lead to the magnetic exchange in these compounds. The magnetic susceptibility, χ, is a measure of the response of a sample to an applied magnetic field. It is defined as the magnetization per unit field. The Curie law ( ) describes the relationship between the susceptibility and temperature, obeyed by true paramagnetics. Samples that do not follow the Curie law are often modelled by the Curie-Weiss law (

, where θ is the Weiss constant and is proportional to the spin, S, the g-factor and the exchange constant, J.

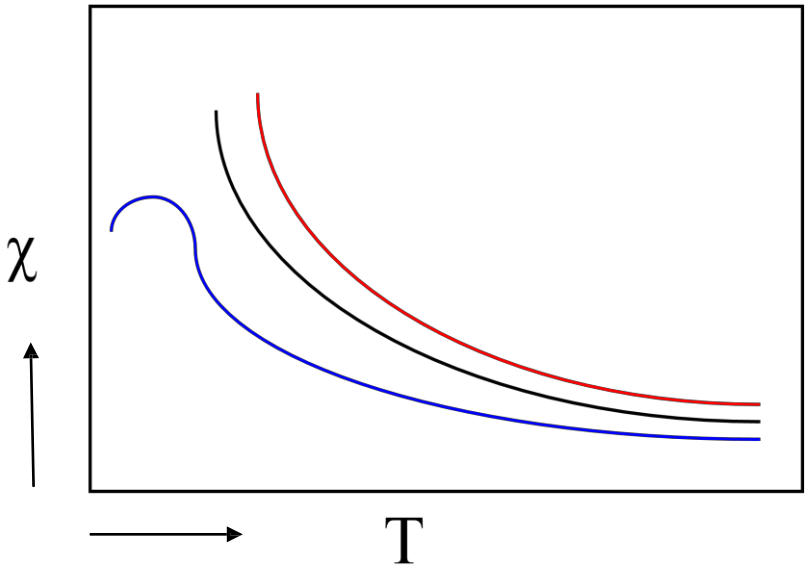

Figure 1.3 For an antiferromagnetic system a plot of X vs T to reach maximum X at low temperature, T (low T means kT is lower than magnetic energy).

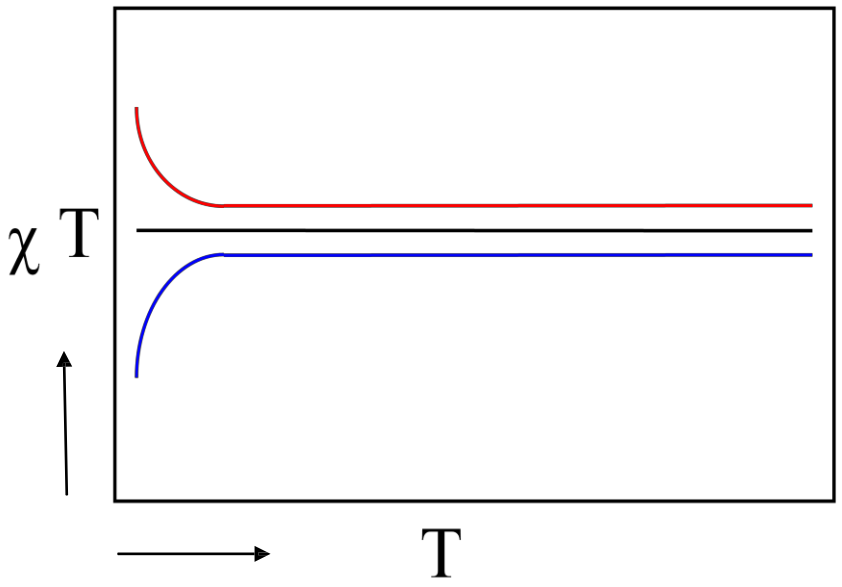

Figure 1.4 A plot of XT vs T should decrese at low temperature for an antiferromagnetic system

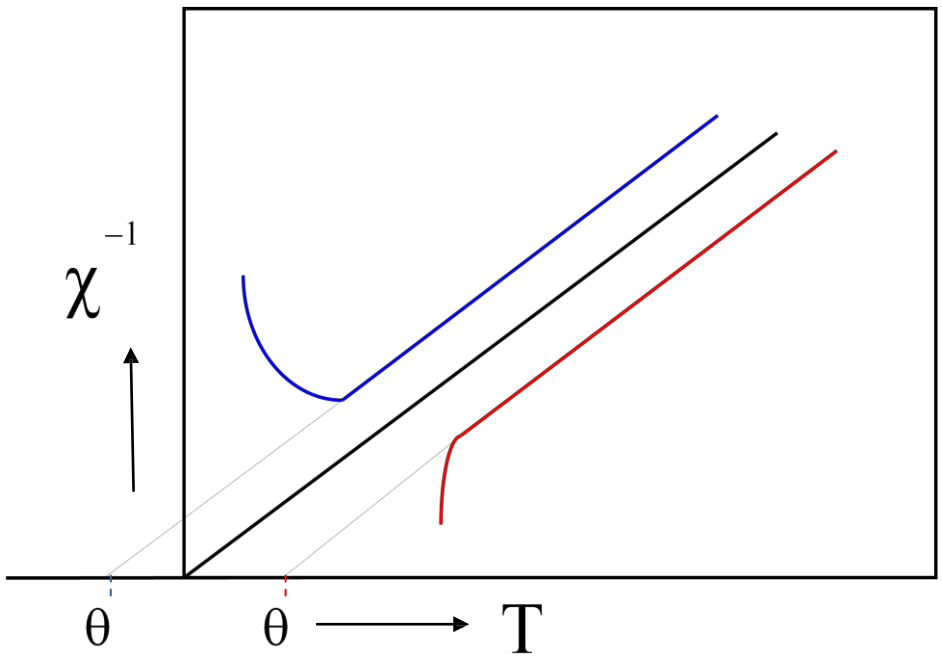

Figure 1.5 For antiferromagnetic systems a graph of X^{-1} vs T should increase at low temperature. The extrapolated intercept gives θ, the Weiss constant which is proportional to J, the magnetic strength

\

The crystal packing, and the distance and angles of the Cu-X···X-Cu contacts is known to affect the magnetic susceptibility of such complexes. Changes to the crystal packing can be made by changing the cationic part of the molecule.

Some general trends have been observed, particularly shorter X···X distances and larger Cu-X···X angles lead to stronger magnetic exchange. The large number of structural parameters that have been shown to affect the magnetic exchange through the double halide bridge interactions (e.g. degree of distortion of the CuX_4^{2-} tetrahedra, Cu-X bond lengths, X···X distances, Cu-X···X angles, etc) mean no definitive magnetostructural correlations can be made due to the limited number of compounds available for comparison[23].

During Drumheller *et al.*[24] studies of $(H_3NCH_2CH_2NH_3).CuCl_4$, a compound made up of sheets of square planar $CuCl_4^{2-}$ ions where the layers were linked by Cu-Cl-Cu bridges, an important observation was made that the antiferromagnetic exchange between the layers was almost 60 times larger than the predicted value based on the number of atoms involved in linking the sheets[25]. Further work by the same group with a series of alkyldiammonium salts, showed similar results and deduced that the strength of the metal exchange was not a function of the distance between metal ions, but rather the distance between the halide ions[26]. The same work reported two other important observations. Firstly, a stronger exchange occurs through a bromide – bromide bridge, compared to equivalent chloride analogues. Secondly, the compound $[H_3N(CH_2)_4NH_3].CuCl_4$ did not fit the same trends as other compounds in the same series. One possible explanation they noted was the Cu-Cl···Cl-Cu pathway was not linear like the other complexes. This was one of the earlier cases where it was suggested that the exchange was dependent on the Cu-X···X-Cu geometry, as well as the halide-halide distances, as the work of van Kalkeren and co workers had suggested[27].

Substituted pyridinium tetrahalocuprates have been frequently used in the study of 2D antiferromagnetic materials as many subtle adjustments such as, the geometry and modes of interactions can be made. Turnbull *et al*. have previously studied the bis(2-amino-5-S-pyridinium)Cu(II)X_4 [2A5SP] family, where S= Me, Cl, Br, F or I and X= Cl or Br [6, 12, 16, 28-30].

Within this family, the crystal packing is affected by the size of the S-substituent, as well as the hydrogen-bond donating properties of the amino group, and the pyridine N-H.

F.M. Woodward et al.[6] started to see some magnetostructural correlations within the 2A5SP family. The compounds compared were $(2A5MP)_2CuBr_4$[31], $(2A5MP)_2CuCl_4$[31], $(2A5CP)_2CuBr_4$[30], $(2A5CP)_2CuCl_4$[32] and $(2A5BP)_2CuBr_4$[6]. All the compounds compared in this series are made up of C-centred layers of CuX_4^{2-} anions separated by neighbouring layers of pyridinium cations. The separation between CuX_4^{2-} anions is due to the 5-substituent protruding into the anion layer. Changing the size of the 5-substituent changes the separation of anions, therefore changing the Cu-X···X-Cu distance, and ultimately the strength of magnetic interaction (J).

A comparison between the bromo and chloro tetrabromocuprates started to show how much effect the size of the substituent had on the overall packing. Chlorine has a Van der Waals radius of 1.75Å, and Bromine 1.85Å. Although they are not greatly different, the chloro compound had intra-layer contacts of 4.30Å with a J value of 8.50K[30], where the bromo compound had intra-layer contacts of 4.39Å with a J value of 6.95K[6]. This shows that even small changes in the size can have a reasonable effect on the strength of the magnetic exchange. However a similar trend is not the case when going from $CuBr_4^{2-}$ to $CuCl_4^{2-}$ tetrahedra. Chlorides are 6% smaller than bromides; with the decrease in van der Waals radii and a shorter copper-halide bond length results in much less halide-halide overlap due to a larger distance between chlorides relative to the van der Waals radii. This is emphasised,

when the tetrachloro and tetrabromo analogues of 2A5CP are compared, with a large decrease in J, from 8.72K for tetrabromo and 1.14K for tetrachloro, with little or no difference in the halide...halide distances of 4.30Å and 4.34Å. With these factors taken into account, the observed trend that J increased as unit cell volume decreased for copper tetrabromide compounds, and not for copper tetrachloride compounds makes sense.

This thesis will extend this work, with the synthesis of the 5-amino-2-substituent analogues of these compounds discussed in chapter 2. The 5A2SP series was chosen as it maintains the overall size and shape of the cations compared to their 2A5SP analogues, but could have significantly different hydrogen bonding capabilities with the amino group no longer adjacent to the pyridine nitrogen.

To date most work on tetrahalocuprates has looked at changing the nature of the cationic portion of the molecule and how this affects the compounds structure and the geometry around the tetrahalocuprate anion. No work as been reported in the literature exploring structuralmagneto correlations in tetrahalocuprates containing mixed halogens giving the structure of CuX_aY_b where X = Cl, Y = Br, and a+b = 4. Various isomers of dimethylpyridinium (lutidine) were chosen for this part of the investigations as they do not have any halogens or conventional hydrogen bonding substituents such as amino groups. Having different analogues with the methyl groups in different positions only changes the geometry of the cation, with minimal influence on the electronic properties, isolating the effects of having mixed halide anions. A few studies of dimethylpyridinium tetrahalocuprate(II) complexes have been reported in the literature dating back to 1974[33]. B.F. Ali and co-workers reported the structures of *bis*(2,6-Lutidinium) tetrachloro, and tetrabromocuprate(II), where they investigated the role of intermolecular interactions (C/N-H...X), π...π stacking and X...π, and how they influenced the crystal packing. This group

concluded that, by having significantly different size anions with (Br much larger than Cl) the structural properties were greatly changed which may lead to changes in other properties of the compounds[34]. In 1976 Guiseppe Marcotrigiano and co-workers[35] investigated the effects of having mixed-tetrahalocuprates using piperazinium as the cation. It was found that mono halide CuX_4 anions were commonly a 'flattened tetrahedra' in between tetrahedral and square planar geometry, whereas the mixed halide anions were closer to square planar geometry. Mark Turnbull and co-workers synthesised *bis*(2,3-dimethylpyridinium)tetrabromocuprate, with magnetic results showing they had prepared a two-leg, strong rail antiferromagnetic spin ladder with $J_{rung} = 3.10^{cm-1}$ and $J_{rail} = -6.02^{cm-1}$[19]. In recent unpublished work by Jan Wikaira involved 2,3-dimethylpyridinium cations. A series was produced using different ratios of $CuCl_2$ to $CuBr_2$ with the same ratios of the corresponding acid. The aim of this was to investigate whether bromine or chlorine was dominant in the anion structure and how these mixed anions affected the structural and magnetic properties of the compounds. Early results showed a strong dominance of Br to Cl in the anions. Only bromine was present in the anions in compounds made from a solution containing less than about 20% chlorine, as would be expected with Br being much larger and more electronegative than Cl. Some compounds gave some interesting magnetic results leading to expanding the study using other dimethylpyridine analogues. The large number of lutidine isomers makes it ideal to further study mixed halide systems.

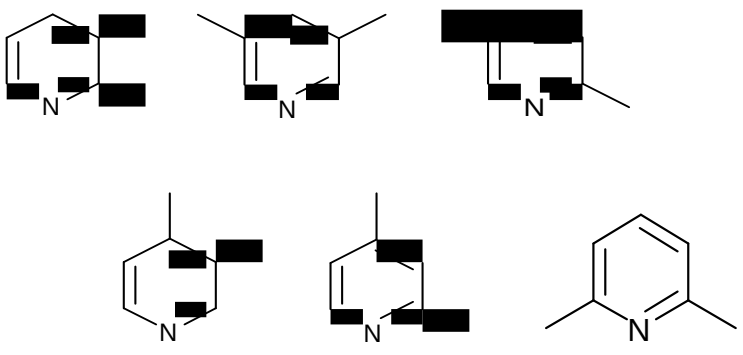

Figure 1.6 The different isomers of dimethypyridine.

As can be seen in figure 1.6, the different isomers of lutidine provide a range of different geometries without greatly changing the hydrogen bonding or electronic properties of the cation. This minimises variables and was hoped to give some insight on how much the cation geometry influences the geometry of the cuprate anion. The aim of this section of work, as discussed in chapter 3, was to make and study series of mixed halide tetrahalocuprates using different dimethylpyridine isomers, to see the effect of changing the shape of the cation, and of having mixed halide anions.

Imidazolium ions (a general structure is shown in Figure 1.7) are commonly used as

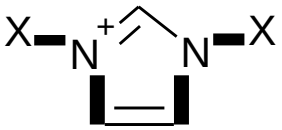

Figure 1.7

N-Heterocylcic carbenes, used for catalysis of a number of reactions. As a cation is necessary in the formation of tetrahalocuprates, imidazolium ions may be an ideal choice as they must have a positive charge due to the N,N substitution off the molecule. Usually the organic cations of tetrahalocuprates are generally achieved by acid protonation using concentrated HCl or HBr. As well as protonation, the acid is used as the source of the halogen atoms to give the correct stoichiometry to form tetrahalocuprates. Again imidazolium molecules remove the acid requirement as a large number are made as salts, often with Br^- or Cl^- as the counterions. With a number of synthetic routes to make these molecules a wide range of different ions can be achieved. The aim of this section of work was to synthesise a range of imidazolium salts, and test their suitability for the formation of tetrahalocuprate complexes with possible magnetic exchange pathways.

Hydrogen bonding and other weak through space interactions, such as π-π stacking and X···π interactions also play an important role in the structure of these compounds. As may be expected with amino-substituted-pyridinium cations there are different modes through which hydrogen bonding may occur. There are three types of hydrogen bond donors typically seen in these compounds; (1) Hydrogen of protonated pyridic nitrogen (commonly from acid generation of cation), (2) Simple hydrogen bonding from aminic hydrogen and (3) Bifurcated hydrogen bonding between a single pyridic hydrogen and two halide ions[36], shown in figure 1.8.

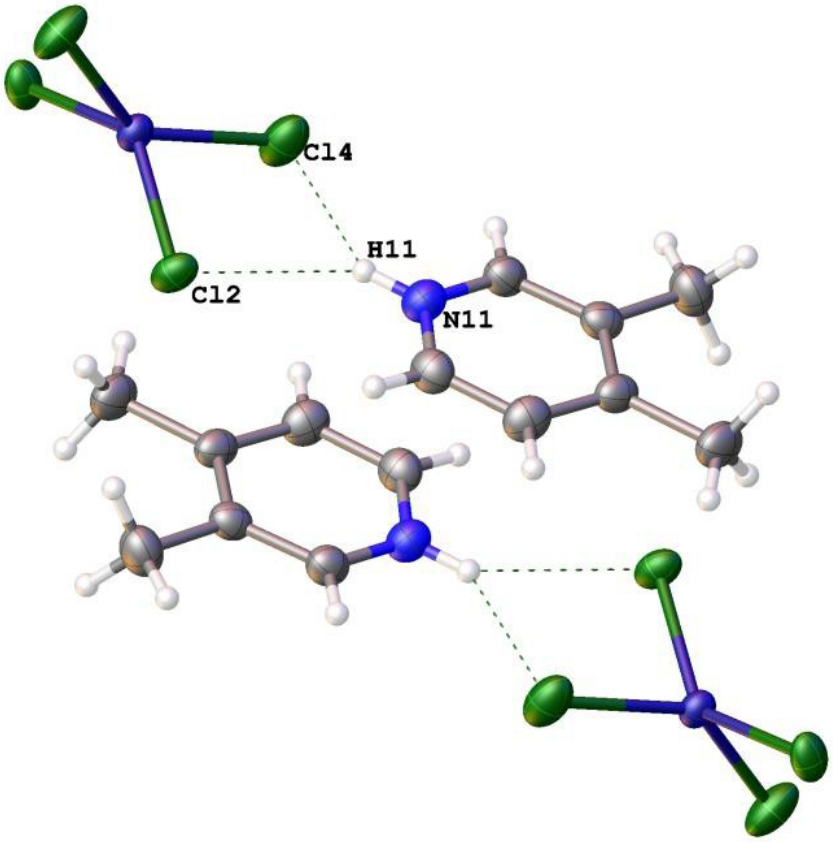

Figure 1.8 Example of bifurcated hydrogen bonding in bis(3,5-dimethylpyridinium)$CuCl_4$ complex

The crystal structure of (2-amino-3-chloro-5-trifluoromethyl pyridinium)$_2$CuBr$_4$ ((TMCAPH)$_2$CuBr$_4$), (figure 1.9) a structure previously reported by Jan Wikaira and co-workers[37] is an excellent example containing hydrogen bonds of types (1) and (2).

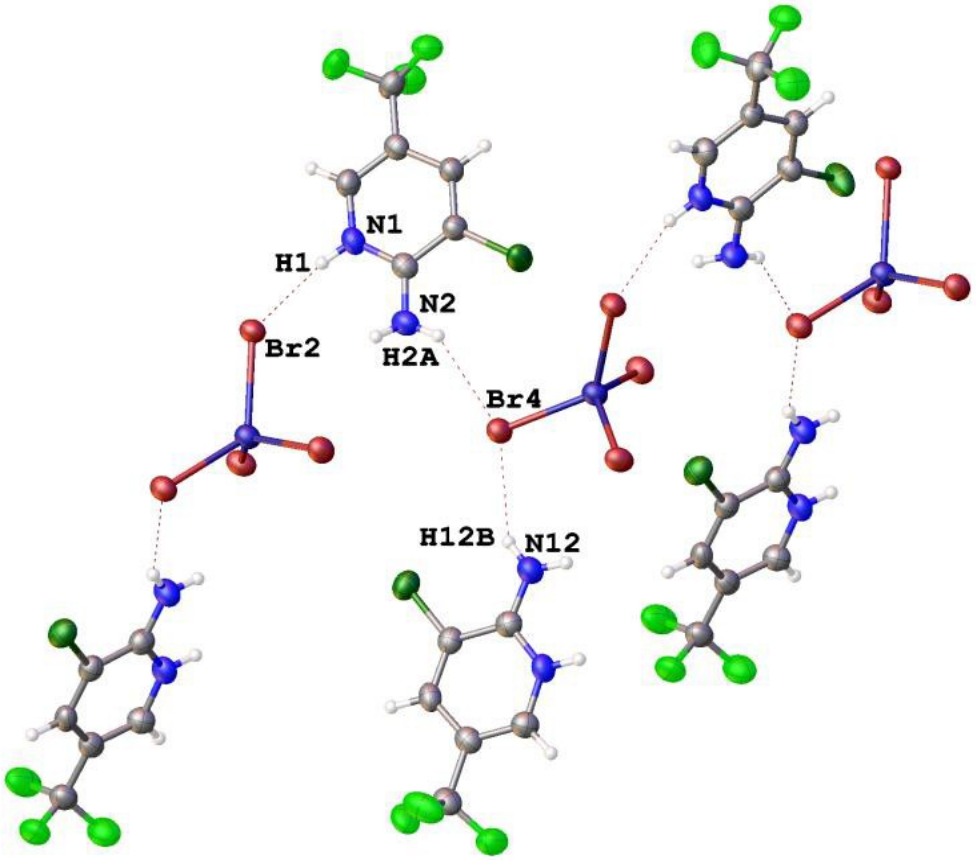

Figure 1.9 Hydrogen bonding between $CuBr_4^{2-}$ anions and pyridinium ions in (TMCAPH)$CuBr_4$.

Table 1.1 A representative set of hydrogen bonds for figure 1.9 (Å and °)

D-H···A	d(H...A)	d(D···A)	<(DHA)
N1-H1...Br2	2.398	3.209	157.42
N2-H2A...Br4	2.651	3.405	145.27
N12-H12B...Br4	2.649	3.416	149.10

Hydrogen bonding through aminic hydrogens is generally weaker than pyridinic hydrogens, due to the lone pair of the aminic nitrogen not being involved in hydrogen bonding, rather in resonance with the pyridine ring's π system. Three types of hydrogen bonding acceptor arrangements are also commonly seen[36], particularly in substituted amino-pyridinium complexes. (1) One halogen atom forms a single hydrogen bond to aminic or pyridic hydrogen atom as seen in figure 1.8 (N1-H1···Br2). (2) A single halogen forms two hydrogen bonds to two different cations, also shown in figure 1.9 (N2-H2···Br4···H12B-N12). (3) Bidentate hydrogen bonding where one halogen atom forms two hydrogen bonds between aminic and pyridic hydrogens of the same cation, shown in figure 1.10 (N1A-H1A¨Cl1¨H2A-N2A).

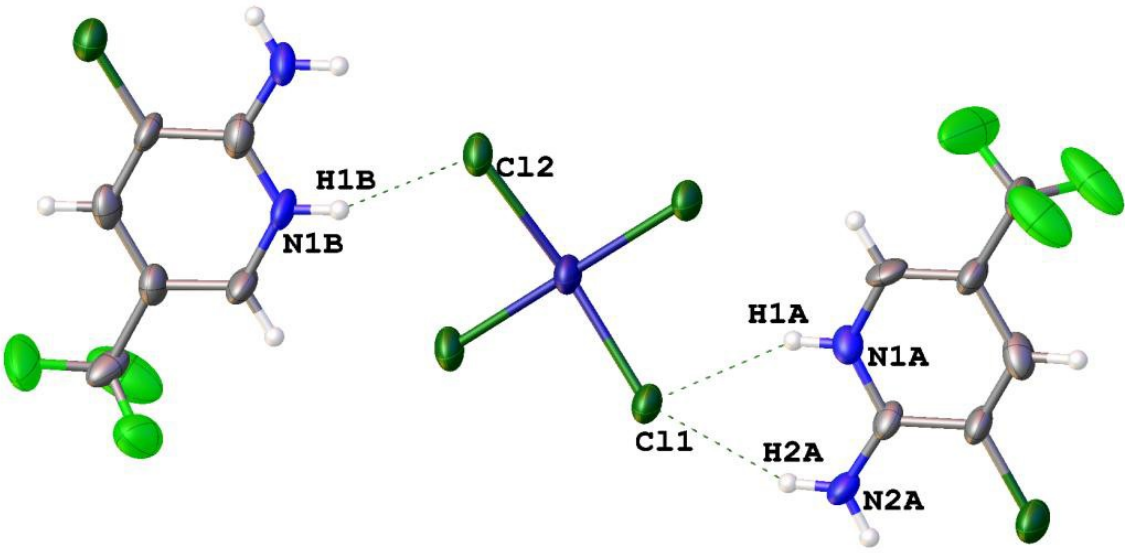

Figure 1.10 Hydrogen bonding in $(TMCAPH)_2CuCl_4$

Table 1.2 A representative set of hydrogen bonds for figure 5 (Å and °)

D-H···A	d(H...A)	d(D···A)	<(DHA)
N1B-H1B...Cl2	2.39	3.197(7)	156.2
N2A-H2A...Cl1	2.47	3.256(8)	152.8
N1A-H1A...Cl1	2.50	3.287(8)	153.0

The strength of hydrogen bonding is described in table 1.3[38].

Table 1.3 Classification of strong, moderate and weak hydrogen bonding. The numerical values are guidelines only

	Strong	**Moderate**	**Weak**
bond lengths, H···A (Å)	1.2 – 1.5	1.5 - 2.2	> 2.2
X···A (Å)	2.2 – 2.5	2.5 - 3.2	> 3.2
bond angles (°)	170 - 180	> 130	> 90

Weaker supramolecular interactions such as π-π stacking are often observed in structures where the cation is an aromatic ring system. The usual π interaction is an offset or slipped stacking, *i.e.* the rings are parallel displaced. The ring normal and the vector between the ring centroids form an angle of about 20° up to centroid–centroid distances of 3.8 Å[39]. The possible π stacking interactions can be seen in figure 1.11

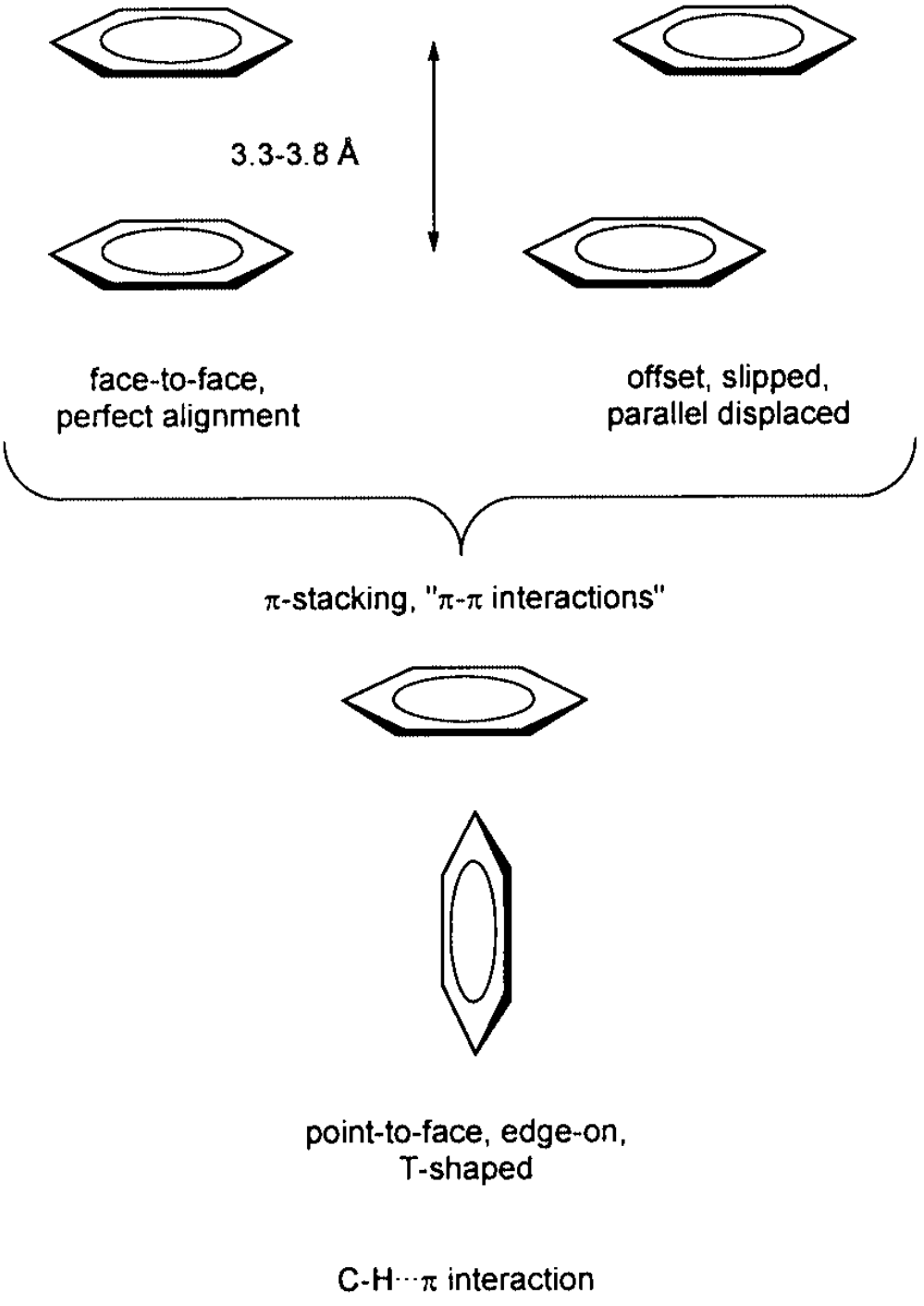

Figure 1.11 Principle orientations of π stacking interactions

Weaker supramolecular interactions such as π-π stacking are often observed in structures where the cation is an aromatic ring system. The degree π-π stacking is dependent on the size and position of the ring substituents. π-π stacking is seen more in compounds with minimal steric bulk, such as in bis(2-Amino-5-fluoropyridinium)$CuBr_4$[29], and *bis*(5-amino-2-methylpyridinium)$CuCl_4$, shown below in figure 1.11. P1, P2 and P3 represent the centroids of the aromatic rings. The distance between P1 and P2 is 3.797(18)Å, and 3.774(18)Å between P2 and P3.

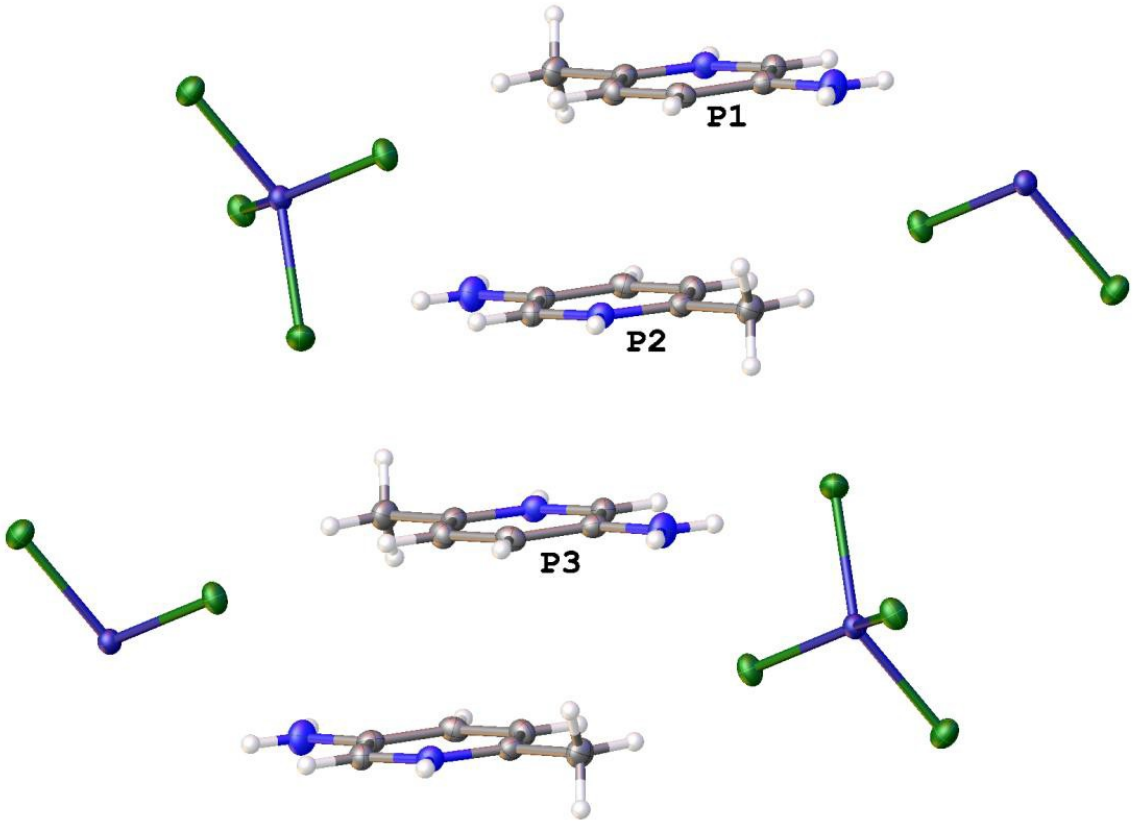

Figure 1.11 π-π stacking interactions in bis(5-amino-2-methylpyridinium)$CuCl_4$

1. Pelissetto, A. and E. Vicari, *Critical phenomena and renormalization-group theory.* Phys. Rep., 2002. **368**(6): p. 549-727.
2. Dagotto, E. and T.M. Rice, *Surprises on the way from one- to two-dimensional quantum magnets: the ladder materials.* Science (Washington, D. C.), 1996. **271**(5249): p. 618-23.
3. Anderson, P.W., et al., *Resonating-valence-bond theory of phase transitions and superconductivity in lanthanum copper oxide (La2CuO4)-based compounds.* Phys. Rev. Lett., 1987. **58**(26): p. 2790-3.
4. Sokol, A. and D. Pines, *Toward a unified magnetic phase diagram of the cuprate superconductors.* Phys. Rev. Lett., 1993. **71**(17): p. 2813-16.
5. Carlin, R.L., et al., *Magnetochemistry of copper(II): exchange interactions in catenated acetatodiamminebromocopper.* Inorg. Chem., 1986. **25**(11): p. 1786-9.
6. Woodward, F.M., et al., *Structure and magnetic properties of (5BAP)2CuBr4: magneto-structural correlations of layered S = 1/2 Heisenberg antiferromagnets.* Inorg. Chim. Acta, 2001. **324**(1,2): p. 324-330.
7. Hatfield, W.E. and J.H. Helms, *From the magnetic susceptibility of clusters to the magnetic susceptibility of chains with novel structures.* Mater. Sci., 1992. **17**(2): p. 21-31.
8. Ueda, K., et al., *Theoretical study and comparison with experiments for atacamite, Cu2Cl(OH)3.* Mol. Cryst. Liq. Cryst. Sci. Technol., Sect. A, 1997. **306**: p. 33-40.
9. Matsumoto, T., et al., *Heat Capacities of the S = 1/2 Two-Dimensional Heisenberg Antiferromagnet Bis(2-amino-5-chloro-pyridinium) Tetrabromocuprate(II) [(5CAP)2CuBr4] and Its Diamagnetic Analogue [(5CAP)2ZnBr4].* J. Phys. Chem. B, 2000. **104**(43): p. 9993-10000.
10. Turnbull, M.M., et al., *Synthesis, structure and magnetic susceptibility of two 5-nitro-2-aminopyridinium cuprates: (5-NAP)2CuCl4 and the quantum magnetic ladder (5-NAP)2CuBr4.H2O.* Mol. Cryst. Liq. Cryst. Sci. Technol., Sect. A, 2002. **376**: p. 469-476.
11. Halvorson, K. and R.D. Willett, *Structures of ethylenediammonium tetrabromocuprate(II) and propylenediammonium tetrabromocuprate(II).* Acta Crystallogr., Sect. C Cryst. Struct. Commun., 1988. **C44**(12): p. 2071-6.
12. Turnbull, M.M., C.P. Landee, and B.M. Wells, *Magnetic exchange interactions in tetrabromocuprate compounds.* Coord. Chem. Rev., 2005. **249**(23): p. 2567-2576.
13. Minguez Espallargas, G., et al., *Reversible Extrusion and Uptake of HCl Molecules by Crystalline Solids Involving Coordination Bond Cleavage and Formation.* J. Am. Chem. Soc., 2006. **128**(30): p. 9584-9585.

14. Jasiewicz, B., et al., *Crystal structure, spectroscopy and magnetism of selected (-)sparteine and alpha -isosparteine tetrahalocuprate salts.* J. Mol. Struct., 2006. **794**(1-3): p. 311-319.
15. Awwadi, F.F., R.D. Willett, and B. Twamley, *The Aryl Chlorine-Halide Ion Synthon and Its Role in the Control of the Crystal Structures of Tetrahalocuprate(II) Ions.* Cryst. Growth Des., 2007. **7**(4): p. 624-632.
16. Turnbull, M.M., et al., *Synthesis, structure and magnetic behavior of bis(2-amino-5-fluoropyridinium) tetrachlorocuprate: A magnetic ladder.* Abstracts of Papers, 234th ACS National Meeting, Boston, MA, United States, August 19-23, 2007, 2007: p. INOR-874.
17. Zhong, C., et al., *Syntheses, structures, and properties of a series of metal ion-containing dialkylimidazolium ionic liquids.* Bull. Chem. Soc. Jpn., 2007. **80**(12): p. 2365-2374.
18. Staniland, S.S., et al., *Structural and Magnetic Properties of [BDTA]2[MCl4] [M = Cu (1), Co (2), and Mn (3)], Revealing an S = 1/2 Square-Lattice Antiferromagnet with Weak Magnetic Exchange.* Inorg. Chem., 2006. **45**(15): p. 5767-5773.
19. Shapiro, A., et al., *Synthesis, Structure, and Magnetic Properties of an Antiferromagnetic Spin-Ladder Complex: Bis(2,3-dimethylpyridinium) Tetrabromocuprate.* J. Am. Chem. Soc., 2007. **129**(4): p. 952-959.
20. Haddad, S.F. and R.H. Al-Far, *Crystal Structure of Three Isomorphous Compounds of 2,5-Dibromopyridine with Tetrahalometalate(II) Ions.* J. Chem. Crystallogr., 2008. **38**(9): p. 663-669.
21. Adams, C.J., et al., *Solid state synthesis of coordination compounds from basic metal salts.* CrystEngComm, 2008. **10**(12): p. 1790-1795.
22. Bai, J., et al., *Theoretical study of crystal structures and intermolecular interactions in isomorphous adducts [2-ClPyH]+2[MCl2-4](M = Co, Cu, Ni).* Gaodeng Xuexiao Huaxue Xuebao, 2007. **28**(6): p. 1113-1116.
23. Tremelling, G.W., et al., *Transition metal complexes of 2-amino-3,5-dihalopyridines: Syntheses, structures and magnetic properties of (3,5-diCAPH)2CuX4 and (3,5-diBAPH)2CuX4.* Dalton Trans., 2009(47): p. 10518-10526.
24. Snively, L.O., et al., *Magnetic susceptibility of 1,2-ethanediammonium tetrachlorocuprate: a layered structure with strong interlayer magnetic coupling.* Phys. Rev. B Condens. Matter, 1979. **20**(5): p. 2101-4.
25. De Jongh, L.J. and A.R. Miedema, *Simple magnetic model systems.* Advan. Phys., 1974. **23**(1): p. 1-260.
26. Snively, L.O., G.F. Tuthill, and J.E. Drumheller, *Measurement and calculation of the superexchange interaction through the two-halide bridge in the eclipsed layered compounds [NH3(CH2)nNH3]CuX for*

n = 2-5 and X = Cl4 and Cl2Br2. Phys. Rev. B Condens. Matter, 1981. **24**(9): p. 5349-55.
27. Van Kalkeren, G., W.W. Schmidt, and R. Block, *Superexchange in insulators: comparison of different methods.* Physica B+C (Amsterdam), 1979. **97**(4): p. 315-37.
28. Giantsidis, J., et al., *S = 1/2 quantum Heisenberg antiferromagnet ladders.* Synth. Met., 2001. **122**(3): p. 517-522.
29. Li, L., et al., *Synthesis, structure, and magnetic behavior of bis(2-amino-5-fluoropyridinium) tetrachlorocuprate(II).* Inorg. Chem. (Washington, DC, U. S.), 2007. **46**(26): p. 11254-11265.
30. Woodward, F.M., et al., *Two-dimensional S = 1/2 Heisenberg antiferromagnets: Synthesis, structure, and magnetic properties.* Phys. Rev. B Condens. Matter Mater. Phys., 2002. **65**(14): p. 144412/1-144412/13.
31. Place, H. and R.D. Willett, *Structure of bis(2-amino-5-methylpyridinium) tetrachlorocuprate(II) and bis(2-amino-5-methylpyridinium) tetrabromocuprate(II).* Acta Crystallogr., Sect. C Cryst. Struct. Commun., 1987. **C43**(6): p. 1050-3.
32. Hammer, P.R., et al., *Magnetic studies of the two-dimensional, S = 1/2 Heisenberg antiferromagnets (5CAP)2CuCl4 and (5MAP)2CuCl4.* J. Appl. Phys., 1997. **81**(8, Pt. 2A): p. 4615-4617.
33. Satyanarayana, D. and B.K. Mohapatra, *Lutidinium tetrahalocuprates(II).* Chem. Zvesti, 1974. **28**(6): p. 753-6.
34. Ali, B.F., R. Al-Far, and S.F. Haddad, *Hydrogen Bonded, pi...pi Stacked and X...pi Framework Structures in Bis(2,6-Lutidinium) Tetrahalocuprate(II) Complexes.* J. Chem. Crystallogr., 2010. **40**(8): p. 696-701.
35. Marcotrigiano, G., L. Menabue, and G.C. Pellacani, *Tetrahalo- and (mixed-tetrahalo)cuprates of the piperazinium dication. Coordination geometry changes in some CuX42- anions.* Inorg. Chem., 1976. **15**(10): p. 2333-6.
36. Haddad, S.F., M.A. AlDamen, and R.D. Willett, *The role of non-classical supramolecular interactions in the structures of 2-amino-4,6-dimethylpyridinium tetrahalocuprate (II) salts.* Inorg. Chim. Acta, 2006. **359**(2): p. 424-432.
37. Wikaira, J.L., et al., *Transition metal complexes of 2-amino-3-chloro-5-trifluoromethylpyridine: syntheses, structures, and magnetic properties of [(TMCAPH)2CuBr4] and [(TMCAPH)2CuCl4].* J. Coord. Chem., 2010. **63**(17): p. 2949-2964.
38. Steiner, T., *The Hydrogen Bond in the Solid State.* Angewandte Chemie International Edition, 2002. **41**(1): p. 48-76.
39. Janiak, C., *A critical account on [small pi]-[small pi] stacking in metal complexes with aromatic nitrogen-containing ligands.* Journal of the Chemical Society, Dalton Transactions, 2000(21): p. 3885-3896.
40. Patyal, B.R., B.L. Scott, and R.D. Willett, *Crystal-structure, magnetic-susceptibility, and EPR studies of bis(piperidinium)*

tetrabromocuprate(II): a novel monomer system showing spin diffusion. Phys. Rev. B Condens. Matter, 1990. **41**(3): p. 1657-63.

41. Zhou, P., et al., *Novel low-dimensional spin 1/2 antiferromagnets: two-halide exchange pathways in A2CuBr4 salts.* J. Appl. Phys., 1991. **69**(8, Pt. 2B): p. 5804-6.

40. *Private communication*, Prof Mark M. Turnbull, Carlson School of Chemistry and Biochemistry, Clark University, 950 Main St., Worcester, MA 01610, 508-793-7167

41. Chu, Y., H. Deng, and J.-P. Cheng, *An Acidity Scale of 1,3-Dialkylimidazolium Salts in Dimethyl Sulfoxide Solution.* The Journal of Organic Chemistry, 2007. **72**(20): p. 7790-7793.

Chapter 2

5-amino-2-substituted-pyridinium tetrahalocuprates

2.1 Introduction

Recent work by Turnbull and co-workers has involved a series of 2-amino-5-substituted-pyridine tetrahalocuprates. Even with the relatively small number of compounds studied within this series some trends in magneto-structural correlations have started to emerge. As with the majority of tetrahalocuprates, the 2-amino-5-substituted compounds crystallise into separate, isolated layers of CuX_4^{2-} anions, and cations. The separation of the CuX_4^{2-} anions depends on the size of the 5-substituent which protrude into the anion layer. As the magnetic exchange interactions occur via halide...halide contacts between tetrahalocuprates, the strength of exchange can to some degree be tuned by the size of the 5-substituent. It was found that the tetrabromocuprates had better exchange than their tetrachlorocuprate counterparts. This was due to the van der waals radii, and the Cu-chloride bond length both being much smaller for the tetrachlorocuprates, meaning less orbital overlap and therefore less magnetic exchange. As would be expected, within the tetrabromocuprates, the smaller the S group, the larger the magnetic exchange, J. The compounds with S = methyl had the weakest exchange. This was due to the shape of the methyl group, making it the largest S, resulting in the greatest anion separation. The tradeoff however, for having a smaller substituent is it lessens the isolation between anion layers, which is also needed for good magnetic exchange, as well as the short intralayer halide···halide contacts. The ultimate aim, therefore, would be to find a compromise between the anion separation within each layer, and the degree of isolation between anion layers. Some trends between magnetic exchange and some key crystallographic parameters have also been noted. The main parameters of interest

are the halide...halide contact distances between tetrahalocuprates within an anion layer, which is a direct indication of the amount of molecular wave function overlap. The interlayer halide···halide distance also indicates the degree of isolation between layers. The volume of the unit cell contains all of this information, and is an obvious indicator of both the isolation between anion layers, and the distance between the tetrahalocuprates.

Table 2.1 Structural and magnetic parameters of interest from some previously reported 2A5SP compounds

Compound	J (K)	Intralayer X···X contact (Å)	Interlayer X···X contact (Å)	Unit cell Vol (Å^3)	Reference
$(5MAP)_2CuBr_4$	6.64	4.55	4.97	1910.1(6)	[31]
$(5BAP)_2CuBr_4$	6.95	4.39	4.85	1856.7(11)	[6]
$(5CAP)_2CuBr_4$	8.72	4.30	4.83	1804.1(11)	[30]
$(5MAP)_2CuCl_4$	0.76	4.55	5.08	1776.2(1)	[31]
$(5CAP)_2CuCl_4$	1.14	4.34	4.94	1661.56(11)	[32]

With the large range of 2-amino-5 substituent complexes already reported, which include the tetrachlorocuprate and tetrabromocuprates of the 2-amino complexes with the substituents being F, Cl, Br, I and Me (figure 2.1)

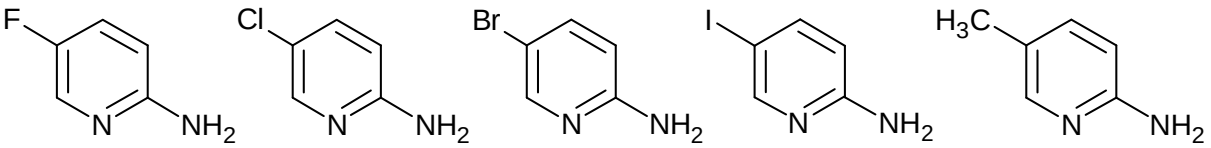

Figure 2.1 2-amino-5-substituent family previously studied

It was proposed to make the 5-amino-2-substituent analogues of the compounds. The 5-amino-2-substituent series of tetrahalocuprates was chosen for study as the cation portion of the compounds to maintain a similar overall size and shape compared to the 2-amino analogues. The main difference between the two series is the hydrogen bonding geometries. The two hydrogen bonding modes for both series of compounds are through the amino groups and the protonated pyridine nitrogen atoms. There is an increase of the angle between

the two hydrogen bonding sites (figure 2.2) from approximately 60° for the 2-amino series where the two groups are at adjacent positions on the pyridine rings, to about 120° in the 5-amino series where the two groups are two positions apart on the pyridine ring. As hydrogen bonding has been shown to be an important factor in the stability of these compounds, the change in the geometry was hoped to lead to some noticeable differences between the different families.

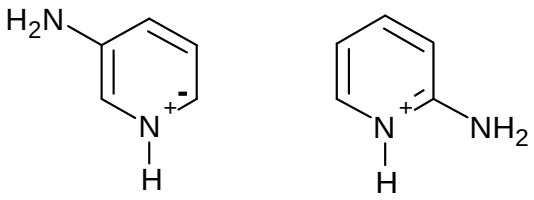

Figure 2.2 The different angles between the hydrogen bonding N groups for 5A2SP and 2A5SP

As the only change between the two series is the exchange of the amino and substituent positions, some insight into the features that have the greatest influence on the crystal packing may be seen. The question posed was, “Does the nature and geometry of the hydrogen bonding greatly affect the packing, or is the size of the substituent the main determinant of the crystal packing, and therefore magnetic properties?”.

2.2a 5-amino-2-methyl tetrachlorocuprate

Reaction of copper(ll) chloride with 2 equivalents of 5-amino-2-methylpyridine in water acidified with HCl gave $(5A2MP)_2CuCl_4$. Single crystals suitable for X-ray diffraction were obtained by slow evaporation. The compound crystallises in the monoclinic space group C2/c. Full tables are available in the crystallography appendix.

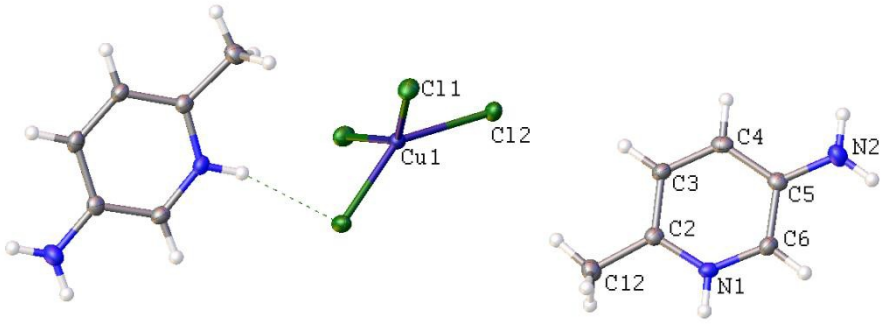

Figure 2.3 Molecular unit of **2.2a**, shown with 50% probability thermal ellipsoids. The labelled atoms are those in the asymmetric unit, with the unlabelled atoms generated by symmetry

The molecular unit shown in figure 2.3 contains a single $CuCl_4$ anion and two 5-amino-2-methylpyridinium cations, which is the usual motif in these type of compounds. The Cu-Cl bond lengths are normal with an average of 2.254(7)Å. The anion geometry lies between square planar and tetrahedral with trans angles of 142.18(4)° and 143.56(4)°. The pyridine cations are nearly planar with an angle of 2.77(19)° between N2 and C12. The amine groups are close to planar with respect to the plane of the ring with the angle N2-C5-C2 being 178.5(2)°. The amines are not angled with respect to the plane of the ring with the angles C6-C5-N2, 121.3(3)°, and N2-C5-C4 121.7(3)°. The methyl groups however are leaning slightly towards the pyridine nitrogen with the angles C12-C2-N1 118.4(3)°, and C12-C2-C3 125.1(3)°. The methyl group also sits slightly out of the plane of the ring with an angle N2-C5-C4 175.5(2)°. The crystal packing can be described as layers of $CuCl_4^{2-}$ anions separated by layers of the cations, shown in figure 2.6. The different layers form almost flat sheets which are well isolated. Weak π-π stacking may affect the stability, with interplanar distances of 3.794(18)Å and 3.774(18)Å between cation centroids, also visible in figure 2.4

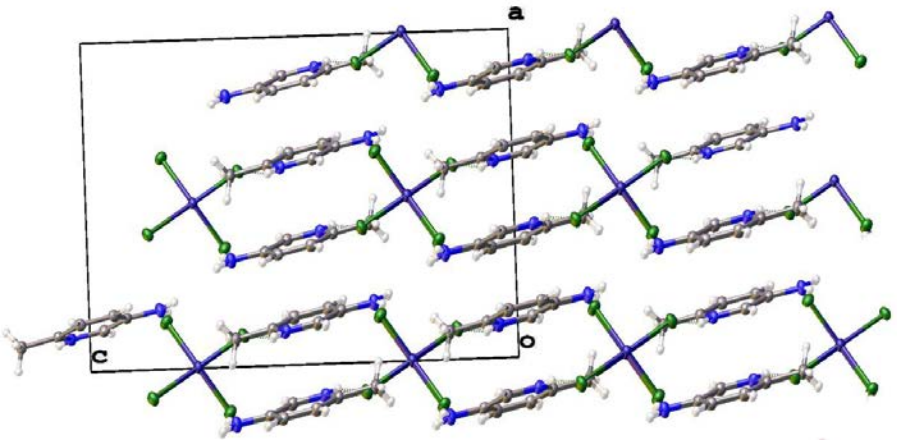

Figure 2.4. Packing of 5A2MP.$CuCl_4$. View of *ac*-plane shows the isolated anion and cation layers

The structure is stabilised by hydrogen bonding between the pyridinium hydrogen atoms to the chloro ions of the tetrachlorocuprate anions. Hydrogen bonding interactions between the amino groups and chloride ions are also present, however are much weaker and on the outer limits of a N-H···Cl hydrogen bond interaction[38]. Details of hydrogen bonding are in table 2.2. and are shown in figure 2.5

Table 2.2 A representative set of hydrogen bonds for 5A2MP (Å and °)

D-H...A	d(H...A)	d(D...A)	<(DHA)
N1-H1...Cl1	2.501	3.177(2)	155.24
N2-H2A...Cl2	2.610	3.448	159.49
N2-H2B...Cl2	2.870	3.521	132.05

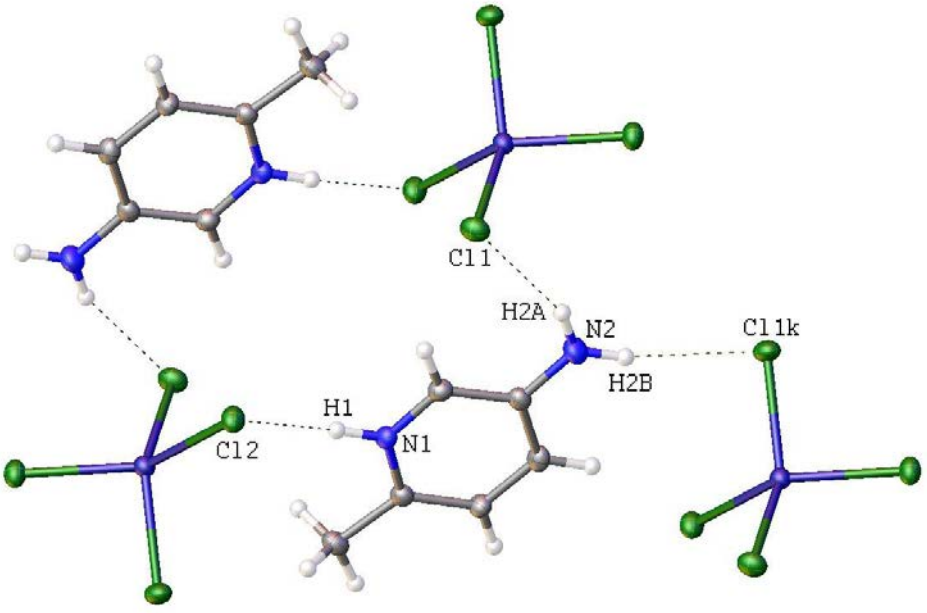

Figure 2.5 The different hydrogen bonding interactions in compound **2.2a.**

Measurement of chloride¨chloride contacts reveals a potential magnetic pathway (figure 2.6). With regard to the anion layers, the intra-layer contact between Cl1 and Cl2 is 4.3360(9)Å with angles Cu1-Cl1···Cl2 being 152.90(3)° and Cu1-Cl2···Cl1 119.00(3)°, and the dihedral angle 33.21(7)°. The shortest inter-layer contact is between Cl2···Cl2f with a distance of 5.3568(14)Å, and both Cu-Cl2···Cl2 angles 114.12(3)°. The dihedral angle is 180° as required by symmetry. Compared to the previous analogue, (2MAP.$CuCl_4$[31]), where the methyl and amino groups are in opposite positions, which had inter-layer contacts of about 4.55Å, and intra-layer contacts of about 5.08Å. The intra contacts are shorter, and inter contacts are longer in 5A2MP.$CuCl_4$ meaning the anion layers are more isolated with shorter contacts which may lead to a larger J value than J = -0.76K of the 2MAP.$CuCl_4$ complex

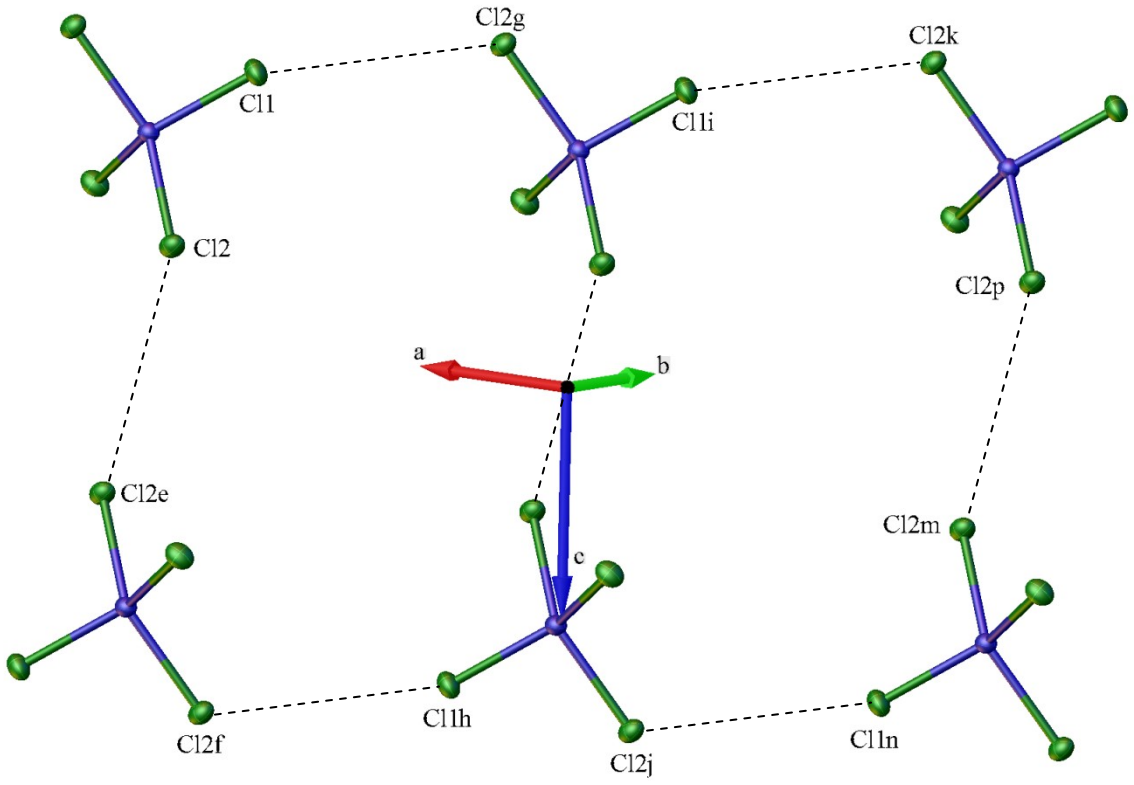

Figure 2.6 Image of the shortest chloride···chloride contacts in compound 2.2a are represented by the dashed lines. The contact distances are Cl2···Cl2f 5.3568(14)Å for the shortest intralayer contact, and Cl1···Cl2g 4.3360(9)Å.

2.2b 5-amino-2-methylpyridine tetrabromocuprate

Reaction of copper(II) bromide with 2 equivalents of 5-amino-2-methylpyridine in conc. HBr gave $(5A6Br2MP)_2CuBr_4$ (**2.2b**). Single crystals suitable for X-ray diffraction were obtained by slow evaporation. The compound crystallises in the orthorhombic in the space group Pbcn.

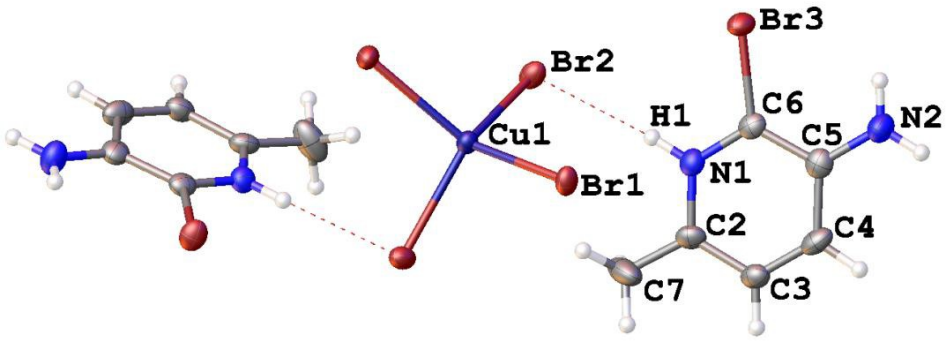

Figure 2.7 Molecular unit of **2.2b**. The labelled atoms are those present in the asymmetric unit, the remaining atoms are generated by symmetry. Br3 is where the pyridine molecules have been brominated at the 6 position. The image is shown with 50% probability thermal ellipsoids.

The molecular unit of **2.2b (**figure 2.7) contains one tetrabromocuprate anion and two pyridinium cations, which is common. However the cation has been significantly changed to become trisubstituded, in this case a bromine atom has been substituted at the C6 position of the pyridine rings.

There is a slight disorder of the pyridine rings, where approximately 5% of the time they are flipped 180°, i.e Br3 and C7 effectively swap positions. The anions have a average Cu-Br bond length of 2.38Å. The trans angles of 129.05(5)° and 130.97(5)° give the anions a geometry in between tetrahedral and square planar, but closer to tetrahedral than square planar.

Hydrogen bonding interactions play a large role in the crystal packing of **2.2b** (figure 2.8). Full details of the hydrogen bond interactions can be seen in table 2.3

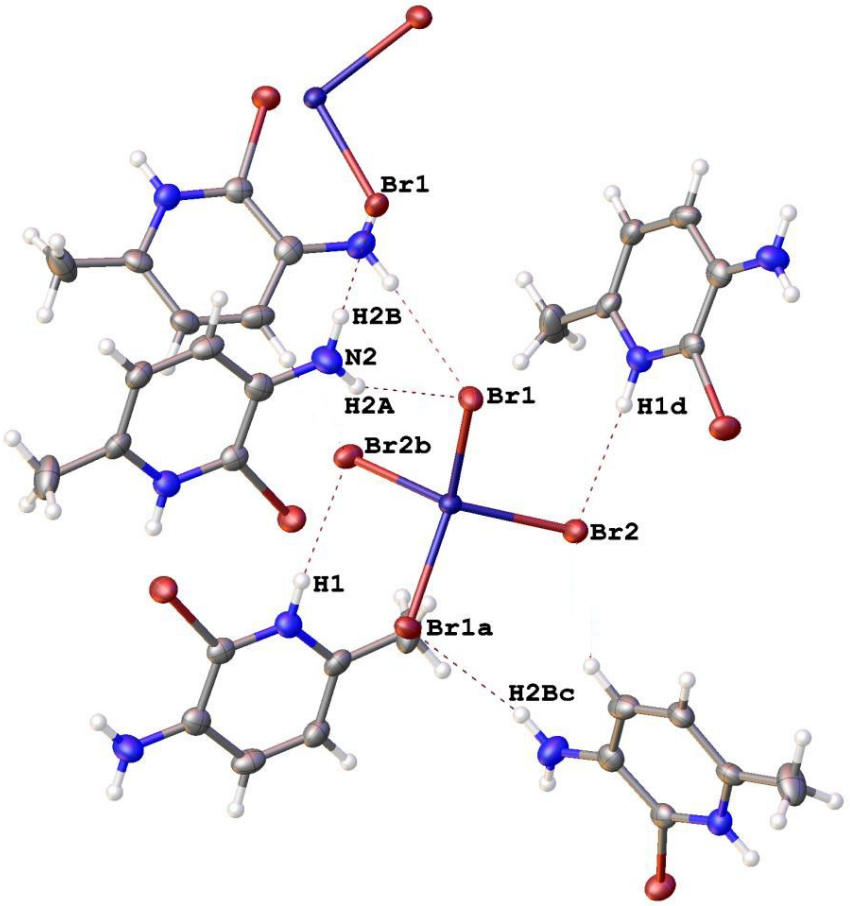

Figure 2.8 Diagram of the different hydrogen bonding interactions in compound 2.2b. The details of the interactions represented by the dashed lines can be found in table 2.3 above

Table 2.3 Details of hydrogen bonding interactions for compound **2,2b**

D-H...A	d(H...A)	d(D...A)	<(DHA)	Symmetry Op.
N1-H1...Br2	2.4607(5)	3.318(5)	174.8(3)	[-x+1, -y+1, -z+1]
N2-H2A...Br1	2.8004(6)	3.581(5)	151.7(3)	[x, y+1, z]
N2-H2B...Br1	2.9136(6)	3.709(5)	154.7(4)	[-x+1/2, y+1/2, z]
N2-H2A...Br3	2.7290(5)	3.141(5)	110.9(3)	

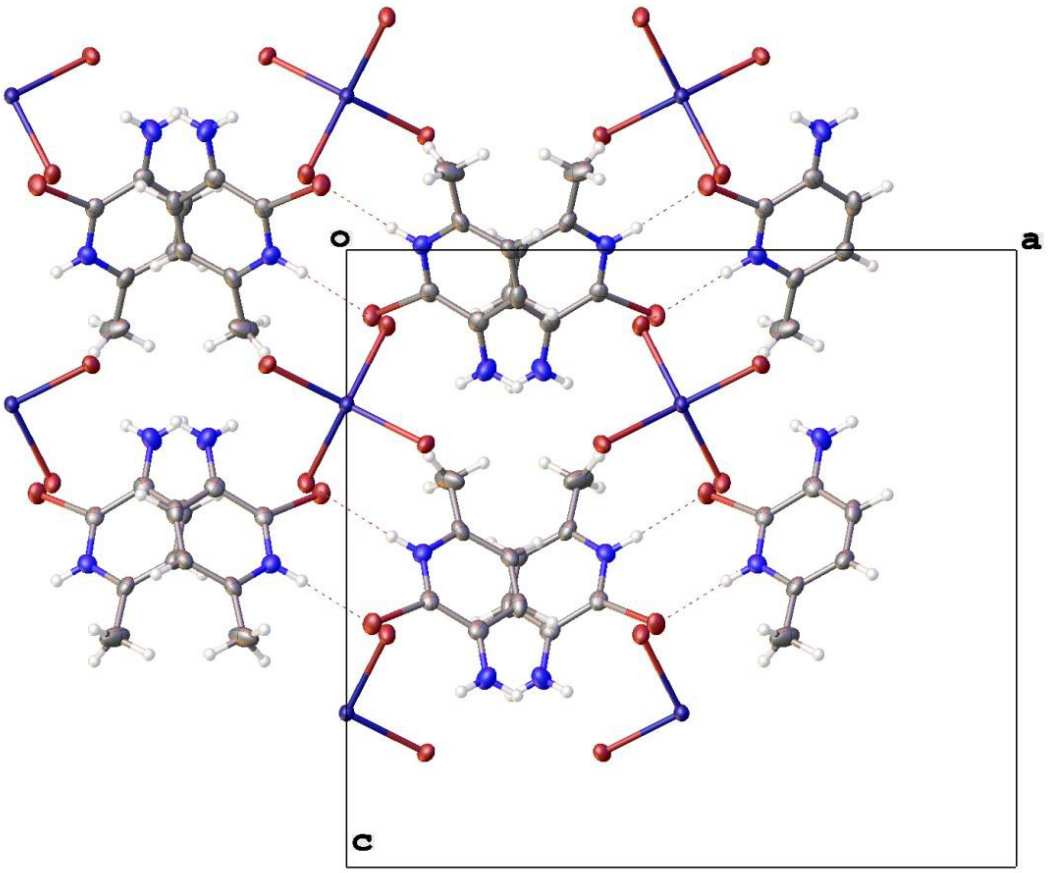

Figure 2.9 Packing diagram of the ac-plane of compound 2.2b, shown with 50% probability thermal ellipsoids. The dashed lines represent hydrogen bonding interactions.

As with the majority of tetrahalocuprates studied, crystals of **2.2b** pack into isolated layers of anions and cations. From the packing diagram viewed of the ac-plane (figure 2.9) the high level of symmetry imposed by an orthorhombic spacegroup can be seen. The pyridine rings alternate orientation along the b-axis, with the bromine atoms inserted into the tetrabromocuprate layers. The angle between the plane of the pyridine rings of the different orientations within each cation layer is 42.6(3)°. As previously mentioned hydrogen bonding interactions play a significant role in the stability of the crystal packing. The anion layers are sandwiched between adjacent cation layers, which have hydrogen bonding interactions between the pyridine nitrogens and the bromines on the pyridine rings. These interactions are represented by the dashed lines that can be seen in figure 2.6.

An alternative view of the crystal packing of **2.2b** (figure 2.10) shows the angle between the pyridine rings between the different cation layers.

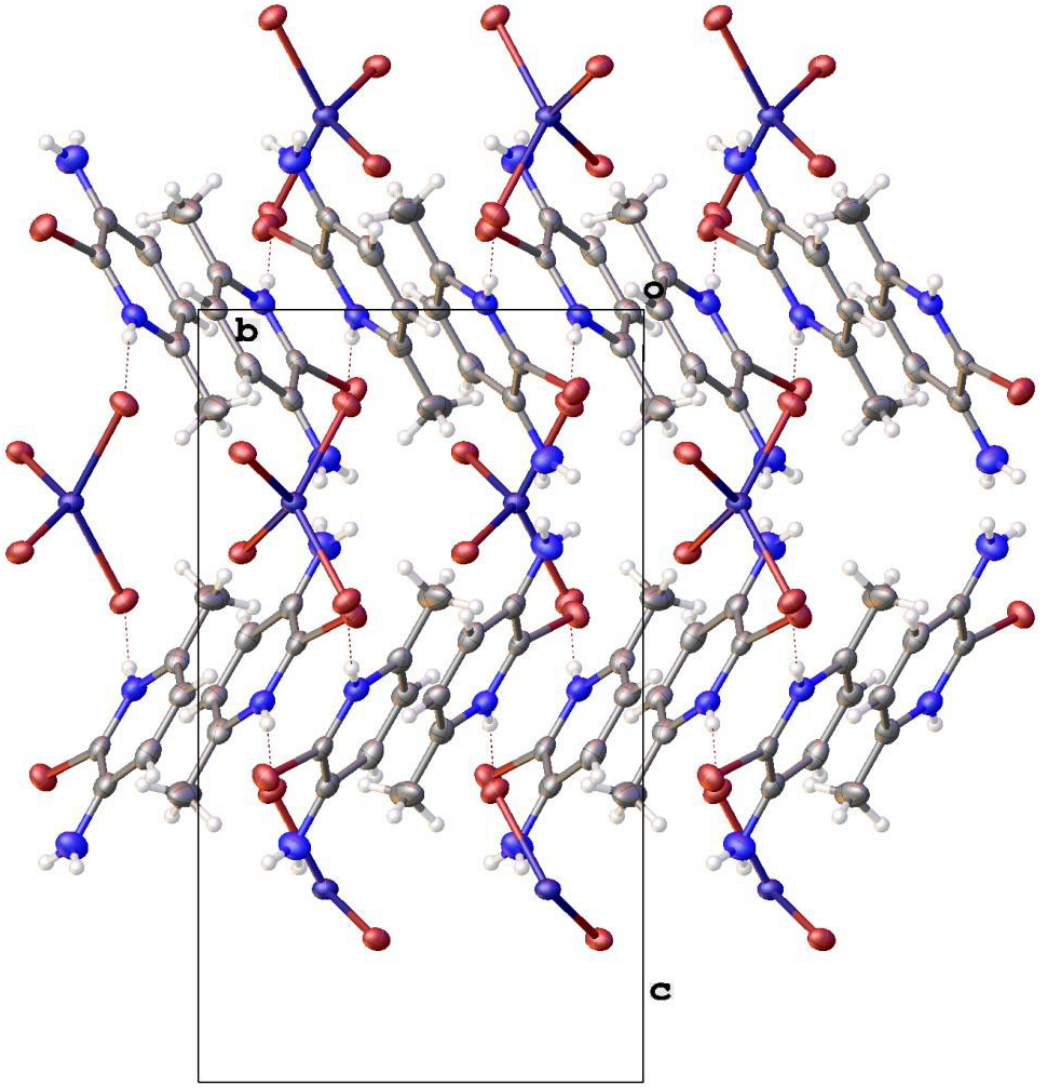

Figure 2.10 Packing diagram of the bc-plane of 2.2b, shown with 50% probability thermal ellipsoids. The alternating orientations of the different anion layers can be seen. The angle between cations of adjacent cation layers is also clearly visible.

5-amino-2-methylpyridine was not an isolated case for the bromine substitution in the 6 position. Both the bromo and iodo pyridines also showed similar substitution (figure 2.11), however did not form the tetrabromocuprates.

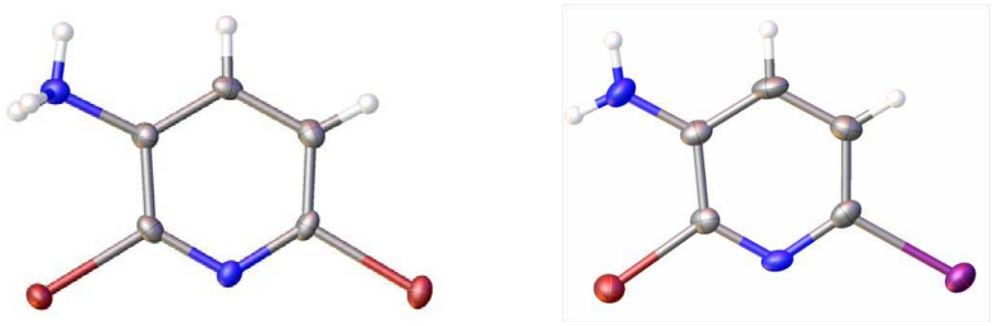

Figure 2.11 Crystal structures of 5-amino-2-bromopyridine and 5-amino-2-iodopyridine, both showing bromination in the 6 position after being in a solution of conc HBr and CuBr2.

This occurrence may be due to electron donating effects of the amino groups leading to the 6 position to carry a slight positive charge, making it more susceptible to nucleophilic substitution. The methyl substituted pyridine also had similar bromination, but formed the tetrabromocuprate complex.

All of the previous 2-amino compounds had the often seen motif of isolated anions and cations, with a 2:1 ratio of cations to anions. This was certainly not the case with the 5-amino family with some interesting results, including tri-copper moieties bound with four pyridinium ions for both the bromine (section 2.4) and chlorine (section 2.3) substituted pyridines when reacted with copper(II) chloride.

2.3 5-Amino-2-Chloropyridine + CuCl2

Reaction of copper (ll) Chloride with 2 equivalents of 5-amino-2-chloropyridine in aqueous concentrated HCl gave $(5A2CP)_2.CuCl_4$ (**2.3**). Single crystals suitable for X-ray diffraction were obtained by slow evaporation. Crystals of this compound are triclinic in the space group P-1. Immediately, from the molecular unit (figure 2.12) it can be seen that the structure of **2.3** is very different to the usual motif of two isolated cations to a single tetrahalocuprate. Instead discrete units of substituted Cu_3 units are formed.

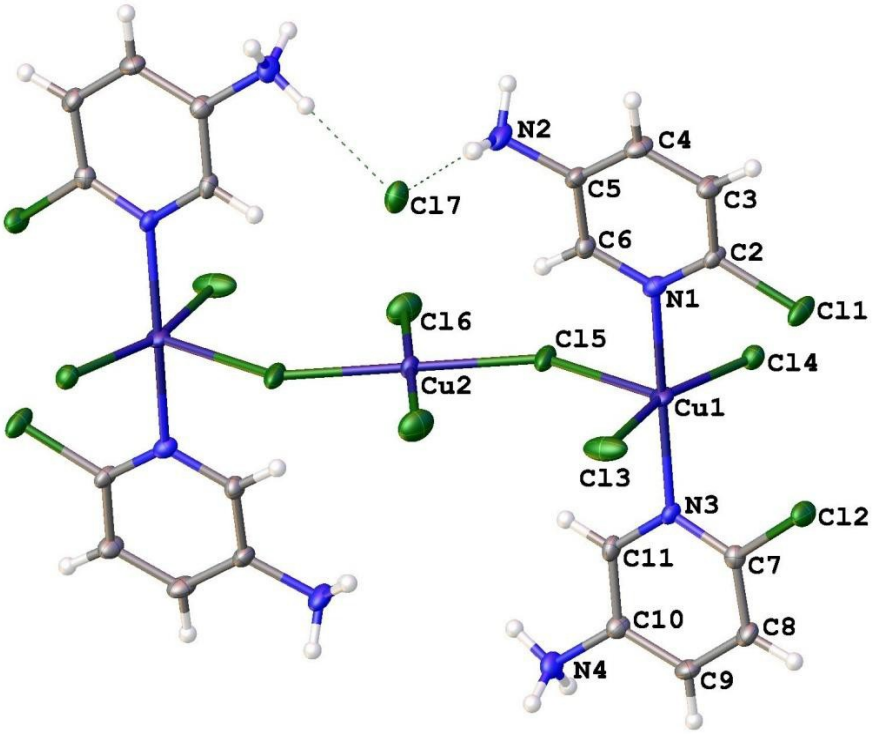

Figure 2.12 Molecular unit of **2.3** shown with 50% probability thermal ellipsoids. The labelled atoms are those present in the asymmetric unit. The unlabelled atoms are generated by symmetry

The main feature of interest in the molecular unit shown in figure 2.9 is the 5 coordinate copper atom, bound to three chloride atoms, and the pyridine nitrogens of two 5-amino-2-chloropyridine molecules. As the pyridine units are bound to the copper through the pyridine nitrogens, the amino groups are protonated instead to give each pyridine a +1 charge. The

pyridine rings attached to a single copper are slightly tilted toward each other, with the angle N3-Cu1-N1 being 170.32(13)°. The chlorine atoms of the pyridines are angled towards each other with an average N-C-Cl angle of 117.08(3)° giving them a through space distance of 3.5281(15) Å suggesting a possible through space halide...halide interaction. The Cu-Cl bond lengths are normal with an average length of 2.28(1)Å, with the exception of the bond between Cu1 and Cl5 which is considerably longer at 2.723(1)Å. The pyridine rings are nearly orthogonal to the copper-choride chain with the average Cl.-Cu.-N angle about Cu1 being 89.52(10)°. The central $CuCl_4$ is almost square planar with angles of 93.55(6)° and 86.45(6)° around the copper. There is a considerable amount of disorder of the bridging copper (Cu2), which has an occupancy of approximately 54%. The atom is likely to be spread over the same position of neighbouring molecules the other 46% of the time.

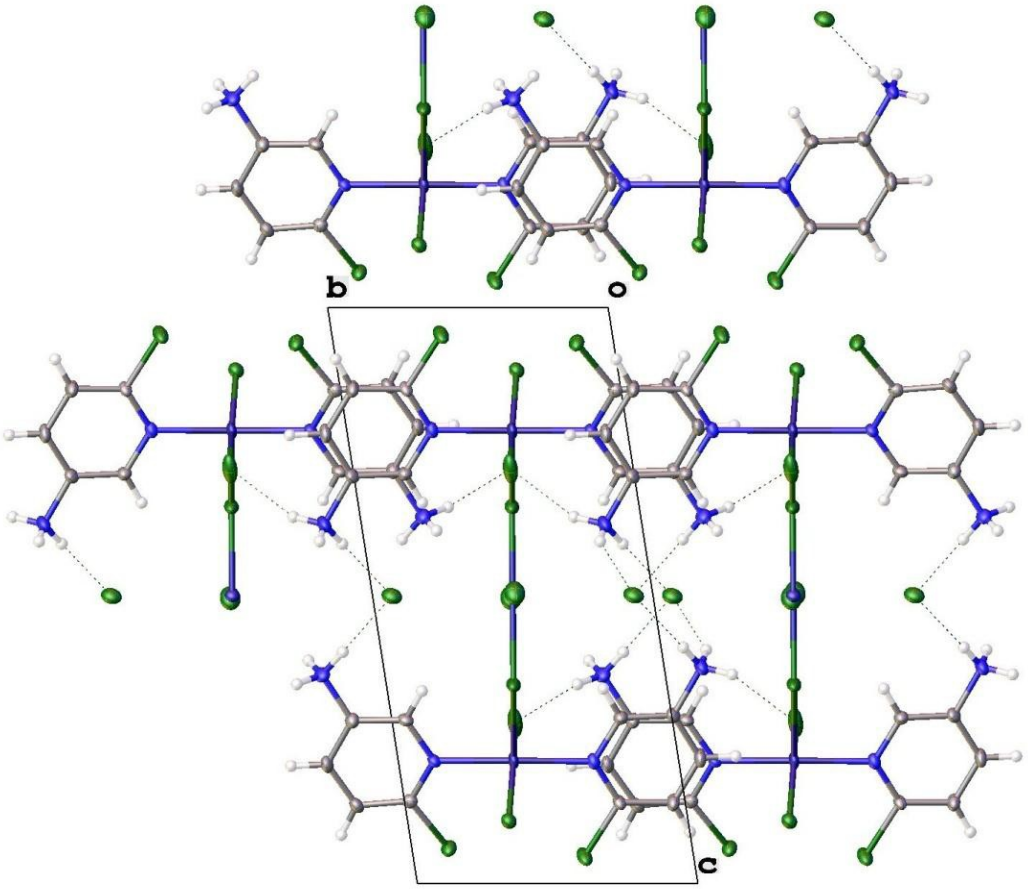

Figure 2.13 Packing diagram of the bc-plane of compound **2.3**. The overlap of pyridine rings between neighbouring units can be seen.

As can be seen in a packing diagram of the bc plane (figure 2.13) staggered layers of the tri-copper units are formed. The layers are in chains. The chains are held together through possible halo···halo interactions as well as possible halo···halide interactions. The halo···halo interactions all fall within the van der Waals radii of the interacting chlorines. The three shortest interactions are Cl2···Cl2 3.493(2)Å, Cl1···Cl1 3.267(2)Å and Cl1···Cl2 3.4319(14)Å. The halo···halide interaction of Cl1···Cl3 3.6965(16)Å may also contribute towards the structure. As can be seen in figure 2.13 there is an overlap of pyridine rings from neighbouring molecules. There is a weak π-stacking interaction between these with a centroid...centroid distance of approximately 3.87Å with a shift if about 1.2Å (figure 2.14).

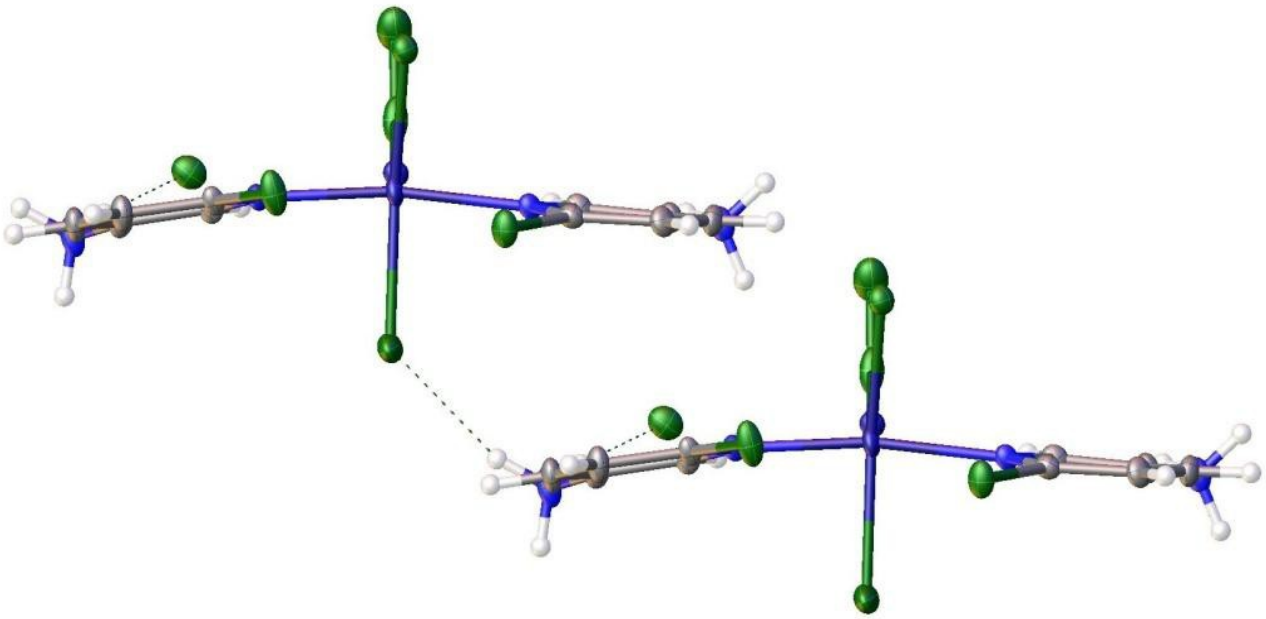

Figure 2.14 View of possible π-stacking interaction between overlapping pyridine rings of neighbouring tri copper molecules in **2.3.**

Hydrogen bonding interactions compliment the π stacking interactions in stabilising the packing structure of compound **2.3**. As can be seen from table 2.4 and figure 2.15 below there are a large number of interactions present. The amino groups are hydrogen bound to chlorine atoms of neighbouring tri-copper chains, eg the interactions between H4A and Cl3. H4C has bifurcating hydrogen bonding, interacting with Cl5 on the neighbouring copper chain, as well as a non-coordination chloride ion, Cl7x.

Table 2.4 Details of hydrogen bonding interactions present in compound **2.3**

D-H...A	d(H...A)	d(D...A)	<(DHA)	Symmetry Op.
N4-H4A...Cl3	2.2269(10)	3.105(4)	168.8(2)	[x-1, y-1, z]
N4-H4B...Cl7	2.239	3.127	175.52	[-x, -y+1, -z+1]
N4-H4C...Cl7	2.5904(11)	3.202(4)	126.6(2)	[x, y-1, z]
N4-H4C ...Cl5	2.6242(11)	3.318(4)	135.4(2)	[x, y-1, z]
N2-H2A...Cl3	2.3865(12)	3.228(4)	157.8(2)	[x, y+1, z]
N2-H2B...Cl7	2.341	3.140	149.34	[-x+1, -y+2, -z+1]
N2-H2C...Cl7	2.2115(10)	3.098(4)	173.5(3)	

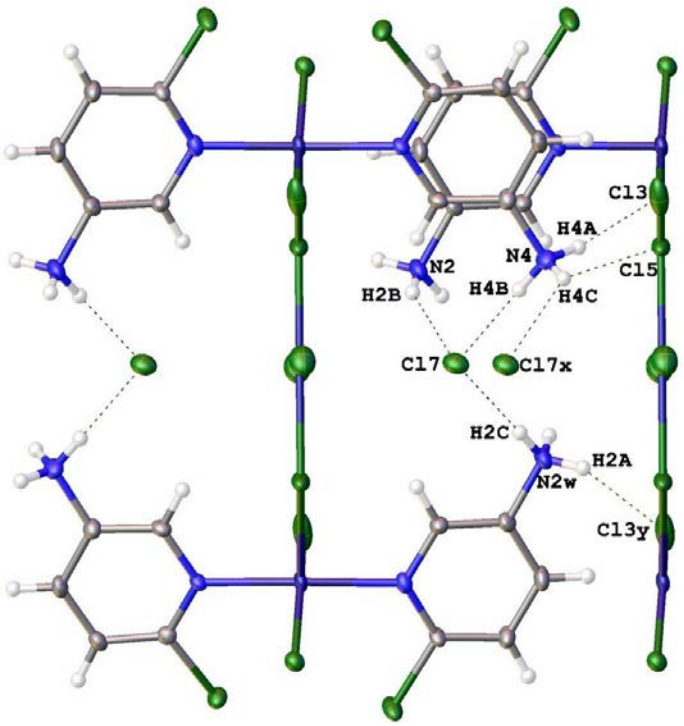

Figure 2.15 Hydrogen bonding interactions present in compound **2.3.**

A diagram of the copper chloride chains (figure 2.16) a possible magnetic exchange pathway can be seen. Details of the chloride···chloride contacts can be seen in table 2.5 below.

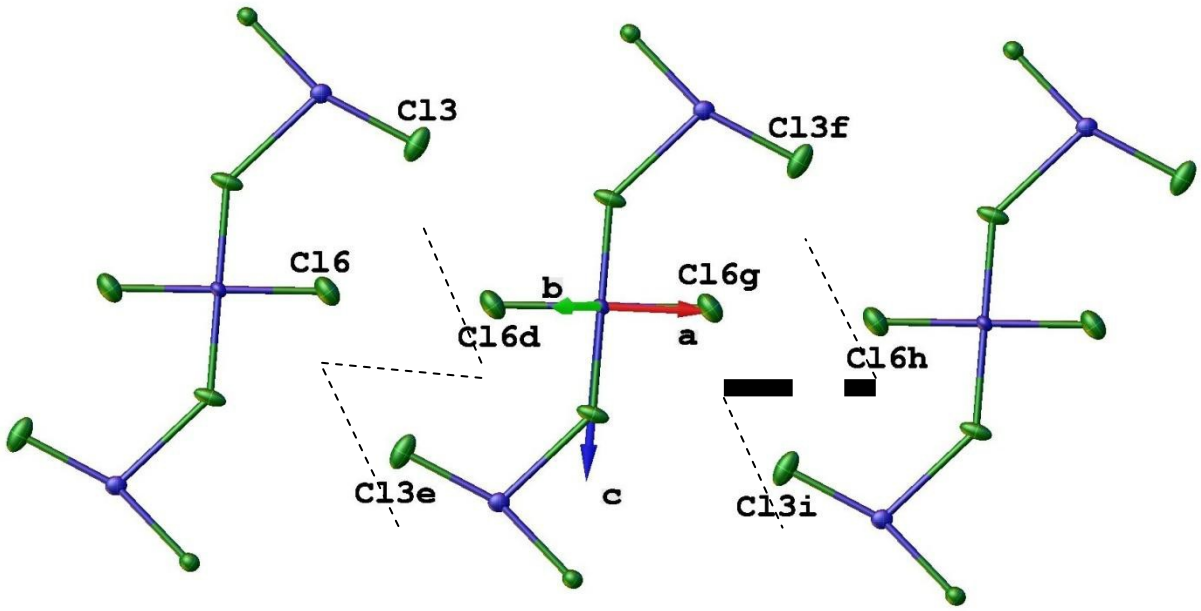

Figure 2.16 Details of the possible magnetic exchange pathway for compound **2.3.** The dashed lines represent possible through space halide···halide contacts The cations have been omitted for clarity.

Table 2.5 Details of the possible magnetic exchange contacts in **2.3**. Figure 1.2 in the introduction shows detail of the θ and T angles.

Contacts	d(Cl···Cl)Å	$\Theta_1{}^0$	$\theta_2{}^0$	τ °
Cl3...Cl6d	3.757(2)	116.15(6)	143.09(7)	176.76(6)
Cl6...Cl6d	3.508(3)	175.23(10)	173.23(10)	180(1)

The magnetic data was fitted using a S = ½ trimer model, with the help of Prof Mark Turnbull[40] and his expertise. The model uses an unreasonable assumption, that the moments at each Cu ion are the same. Since the geometries are different, this is not correct. However, the difference is small so can safely be ignored. In this case it is fairly negligible since the data suggests only very very weak antiferromagnetic interactions. In the ChiT versus T plot, a little bump around 8K, which is likely to be a background problem is visible, and while it would normally have minimal effect, the interactions here are so weak that it is a dominant feature. The fit gives a Curie constant of 0.4 which fits well with the data (three Cu ions so 0.4 x 3 = 1.2) and an exchange constant of virtually zero, J = -0.33(4)K.

Figure 2.17 Graph of Chi x T Vs T for compound **2.3**

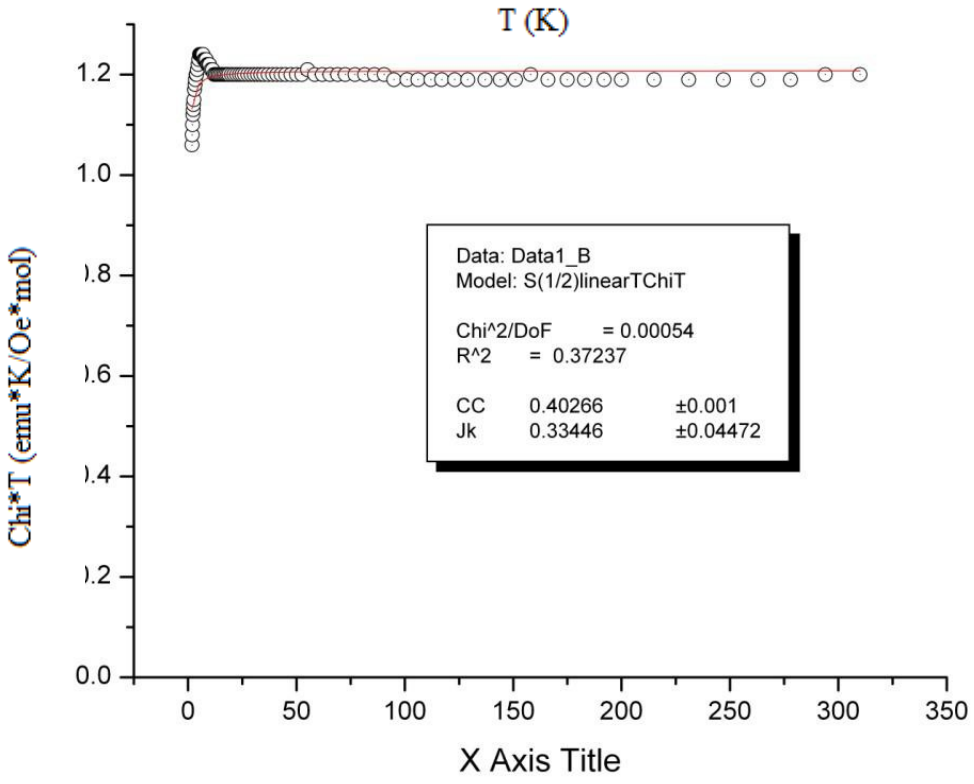

2.4 5-Amino-2-bromopyridine + CuCl2

Reaction of copper (ll) chloride with 2 equivalents of 5-amino-2-bromoopyridine in aqueous concentrated HCl gave $(5A2BP)_2CuBr_4$ (**2.4**). Single crystals suitable for X-ray diffraction were obtained by slow evaporation. This compound crystallises in the orthorhombic in the space group Cmca.

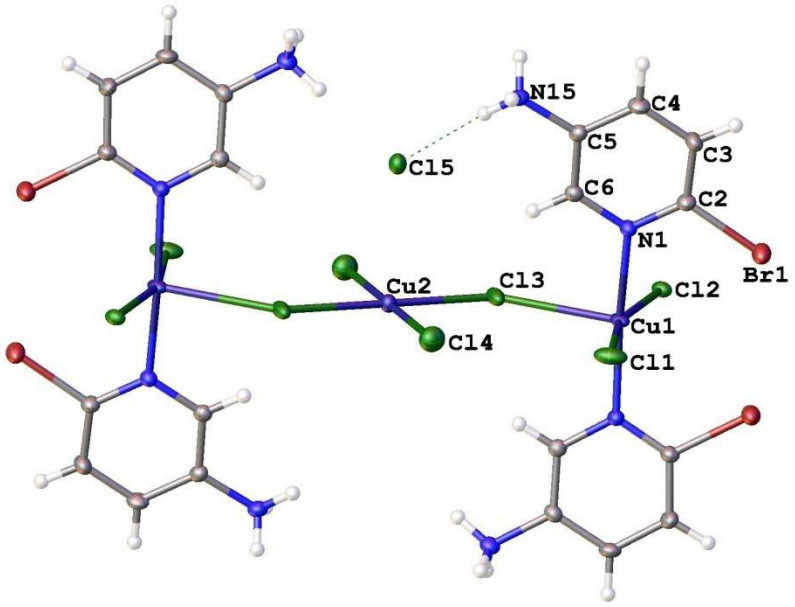

Figure 2.18 Molecular unit of compound **2.4**, shown with 50% probability thermal ellipsoids. The labelled atoms are those in the asymmetric unit. The unlabelled atoms are generated by symmetry using the grow command.

The structure of **2.4** is very similar to **2.3**. The molecular unit, figure 2.18 contains the same bridging tri copper moiety as the 5A2CP analogue. The angle Cu1-Cu2-Cu1 is 180° due to symmetry giving the chains an overall linear shape. The pyridine rings are almost perpendicular to the copper/chloride chain with the angle N1-Cu1-Cl3 being 93.00(12)° and a torsion angle of $177.60(4)^0$. Most of the Cu-Cl bond lengths are normal with an average length of 2.292(2)Å, with the exception of the bond Cu1-Cl3 which is longer than usual at 2.740(2)Å. The angle Cl1-Cu1-Cu2 is 162.12(9)°. The Cu2-Cl3-Cu1 angle is 137.67(10)°. There is a through space distance of 3.685(4)Å between Cl1 and Cl4 which is within the combined van der Waal's radii so it may be influencing the bent arrangement with respect to

the overall linear shape of the Cu/Cl chain. The orientation of the pyridine rings may be stabilised by a through space interaction of 3.5092(9)Å between the pairs of bromine atoms at each end of the copper chains. The interactions are within the sum of their van der Waals radii suggesting it may be a strong enough interaction to provide some structural stability. The pyridine rings attached to a single Cu are slightly angled towards each other with the N1-Cu1-N1 angle being 170.3(2)°. The central $CuCl_4$ is almost square planar with angles of 92.86(9)° and 87.14(9)° around the copper. Similarly to the 5A2CP analogue there is significant disorder of the central copper atom, with an occupancy of about 63%, with the occupancy spread over the same position in neighbouring molecules the remainder of the time. Cl4 is also disordered with an occupancy of approximately 85%.

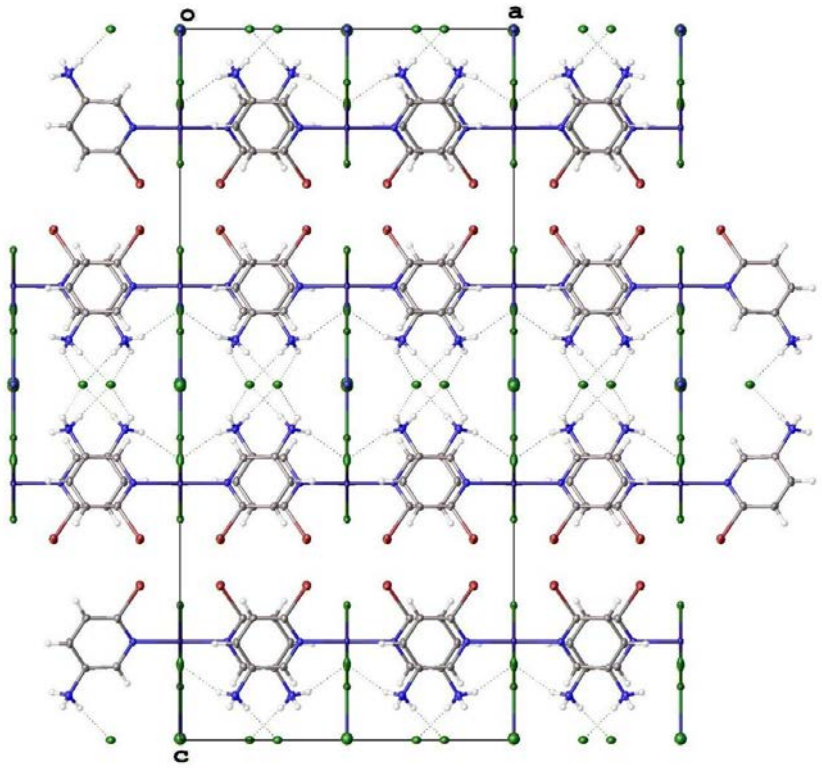

Figure 2.19 packing diagram of the ac-plane, shown with 50% probability thermal ellipsoids. Simialry to the 5A2CP analogue, the overlap of pyridine rings from neighbouring molecules can be seen.

As can be seen in a packing diagram along the ac plane (figure 2.19) staggered layers of the tri-copper units are formed. This staggering leads to what looks like pairs of bromines pointing towards each other. There may be a bromine···bromine interaction between opposite "pairs" with the Br1···Br1 through space distance of 4.4471(6)Å; however the distance of 3.5193(14)Å between Br1 and the Cl2 opposite is likely to have a more significant effect on these layers that are formed. "Pairs" of amino groups also form layers similar to the "pairs" of bromines with free chloride ions in between the pairs.

In figure 2.20 it can be seen that π stacking may play a significant role holding the "sheets" together with the centroids of the above and below pyridines being 3.979Å with small offsets of 1.75Å and 1.55Å for the top and bottom interactions, respectively.

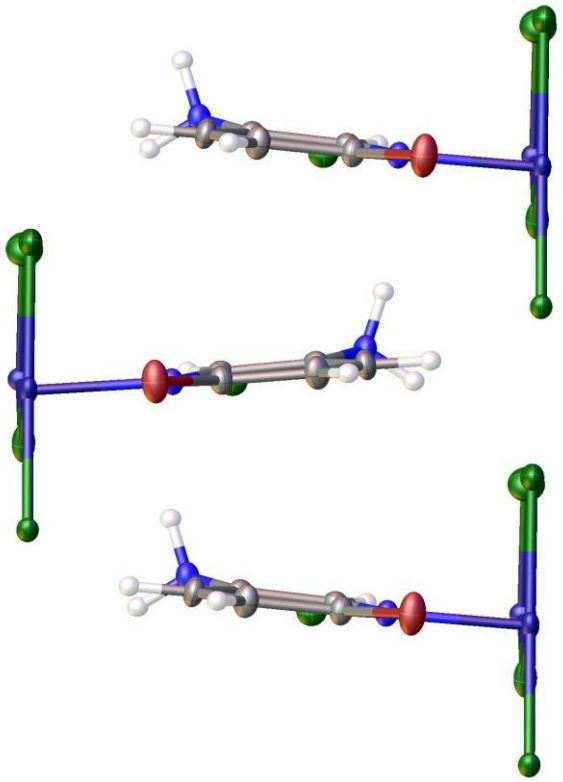

Figure 2.20 view of the possible π-stacking interactions between the overlapping pyridine rings of adjacent molecules.

The non-coordinated chloride ions that can be seen are held in place through hydrogen bonding from the four different pyridine amides. Hydrogen bonding plays a large role in the stability of the structure, as can be seen by all the dashed lines in figure 2.21 representing hydrogen bonding interactions. Details of these interactions are summarised below in table 2.6.

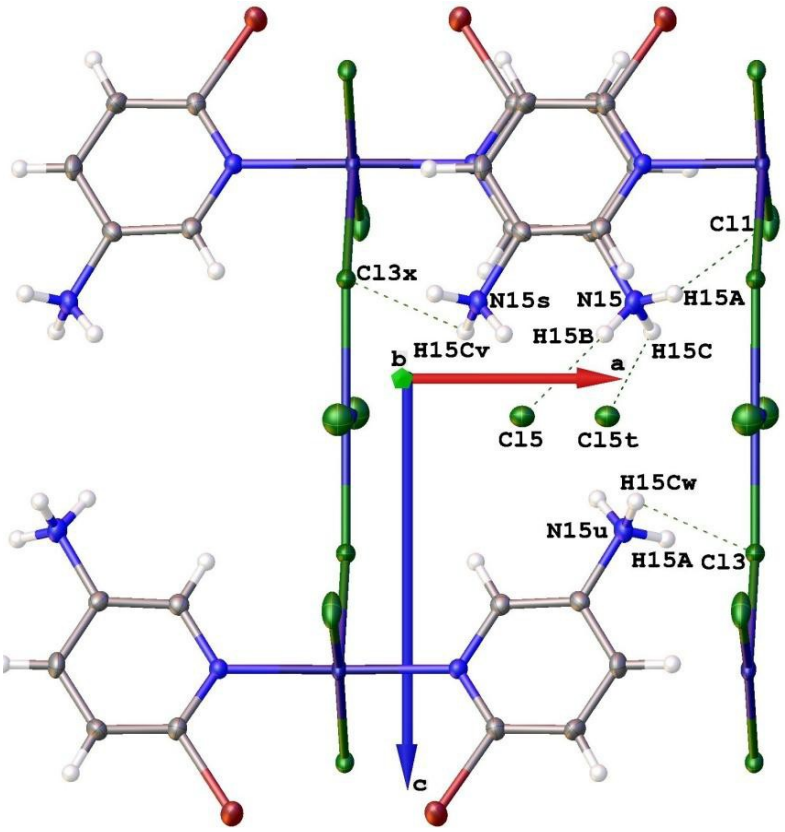

Figure 2.21 Hydrogen bonding interactions in compound **2.4.**

Similarly to compound **2.3**, hydrogen bonding interactions in **2.4** compliment the π stacking interactions in stabilising the crystal packing. As can be seen above in figure 2.21, the interactions are between the aminic hydrogen atoms and chlorine atoms of neighbouring tri copper chains, or to non coordinating chloride ions.

Table 2.6 Table of hydrogen bonding interactions for compound **2.4.**

D-H...A	d(H...A)	d(D...A)	<(DHA)	Symmetry Op.
N15-H15A...Cl1	2.34(2)	3.151(4)	159(3)	[x+1/2, y+1/2, z]
N15-H15B...Cl5	2.218(19)	3.092(4)	173(4)	
N15-H15C...Cl5	2.37(6)	3.160(4)	142(4)	[-x+3/2, -y+1/2, -z+1]
N15-H15C...Cl3	2.89(6)	3.475(4)	121(4)	[x+1/2, y-1/2, z]

2.5 5-amino-2-iodopyridne + CuCl2

Slow evaporation of an aqueous solution of 2 equivalents of 5-amino-2-iodopyridine with copper(II) chloride in concentrated HCl resulted in crystals of 2(5A2IPH).CuO_2Cl_4 (**2.5**) which pack into the triclinic spacegroup P-1. From the asymmetric unit (figure2.22) it can be seen that there are obvious differences when compared to the more common motif of two protonated cations and a single tetrahalocuprate anion. A similar result had been seen previously in three unreported structures partially refined by Mark Turnbull.[40]

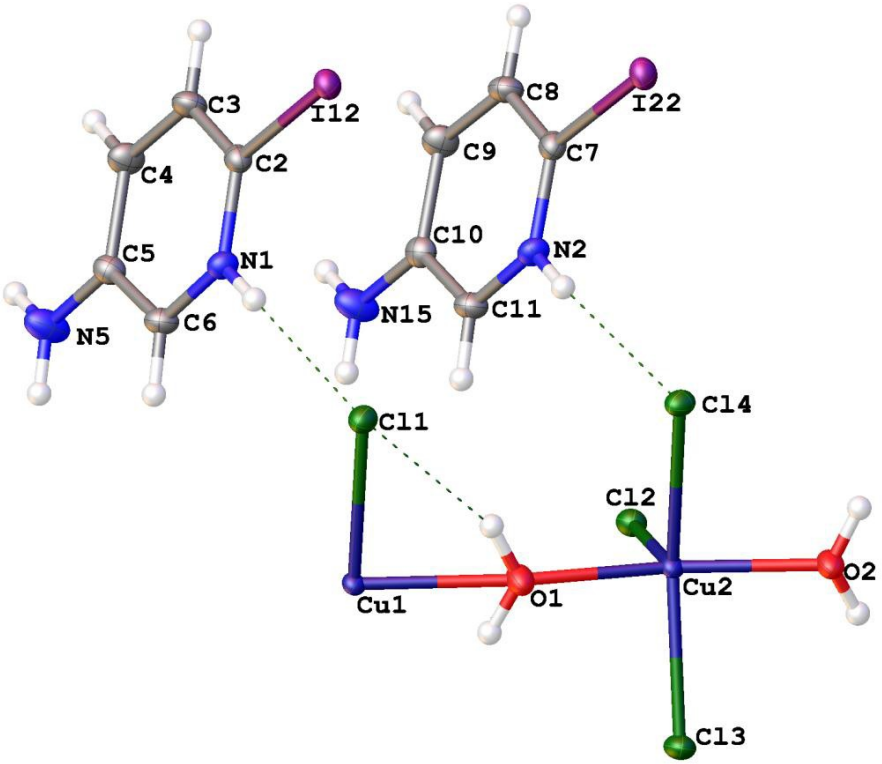

Figure 2.22 Asymmetric unit of compound **2.5**. It is easily seen that the structure differs from the more common motif of two cations to a single tetrahalocuprate anion.

Elucidation of all these structures has been elusive until recently. Prof Geoff Jameson at Massey University is to thank for solving this puzzle.

The following figures (2.23 and 2.24) are made from a search of Cu-OH_2-Cu and Cu-O-Cu bond angles from the Cambridge Structural database[43]. They show that there are other reported structures with similar angles for the Cu-OH2-Cu motif but not the Cu-O-Cu motif.

Figure 2.23 Histogram of Cu-OH_2-Cu bond angles .

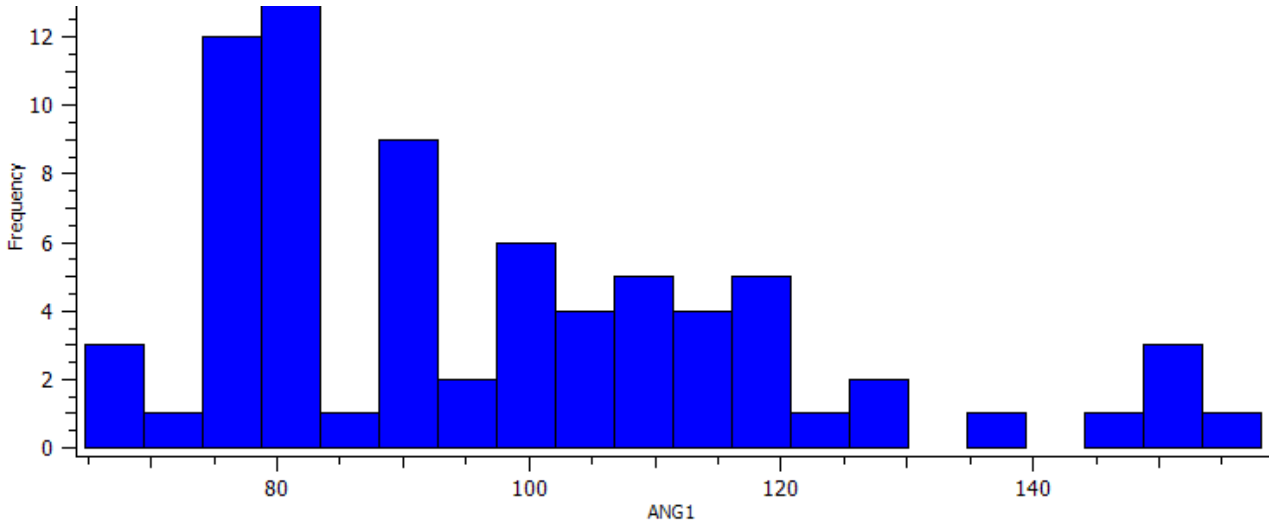

Angle (^{o})

Figure 2.24 Histogram of Cu-O-Cu bond angles.

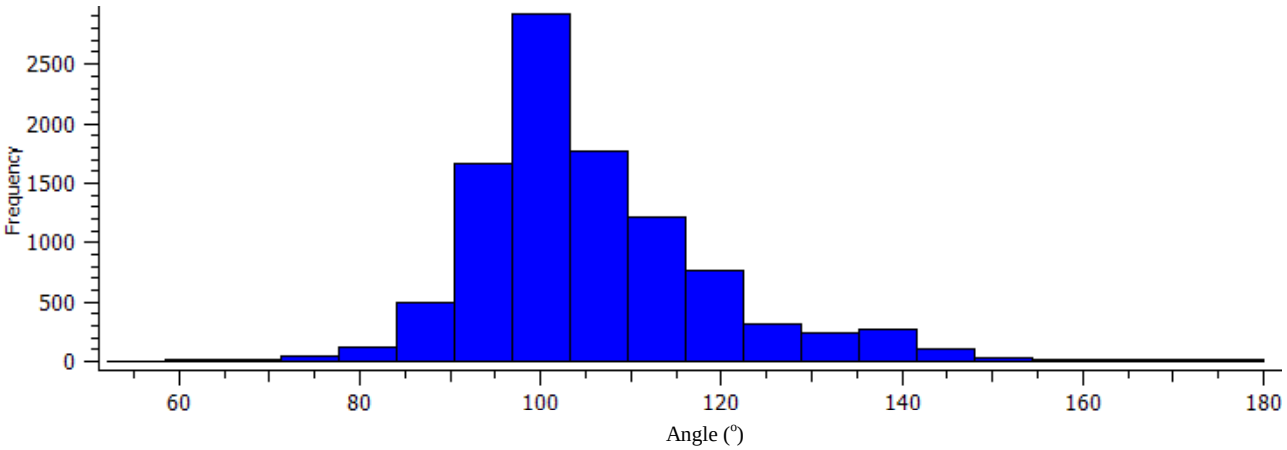

Angle (^{o})

Chains of oxygen bridged copper chloride chains are formed (figure 2.25). Both Cu-OH_2-Cu angles are large for this type of structure (figures 2.23 and 2.24). The angles are Cu1-O1-Cu2, 168.53(16)° and Cu2-O2-Cu1, 166.17(16)°. Hydrogen bonding from the bridging waters may be stabilising the large angle. Details of the interactions are in table 2.6.

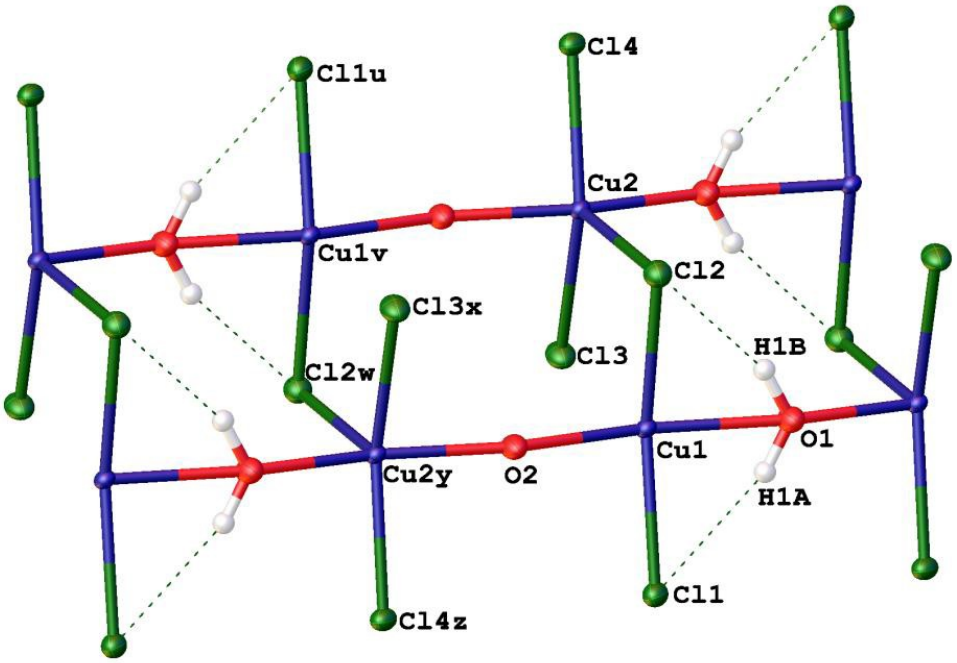

Figure 2.25 Closeup of the copper chloride chains in compound **2.5.** Dashed lines represent hydrogen bonding interactions

There is a large amount of disorder of the copper atoms in the chains with Cu1 having an occupancy of 15%, and 85% for Cu2. This means when Cu1 is there, Cu2 is not, and vice versa. The copper-chlorine bond lengths are normal with an average of 2.2983(9)Å, with the exception of the Cu2-Cl2 bond which is significantly longer at 2.5814(9)Å. The outer chlorines are angled slightly outwards with the angles Cl1-Cu1-Cl2, 164.16(12)° and Cl3-Cu2-Cl4, 158.69(4)°. The chains are almost square with the bridging chlorine angle Cu1-Cl2-Cu2 being 89.02(7)°.

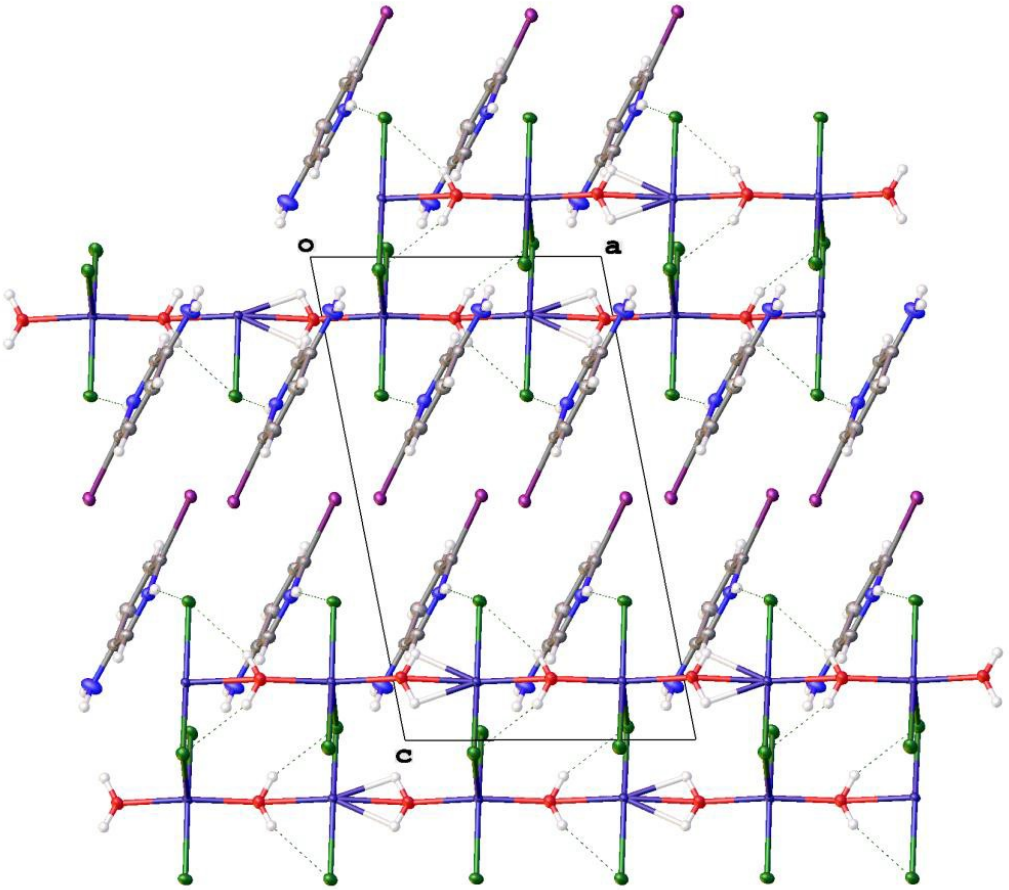

Figure 2.26 Packing diagram of the ac plane of **2.5**, shown with 50% probability thermal ellipsoids.

Compound **2.5** crystallises into isolated layers of pyridine cations and copper chloride chains which run along the a-axis. The packing is in an ABBA type arrangement with double layers of cations and single anion layers (figure 2.26). The pyridines alternate orientation within the double cation layers with the iodine atoms facing away from the chains, and towards the iodine of the other cations in the double layers. The plane of the cations is nearly perpendicular to the ac-plane.

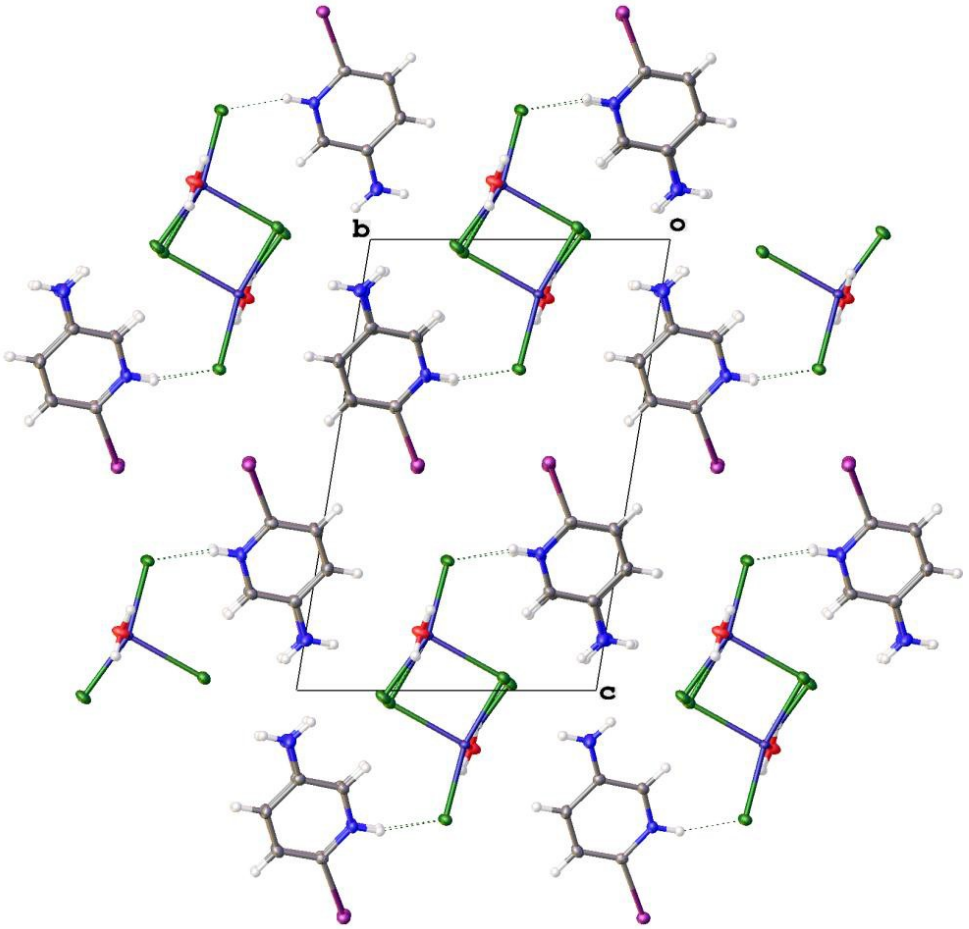

Figure 2.27 Packing diagram of the bc-plane of **2.5**, shown with 50% probability thermal ellipsoids.

A packing diagram of the bc-plane (figure 2.27) shows that hydrogen bonding may be a large contributor to the structural stability of crystals of compound **2.5** (figure 2.28) with the pyridine nitrogens hydrogen bonding to the exterior chlorines of the copper chains being the strongest interaction (average d(H...A), 2.2906(8)Å). The amino groups are also involved in slightly weaker hydrogen bonding interactions with the copper bridged chlorines of the chains (average d(H...A), 2.6257(9)Å). Each hydrogen is interacting with a different neighbouring chain. The combination of the amino and pyridic hydrogen bonding leads to the amino groups of two different cations facing each other, protruding into the anion chain layers (figure 2.25).

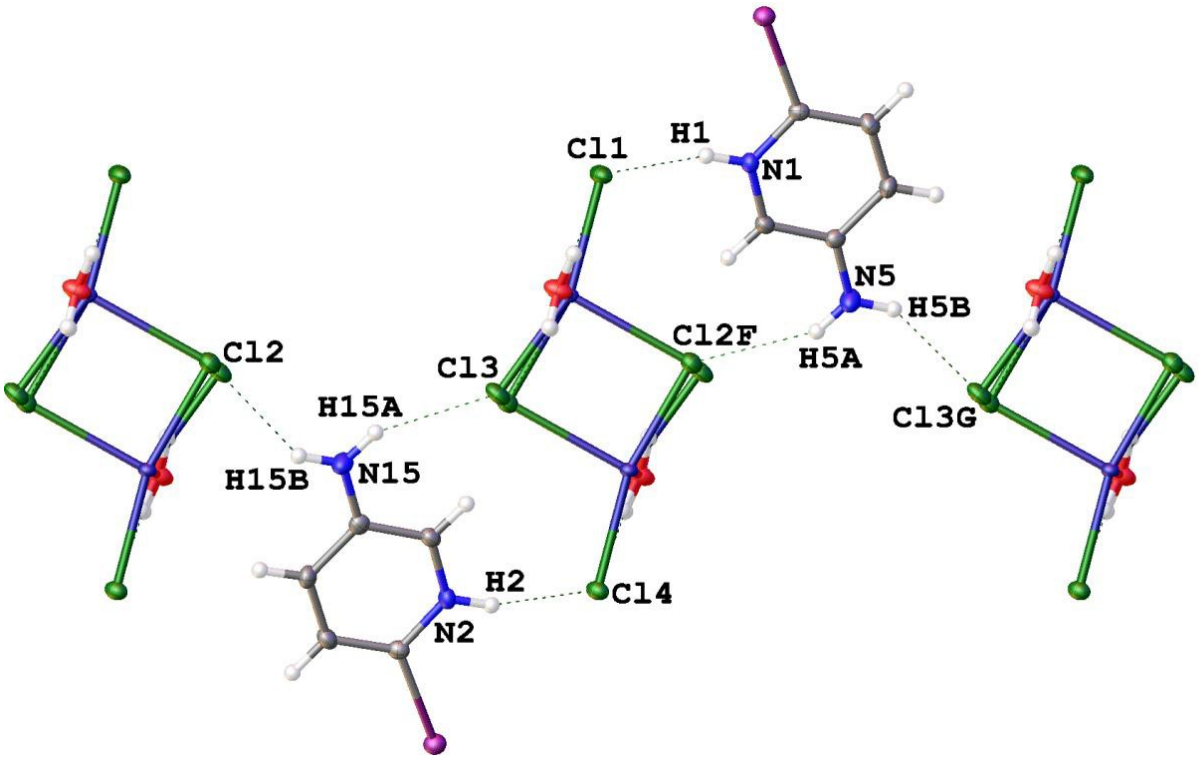

Figure 2.28 Details of the nitrogen donor hydrogen bonding interactions in compound **2.5**. The hydrogen bond interactions are represented by the dashed lines.

Details of the extensive hydrogen bonding interactions in 2.5 are shown in table 2.7. The hydrogen atoms are all in calculated positions.

Table 2.7 Table of hydrogen bonding interactions in compound **2.5.**

D-H...A	d(H...A)	d(D...A)	<(DHA)	Symmetry Op.
N1-H1...Cl1	2.2675(8)	3.085(3)	158.70(18)	
N2-H2...Cl4	2.3136(8)	3.129(3)	158.28(18)	
N5-H5A...Cl2	2.5621(8)	3.341(3)	151.1(2)	[x-1, y, z]
N5-H5B...Cl3	2.6608(9)	3.410(3)	146.3(2)	[x-1, y-1, z]
N15-H15A...Cl3	2.5128(8)	3.310(3)	154.5(2)	[-x+1, -y+1, -z+2]
N15-H15B...Cl2	2.7671(8)	3.499(3)	143.98(19)	[-x+1, -y, -z+2]
O1-H1A...Cl1	2.302(13)	3.071(2)	159(3)	
O1-H1B...Cl2	2.340(15)	3.100(2)	156(3)	[-x+1, -y+1, -z+2]
O2-H2A...Cl2	2.339(15)	3.106(2)	157(3)	[-x+2, -y+1, -z+2]
O2-H2B...Cl1	2.346(12)	3.113(2)	158(2)	[x+1, y, z]

Magnetic data showed that there is no magnetic exchange, within experimental error, in this compound.

2.6 Conclusions

The study of the 5A2SP family as shown that simply swapping the position of the S and amino substituents has had a large effect on the resulting structures of the formed tetrahalocuprates when compared to the previously reported 2A5SP analogues, which all had formed the common structural motif of two unbound, protonated pyridines to one discrete tetrahalocuprate anion.

The 5A2SP series has given some fascinating results, with four different structural types; (1) The usual two isolated cations to one tetrahalocuprate ion, (2) substituted tricopper halide chains, (3) extra substitution of the pyridine ring from unintended experimental conditions and (4) water bridged copper chloride chains for the iodo substituted complex.

The tetrabromocuprates turned out to be very challenging but gave further interesting results. There were unexpected solubility issues when synthesising the tetrabromocuprates making it very difficult to obtain crystals containing the copper bromide. In many cases only the cations crystallised. Many different solvents and crystallising techniques were tried with similar unsuccessful results. There were also multiple instances where again the tetrabromocuprate complexes were not made, but the pyridine was brominated in the 6 position.

Both 5A2BP and 5A2CP when reacted with $CuCl_2$ formed unusual discrete tri-copper chains with two pyridines bound through the nitrogen, to each terminal copper of the chain. From the magnetic data of the 5A2CP compound it may be a reasonable assumption that the 5A2BP compound is likely to have similar very weak antiferromagnetic interactions, as it has a very similar crystal structure to the 5A2CP compound.

The surprises did not cease within this family of compounds, with the iodo substituted pyridine giving interesting results. This was not isolated to 5A2IP.CuCl4 as a similar result was found with the 2-amino analogue from unpublished work by Jan Wikaira. Mark Turnbull also had a similar result many years earlier using the same 2A5IP cation.

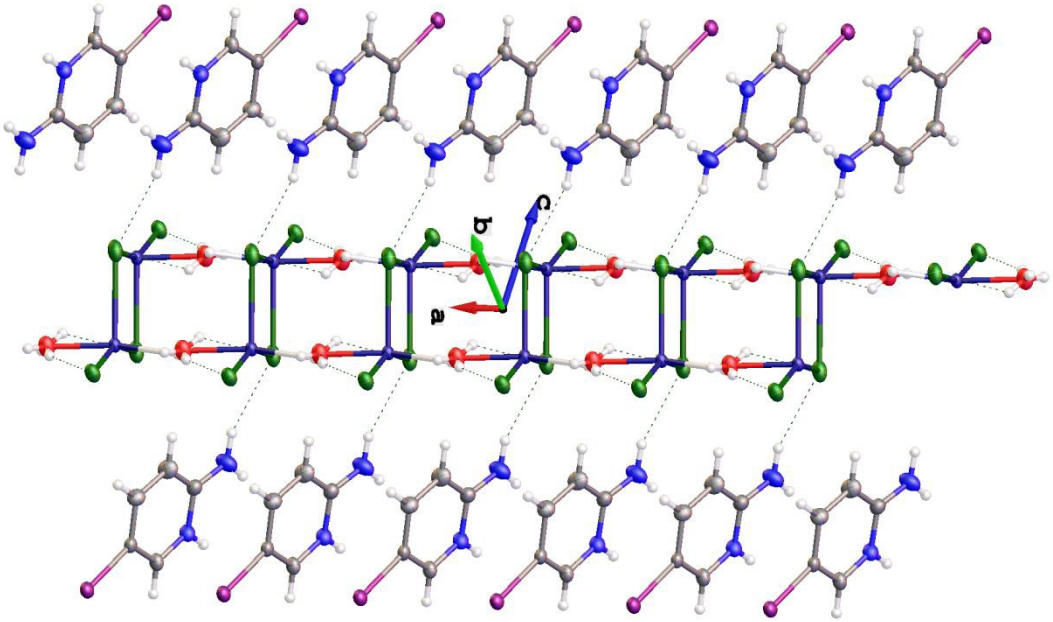

Figure 2.26 View of a single copper chain running parallel to the a-axis

Similarly to Turnbulls 2-amino complex, magnetic data showed that the 5-amino complex has no magnetic interactions within experimental error.

This week another similar iodo structure has been communicated to me, in this case using 3-iodopyridine[44].

Chapter 3

Dimethylpyridinium (DMPY) mixed halogen tetrahalocuprates

3.1 Introduction

The interest in mixed halide, dimethylpyridine systems has been outlined in chapter 1. As can be seen in figure 3.1, the different isomers of dimethylpyridine provide a range of different geometries without greatly changing the hydrogen bonding or electronic properties of the cation. This minimises variables and may give some insight on how much the cation geometry influences the geometry of the cuprate anion, and the overall packing of the crystal lattice.

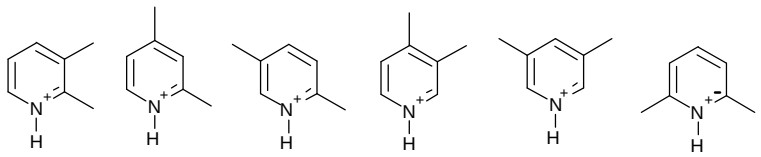

Figure 3.1

A general reaction scheme for the preparation of these compounds can be written as:

$$\mathbf{2dmpy + CuX_2 + 2HX \longrightarrow (dmpyH)_2 + CuX_4^{2-}}$$

Scheme 3.1

where X = Cl and/or Br, and dmpy = dimethylpyridine. The percentage of Cl to Br applies to both the CuX_2 salt and its corresponding acid. For each dmpy isomer, the ratios of 0:100, 5:95, 25:75, 50:50, 75:25, 95:5 and 100:0 Cl to Br were be used.

Synthesising, the mixed halide tetrahalocuprates followed the general method of making tetrahalocuprates, i.e. using a reaction mixture of a 2:1 molar ratio of organic molecule to CuX_2. Acid is added to, a) protonate the organic molecule to form the cations, and b) provide the extra halide ions needed to form the tetrahalocuprates. The only variation of the preparation of mixed halide tetrahalocuprates is the combination of $CuCl_2$ and $CuBr_2$ used to make up the $Cu(II)X_2$ portion of the reaction mixture. This is where the ratios of Cl to Br were applied. The same ratios were applied to the acids to keep the relative amount of the acid and its corresponding metal salt the same.

When refining the crystal structures of the compounds which contained mixed halides on a single position were found by setting the halogen occupancy to free. This showed whether it was a mixed halide or not. If the atom was found to be a mixed halide, the EADP and EXYZ commands were used in the .ins file to constrain the atom to the same position and fix the thermal parameter size. The occupancy percentage of bromide to chloride was found by putting a 1 on the FVAR line for each halogen pair. The Br % values in the compound tables at the start of each section are representative of these values. The copper-halide bond lengths increased as the bromine percentage increased, suggesting that they were representative of the mixed halide-copper bond length. There is likely to be a considerable amount of error in this method as it is fixing the thermal parameter and position of the atoms. The error could be as much as 5%, and further experiments such as Cl/Br elemental analysis would be needed to give a more accurate result. With disruptions from many high magnitude earthquakes, and the cost involved these were not able to be undertaken. With this taken into consideration, the trends can still be analysed using the estimated values.

Throughout this chapter the anion trans angles are often referred to as an indicator of structural changes between two compounds. The trans angles are defined as the two largest halide - Cu - halide angles of a single tetrahalocuprate.

3.2 2,4-dimethylpyridinium mixed halogen tetrahalocuprates

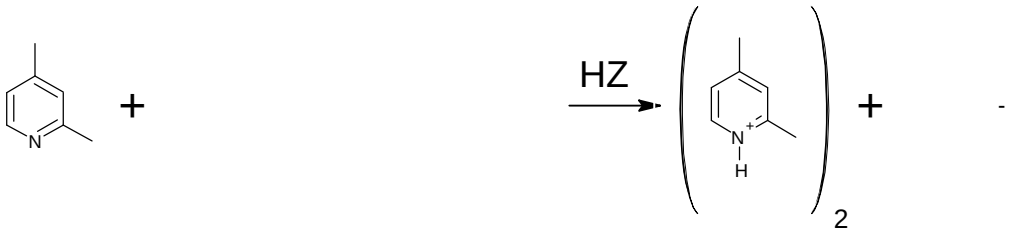

Scheme 3.2

Reaction of 2,4-dimethylpyridine with HX and CuX_2 (X=Cl and/or Br) in aqueous solution gave salts $(2,4\text{-dmpyH})_2CuX_4$. Crystals suitable for single crystal x-ray diffraction were grown by slow evaporation of the aqueous solution. Seven complexes (**3.21**-**3.27**) were prepared with ratios of 0, 5, 25, 50, 75, 95 and 100 of X = Br : Cl, with the ratio applied to the CuX_2 salt and its corresponding acid, as shown in scheme 3.2. All complexes crystallised in the monoclinic spacegroup C2/c. Comparisons of structural features of interest are shown in tables **3.1** and **3.2.**

Table 3.1 Crystallographic features of interest of compounds **3.21**-**3.27**. The interlayer and intralayer contacts are the shortest halide...halide through space interactions.

Compound (Br ratio)	Space group	Cell Volume (Å^3)	Intralayer Contact (Å)	Interlayer Contact (Å)
3.21 (0)	C2/c	1843.2(6)	5.402(1)	5.3606(10)
3.22 (5)	C2/c	1864.91(16)	5.3551(6)	5.3515(4)
3.23 (25)	C2/c	1932.46(18)	5.3983(4)	6.1630(7)
3.24 (50)	C2/c	1931.89(15)	5.4104(4)	6.1627(6)
3.25 (75)	C2/c	1983.18(15)	5.5554(4)	6.1757(6)
3.26 (95)	C2/c	1994.75(15)	5.5722(4)	6.5416(4)
3.27 (100)	C2/c	2001.87(13)	5.3248(5)	5.6312(5)

Table 3.2 Anion structural features of compounds **3.21**-**3.27**

Compound (Br)	Br % of halides *		Trans Angles (°)		Average Cu-X bond length (Å)
	X1	X2			
3.21 (0)	0	0	129.489(2)	133.533(19)	2.2460(4)
3.22 (5)	30.4	18.1	129.92(10)	133.237(19)	2.3400(4)
3.23 (25)	76.8	49.5	129.95(3)	132.39(2)	2.3400(3)
3.24 (50)	68.9	41.2	129.90(2)	132.36(2)	2.3420(4)
3.25 (75)	97.5	100	128.6999(17)	132.310(17)	2.3760(2)
3.26 (95)	100	100	128.61(2)	132.36(2)	2.3810(3)
3.27 (100)	100	100	130.41(3)	130.79(3)	2.3875(4)

* X1 and X2 are the two different halogen atoms present in the asymmetric unit of the crystal structures, where X1 is assigned as the halogen with the largest Br %. The other two halogens of the tetrahalocuprates are related by symmetry so therefore the same as X1 and X2.

As can be seen from tables 3.1 and 3.2 most of the structures are very similar. The two compounds with the greatest differences are those arising from 0 Br, **3.21** and 100 Br, **3.27** in the preparation. These will be discussed in more detail to highlight any structural differences.

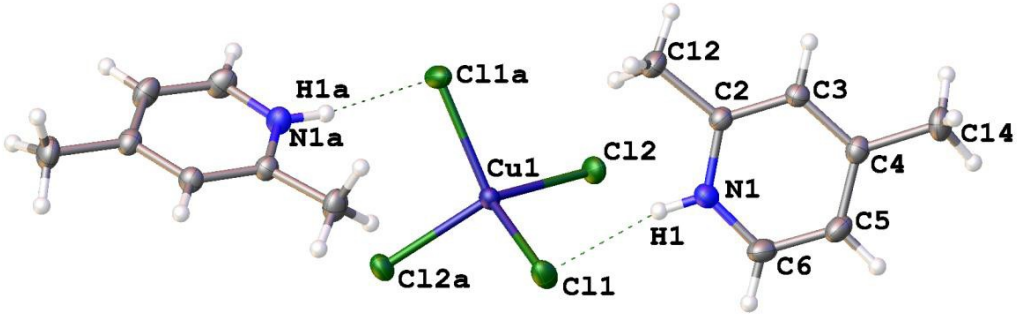

Figure 3.2 Molecular unit of $(2,4\text{-dmpyH})_2CuCl_4$, **(3.21)**, shown with 50% probability thermal ellipsoids

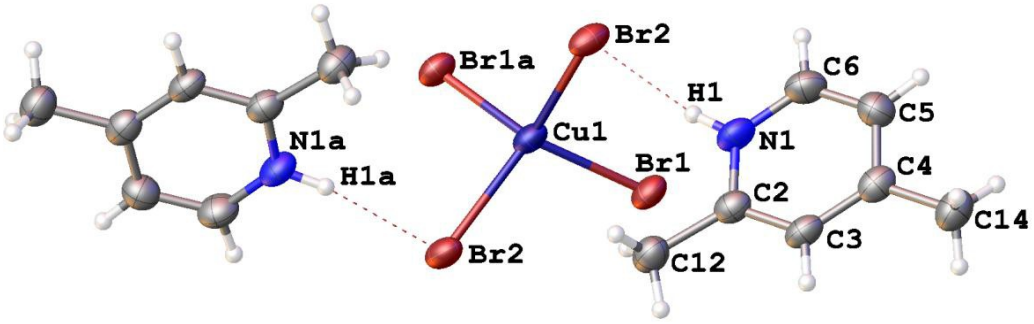

Figure 3.3 Molecular unit of $(2,4\text{-dmpyH})_2CuBr_4$, **(3.27)** shown with 50% probability thermal ellipsoids

The molecular units of **3.21** and **3.27**, figures 3.2 and 3.3, contain two pyridinium cations and a CuX_4^{2-} anion, as expected from the molar ratio of the preparation. For both compounds the asymmetric unit contains a single pyridinium cation and half a tetrahalocuprate anion. The remaining unlabelled atoms are generated by symmetry. Although they both have the same unit cell contents these are in different orientations. The average anion Cu-Cl bond length in **3.21** is 2.2460(4)Å, and the average Cu-Br bond length in (**3.27**) is 2.3876(4)Å. The Cu-X

bond lengths are comparable to the reported 2,6-dmpyH analogues[31]. The anion trans angles are 129.489(2)° and 133.533(19)°, 130.41(3)° and 130.79(3)° for **3.21** and **3.27,** respectively. These trans angles indicate the $CuBr_4$ anion distortion is much more symmetric than that of the $CuCl_4$ anions. Compared to the 3,4-dmpy (**section 3.3**) and 3,5-dmpy (**section 3.4**) isomers in this study the mean trans angle of **3.21** is much smaller than both, however in **3.27** it is smaller than the 3,4 analogue but similar to the 3,5 analogue The structures of both **3.21** and **3.27** are stabilised through hydrogen bonding between the protonated pyridinium nitrogen and a single halide of the anion. No other hydrogen bonding interactions occur in either structure. Full details of the hydrogen interactions can be seen in table **3.3**

Table 3.3 Details of Hydrogen bonding interactions in compounds **3.21** and **3.27**

Compound	D-H···A	d(H···A)	d(D···A)	<(DHA)
$(2,4\text{-dmpyH})_2CuCl_4$	N1-H1...Cl1	2.2600(5)	3.1077(11)	168.63(7)
$(2,4\text{-dmpyH})_2CuBr_4$	N1-H1...Br2	2.3065(3)	3.158(3)	170.4(2)

The structure of **3.21** can be described as alternating layers of cations and CuX_4^{2-} anions running across the ac-plane with the anion and cation layers parallel to the diagonal of the *ac*-plane (figure 3.4). Complex **3.27** also packs into alternating layers of anions and cations, however the difference with respect to the packing view of the ac-plane, figure 3.5, is the layers run parallel to the c-axis, rather than the diagonal, as seen in **3.21.** For both structures the cations within a single layer alternate orientation as a result of the pyridine nitrogen hydrogen bonding to the halides of the anions.

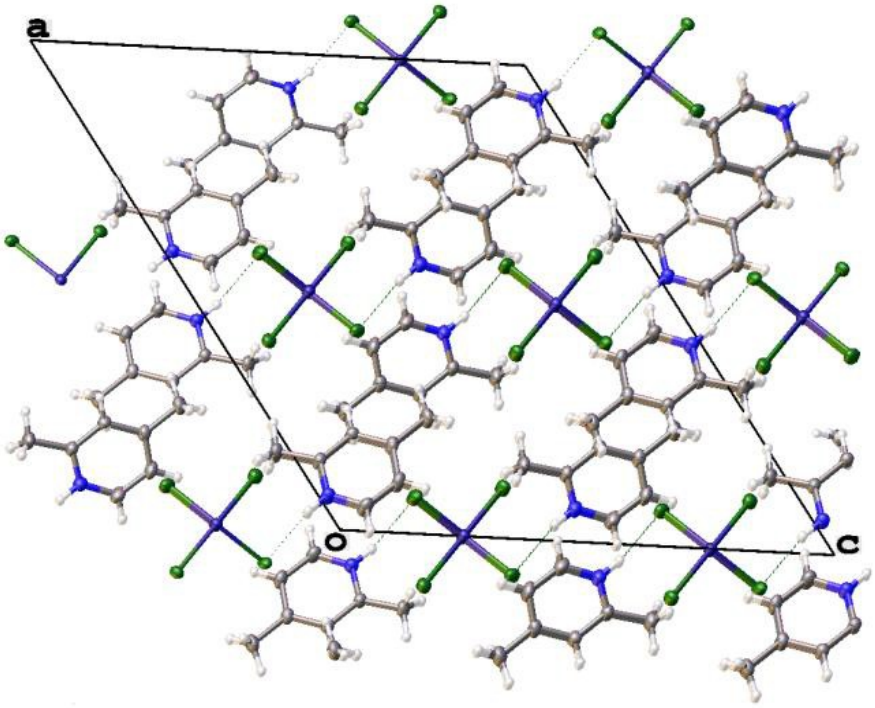

Figure 3.4 Packing diagram of *ac*-plane of $(2,4\text{-dmpyH})_2CuCl_4$ shown with 50% probability thermal ellipsoids. The diagrams show the separate anion and cation layers parallel to the diagonal of the ac-plane.

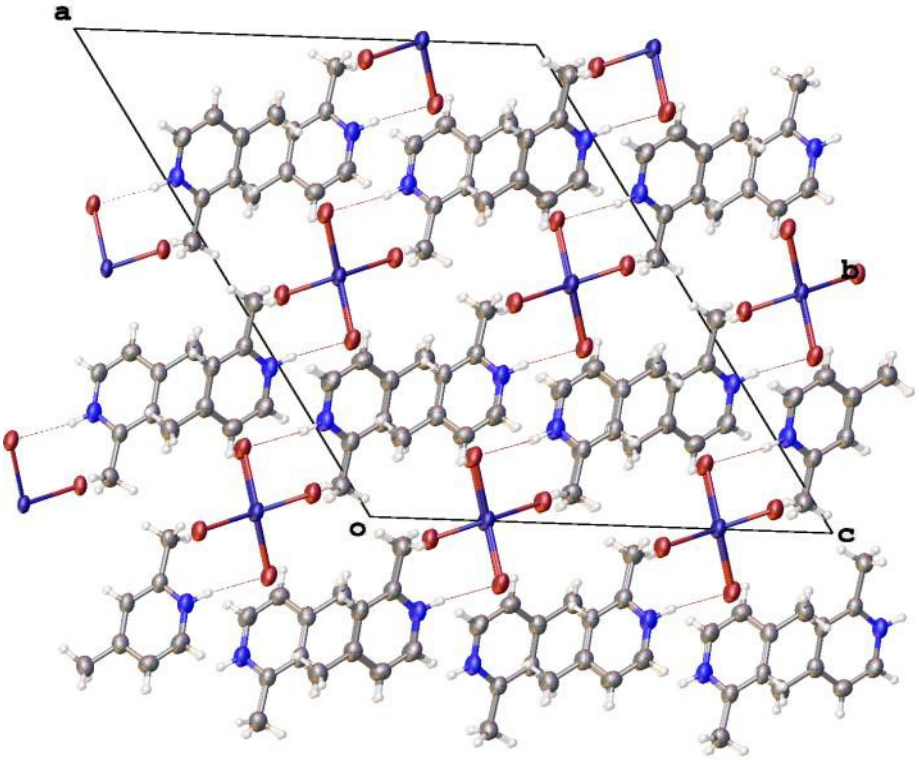

Figure 3.5 Packing diagram of *ac*-plane $(2,4\text{-dmpyH})_2CuBr_4$ shown with 50% probability thermal ellipsoids. The diagrams show the separate anion and cation layers running parallel to the c-axis.

The different packing orientation seen in the ac-plane diagrams, figures 3.4 and 3.5, can be clearly seen when looking at packing diagrams of the ab-plane of both **3.21** and **3.27** as shown in figures 3.6 and 3.7. The angle between the planes of the pyridine rings is very similar for both compounds, with angles of 55.49(6)° and 56.15(15)° for **3.21** and **3.27**, respectively. The slight staggering of the anions within the anion layers leads to the alternating pyridine orientations. This arises from the pyridinium hydrogen bonding and the steric bulk of the methyl groups forcing the rings apart.

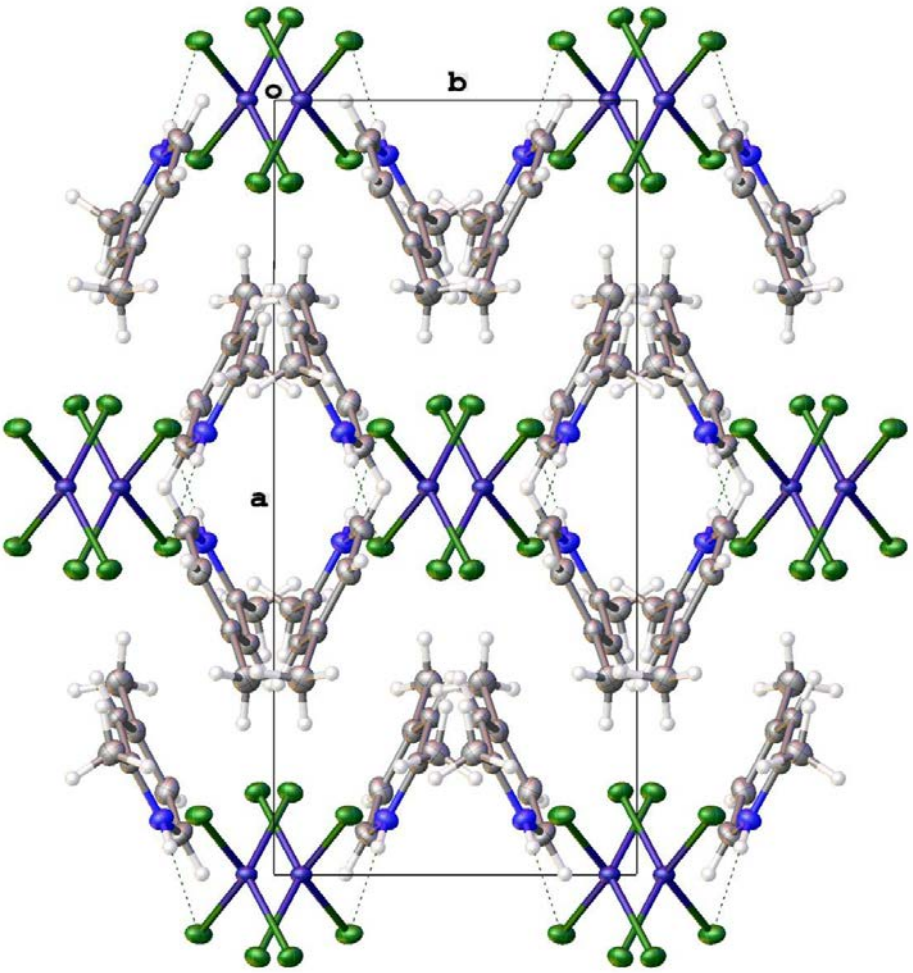

Figure 3.6 Packing diagram of *ab*-plane of **3.21** shown with 50% probability thermal ellipsoids. The angle between the planes of the adjacent pyridine rings can clearly be seen

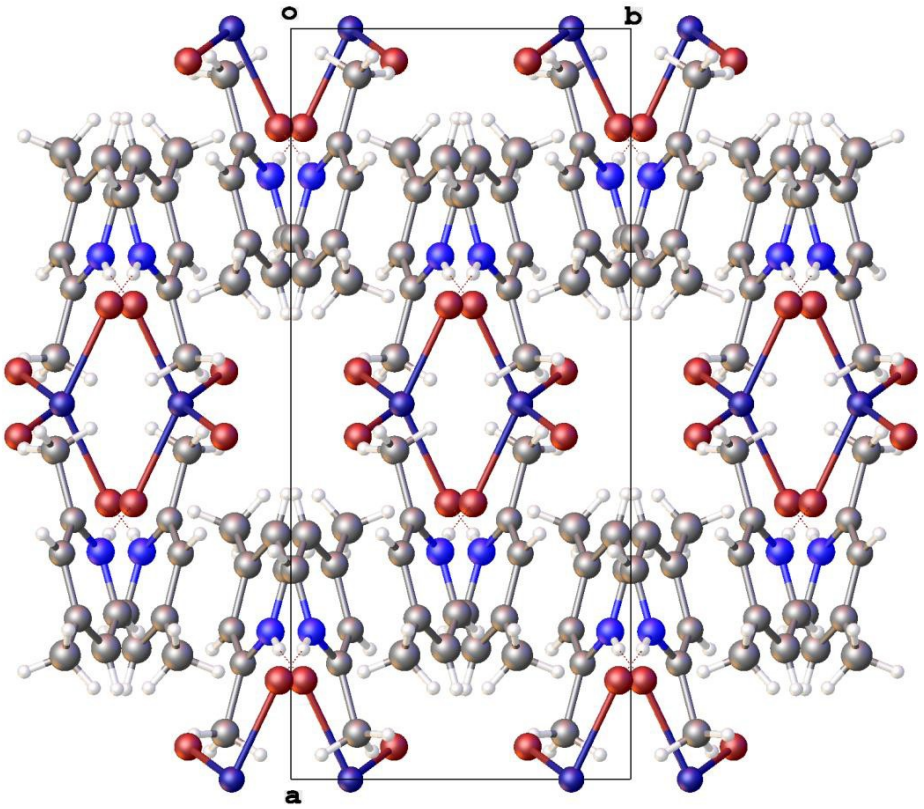

Figure 3.7 Packing diagram of *ab*-plane of **3.27** shown with 50% probability thermal ellipsoids. Similarly to 3.21 this view emphasises the angle between the planes of the alternating cations within a single cation layer

Having a methyl group next to the nitrogen (2 position) in the pyridine ring leads to greater anion separation than the 3,4 analogues where the methyl groups are adjacent on the ring. Being adjacent to the hydrogen bonding pyridinium nitrogen means the methyl group sits between the halides of neighbouring anions leading to the greater separation (figure 3.8). This can be seen by looking at the halo¨halo interactions. The shortest inter and intra-layer contacts for **3.21** are 5.402(1)Å and 5.3606(10)Å, and 5.3248(5)Å and 5.6312(5)Å for **3.27**. For both compounds these are significantly (more than 1Å) larger than their 3,4 dmpyH counterparts.

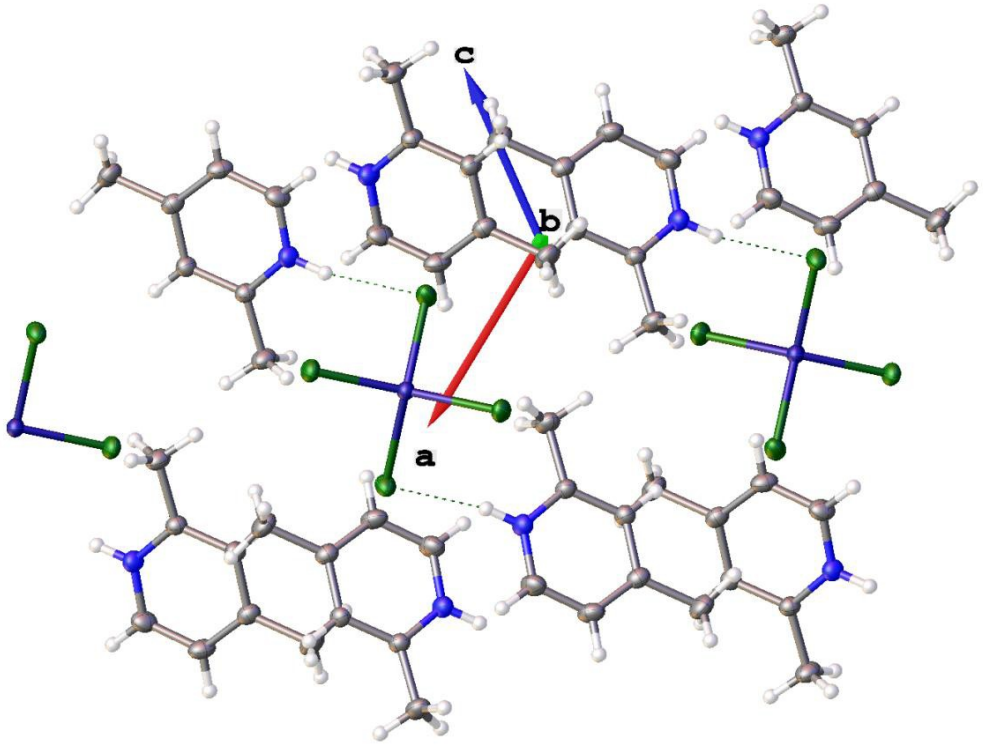

Figure 3.8 Packing diagram of the ac-plane of **3.21** shown with 50% probability thermal ellipsoids. The insertion of the methyl substituents into the anion layer can be seen.

There is unlikely to be any significant magnetic exchange pathways in any of the 2,4 dmpy compounds as all of the halide···halide interaction distances are over 4.5Å[31]. This is likely to be due to there being a methyl group adjacent to the hydrogen bonding nitrogen on the pyridine ring. As the pyridinium nitrogen is hydrogen bonded to halides of the anions, having a methyl group on the adjacent carbon will lead to greater anion separation as it will protrude further into the anion layers compared to the 3,4 and 3,5 isomers.

The compounds which contain mixed halide tetrahalocuprates are isostructural with the single halide compound which has the same trans angle pairs. The changes in structure occur as a slow transition where subtle changes occur in the anion trans angle pairs.

3.3 3,5-dimethylpyridinium mixed halogen tetrahalocuprates

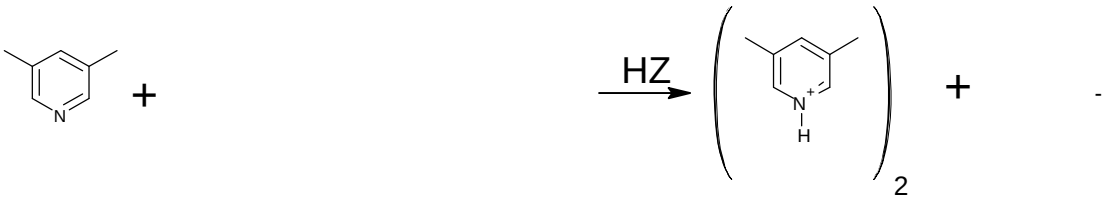

Scheme 3.3

Reaction of 3,5-dimethylpyridine with HX and CuX_2 (X=Cl and/or Br) in aqueous solution gave $(3,5\text{-dmpyH})_2CuX_4$ salts. Crystals suitable for single crystal x-ray diffraction were grown by slow evaporation of an aqueous solution. Seven complexes were made with ratios of 0, 5, 25, 50, 75, 95 and 100 of X = Br to Cl, where the ratio applied to the CuX_2 salt and its corresponding acid, as shown in scheme 3.3. All complexes crystallised in the monoclinic spacegroup C2/c. Comparison of structural features of interest are shown in tables **3.4** and **3.5**

Table 3.4 Crystallographic features of interest of compounds **3.31-3.37**. The interlayer and intralayer contacts are the shortest halide...halide through space interactions between anion halogens.

Compound (Br)	Space group	Cell Volume (Å^3)	Intralayer Contact (Å)	Interlayer Contact (Å)
3.31 (0)	C2/c	1822.37(18)	3.9873(8)	4.6396(8)
3.32 (5)	C2/c	1832.18(10)	3.9893(7)	4.5652(6)
3.33 (25)	C2/c	1901.41(11)	4.0541(5)	4.4821(3)
3.34 (50)	C2/c	1984.62(12)	6.0799(4)	5.1362(3)
3.35 (75)	C2/c	1986.50(11)	6.1036(7)	5.1164(4)
3.36 (95)	C2/c	2006.82(19)	6.1183(7)	5.1355(7)
3.37 (100)	C2/c	2009.95(10)	6.1182(7)	5.1389(5)

Table 3.5 Anion structural features of compounds **3.31-3.37**

Compound (Br %)	Br % of halides * X1	X2	Trans Angles (°)		Average Cu-X bond length (Å)
3.31 (0)	0	0	133.85(2)	139.11(3)	2.2487(4)
3.32 (5)	18.5	5.3	133.88(2)	139.43(2)	2.2780(3)
3.33 (25)	83.1	44.8	133.54(2)	138.600(16)	2.3462(2)
3.34 (50)	92.4	88.7	123.617(18)	135.74(2)	2.3759(3)
3.35 (75)	100	100	123.47(2)	135.62(3)	2.3789(4)
3.36 (95)	100	100	123.45(3)	135.50(4)	2.3841(5)
3.37 (100)	100	100	123.44(2)	135.52(3)	2.3854(4)

* X1 and X2 are the two different halogen atoms present in the asymmetric unit of the crystal structures. The other two halogens of the tetrahalocuprates are related by symmetry so therefore the same as X1 and X2. X1 was assigned as the halide with the highest Br%

Looking at the trans angles in table 3.5, there is a change in the pairings of 133° and 139° for compounds **3.31-3.33**, to 123° and 135° for compounds **3.34-3.37**. There is also jump in cell volume of approximately 80 $Å^3$ at the same point. The combination of these two factors suggests there are two different structure types within the series.

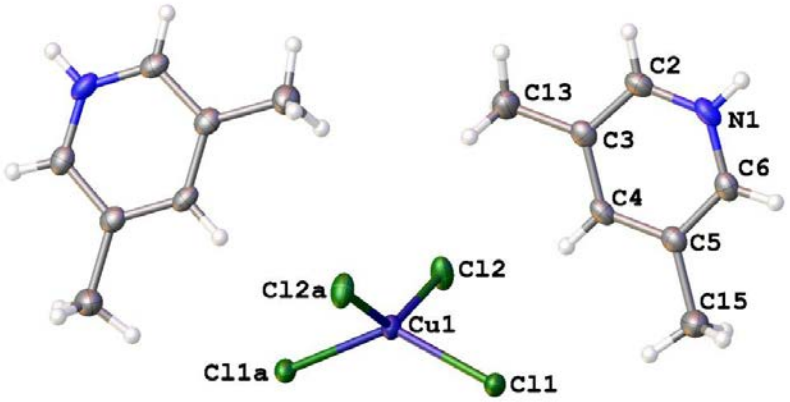

Figure 3.9 Molecular unit of $(3,5\text{-dmpyH})_2CuCl_4$, shown with 50% probability thermal ellipsoids

The molecular unit of Compound **3.31** is shown in figure 3.9. The labelled atoms are those present in the asymmetric unit; the remaining atoms are generated by inversion symmetry. The $CuCl_4^{2-}$ ion is a flattened tetrahedron with a mean trans angle of 136.470(18)° and an average Cu-Cl bond length of 2.249(3)Å. The 3,5-dmpyH cations are hydrogen bonded to the tetrachlorocuprates via N1-H1 to both Cl1 and Cl2 as shown in figure 3.10 and table 3.6.

Table 3.6 Representative table of hydrogen bonding for compuns **3.21** and **3.27**

Compound	D-H···A	d(H···A)	d(D···A)	<(DHA)	Symm. Op
3.31	N1-H1...Cl2	2.6054(6)	3.264(2)	134.28(16)	[x-1/2, -y+1/2, z+1/2]
	N1-H1...Cl1	2.7143(6)	3.262(2)	122.88(15)	[-x+1/2, y-1/2, -z+1/2]
	N1-H1...Cl1	2.7866(6)	3.292(2)	119.11(16)	[x-1/2, -y+1/2, z+1/2]
3.37	N1-H1...Br1	2.4919(4)	3.328(3)	164.2(2)	[x, -y+2, z+1/2]

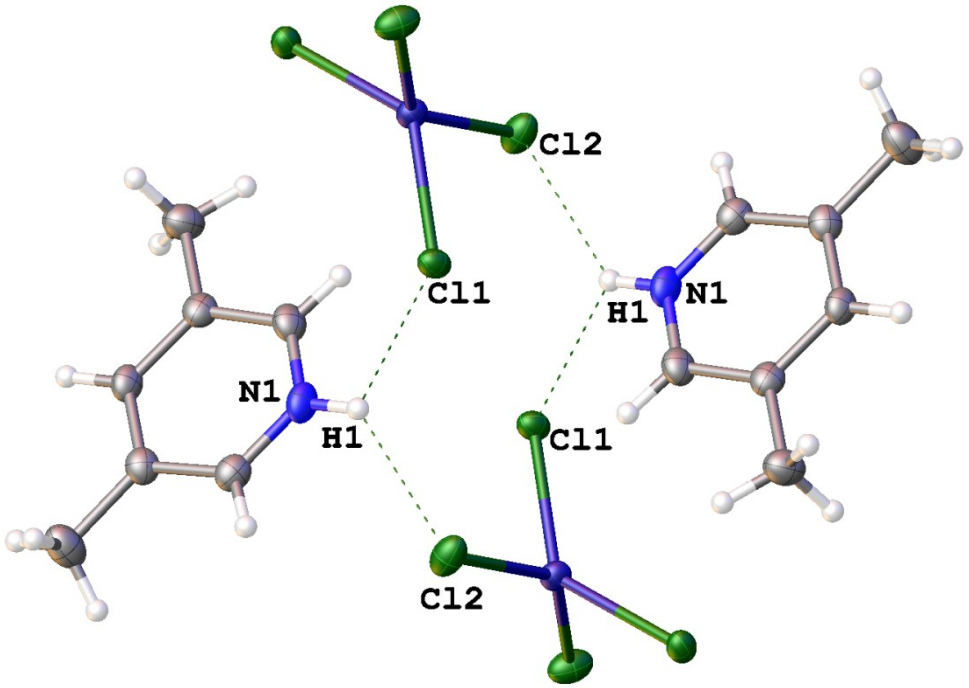

Figure 3.10 Hydrogen bonding interactions of compound 2.31 shown with 50 % probability thermal ellipsoids. The interaction details are in table 2.6. the interactions are represented by the dashed lines.

The compound **3.31** crystallises in layers which run across the *ac*-plane parallel to the c-axis (figure 3.11). Both the anions and cations alternate orientations within a single layer. The plane of the pyridinium cations is nearly orthogonal to the relative plane of the flattened tetrahedral anions (figure 3.12). The packing diagram of the ac-plane (figure 3.12) shows the weak π-stacking interactions between the cations. The π-stacking interactions have approximate centroid...centroid distances of 3.67Å and 3.59Å, with shifts of 0.69Å and 0.98Å. Figure 3.13 shows the extent of the layer separation, as well as the stacking of the cations of alternating orientations.

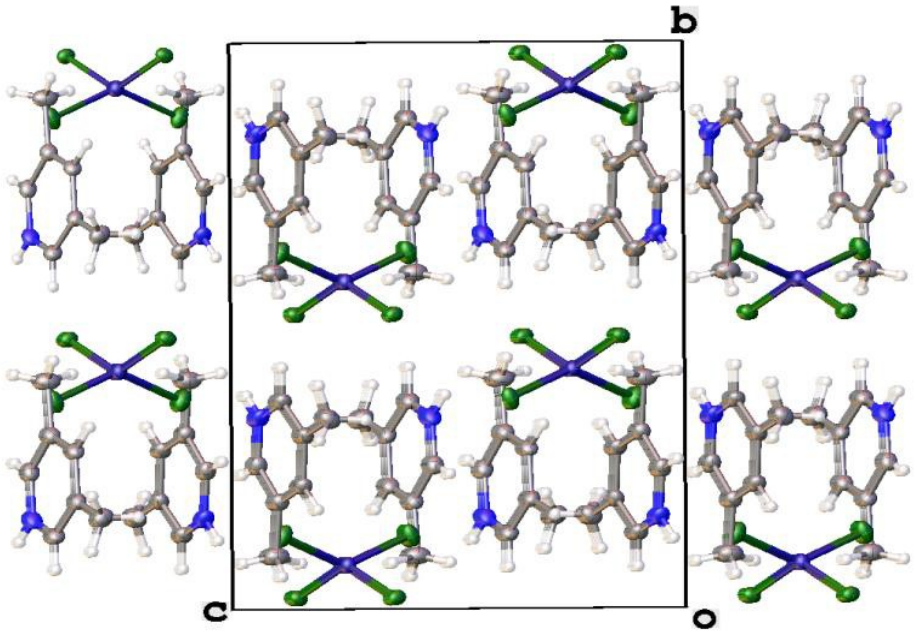

Figure 3.11 Packing diagram of the bc-plane of **3.31**, shown with 50% probability thermal ellipsoids. The separate layers of anions and cations running parallel to the c-axis can be clearly seen.

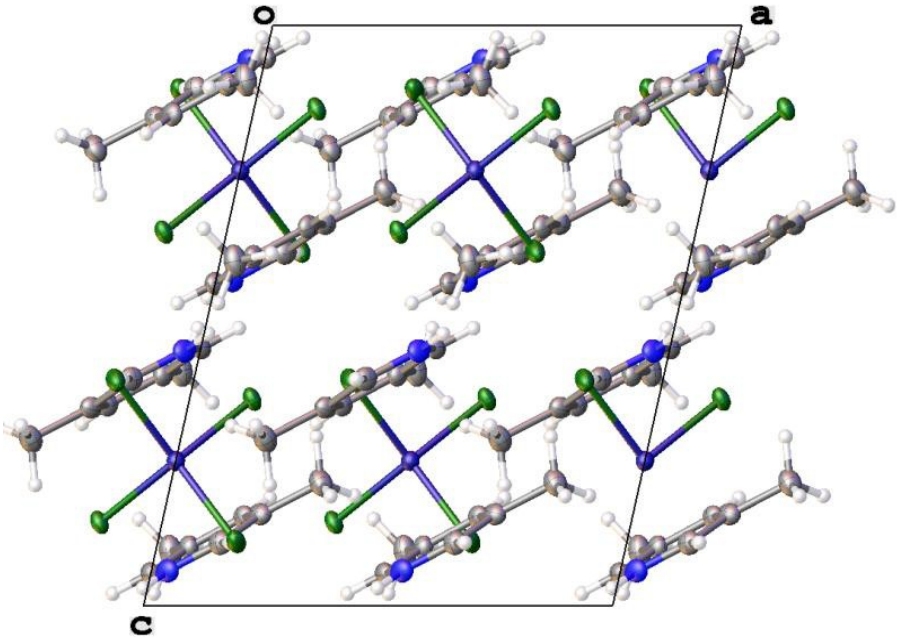

Figure 3.12 Packing diagram of the ac-plane of **3.31** shown with 50% probability thermal ellipsoids. The angle between the planes of the anions and cations can be seen, as well as the weak π-stacking interactions.

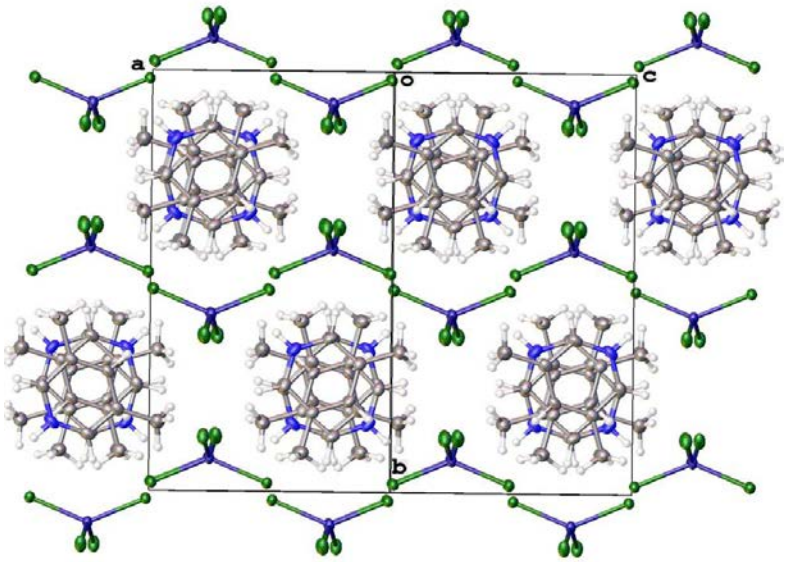

Figure 3.13 Packing diagram between the ab and bc planes, shown with 50% probability thermal ellipsoids. This view emphasises the isolations between the anion and cation layers.

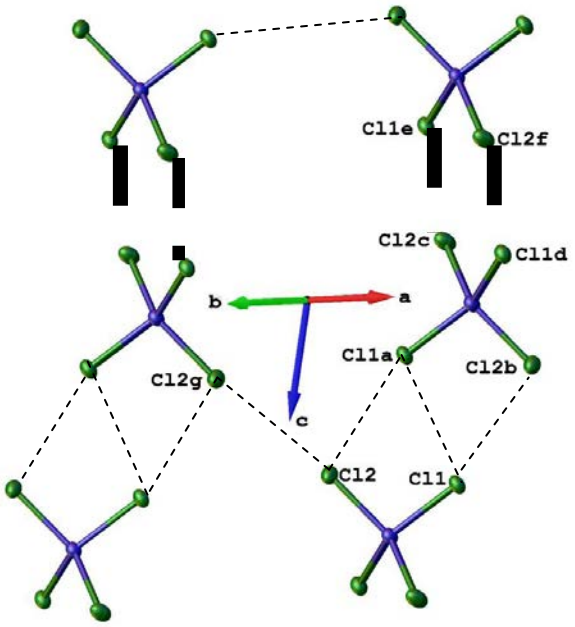

Figure 3.14 Possible magnetic exchange pathway for the type one compounds which have halide...halide contacts of less than 4.5Å. The cations are omitted for clarity.

Figure 3.14 shows a possible 2D ladder magnetic exchange pathway through halide...halide contacts between anions. Using compound **3.31** as an example the interlayer contacts of 4.6396(8)Å can be seen between Cl2···Cl2g (g = [x-1/2, -y+1/2, z+1/2]). Examples of the shorter intralayer contacts are Cl1···Cl1a being 3.952(1)Å and Cl1···Cl2b (b = [x-1/2, -y+1/2, z+1/2]) at 3.9873(8)Å. The same pathway applies to all the compounds with the same structure trans angle pairing as **3.31**, but with their appropriate distances for the interactions.

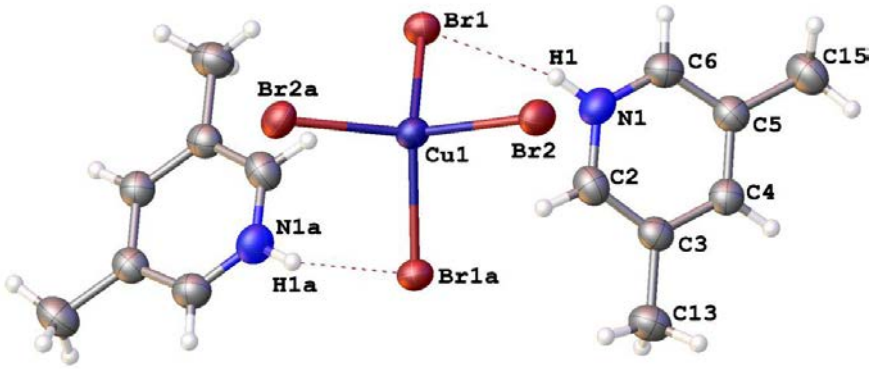

Figure 3.15 Molecular unit of **3.37**. The labelled atoms are those present in the asymmetric unit, the remaining are generated by symmetry. Table 3.6 on page 53 has details of the hydrogen bonding interactions represented by the dashed lines.

Compound **3.37** also crystallises in the spacegroup C2/c with the asymmetric unit containing half of the full structure. The $CuBr_4^{2-}$ ion is also a flattened tetrahedron, however slightly more towards ideal tetrahedral geometry than compounds **3.31-3** with a mean trans angle of 129.48(3)°. The average Cu-Br bond length is 2.3858(4)Å, comparable with other compounds of this type. As in all compounds **3.31-7** the pyridinium ions are hydrogen bonded to the tetrahalocuprates via the pyridinium hydrogen, however there is only a single hydrogen bonding interaction (table 2.6) compared to the three in compound **3.31**.

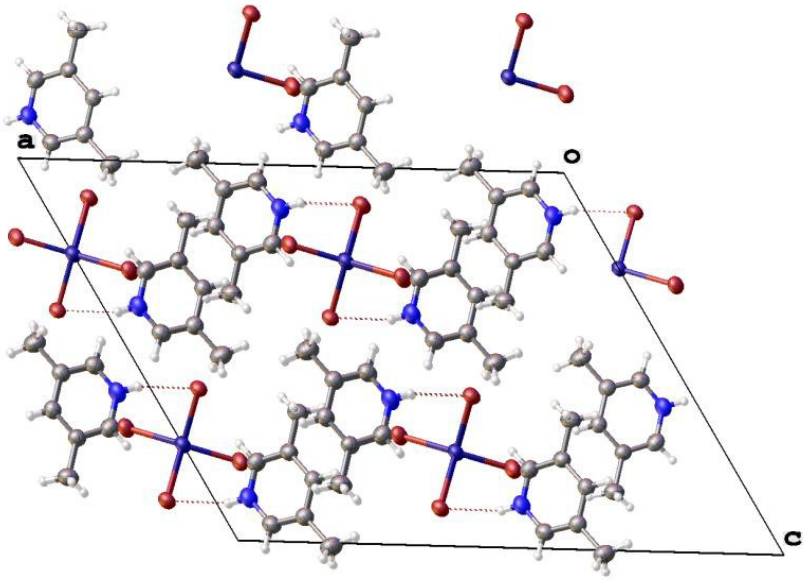

Figure 3.16 Packing diagram of *ac*-plane of compound **3.37**, shown with 50% probability thermal ellipsoids. The isolated layers of anions and cations can easily be seen. The alternating pyridinium orientations can be seen within the cation layers. The dashed lines represent the hydrogen bonding interactions described in table 3.6

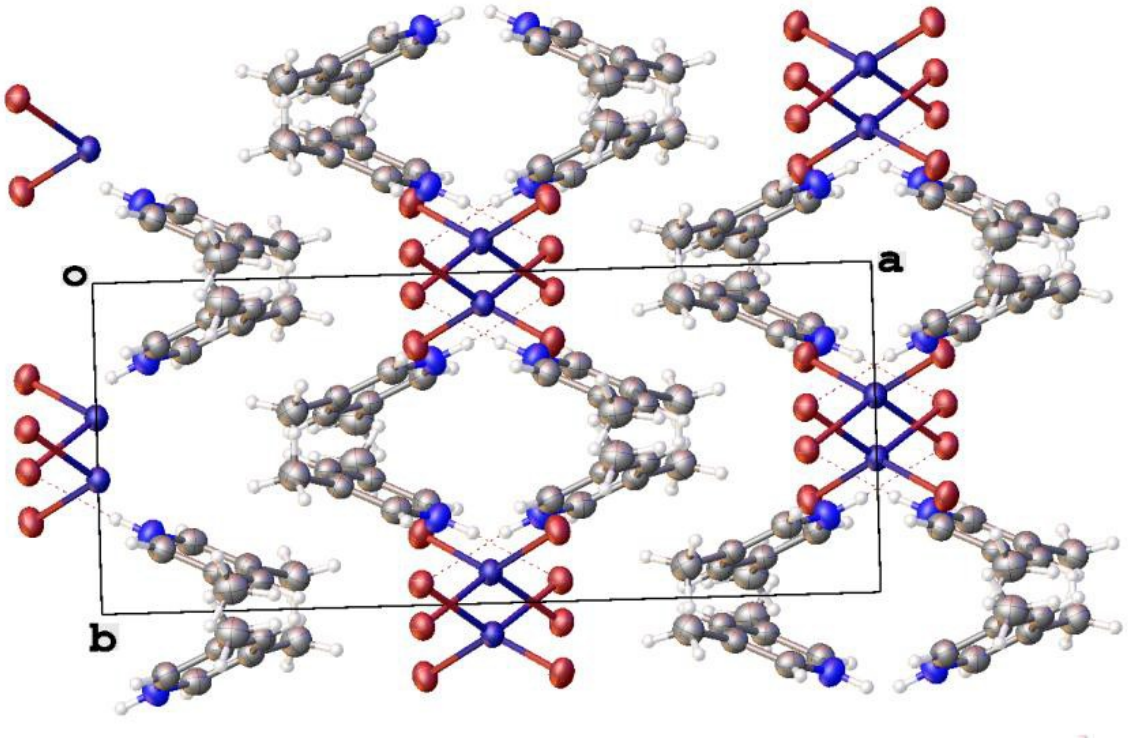

Figure 3.17 The *ab*-plane packing diagram, shown with 50% probability ellipsoids emphasises the angle between the pyridine wings within the cation layers. The angle between the plane of each ring in each of the "pairs" that can be seen is $48.95(16)^0$.

As with all compounds in this series, **3.37** crystallises into layers of separated anions and cations, as can be seen in the packing diagram view of the *ac*-plane (figure 3.16). Compared to the same view of **3.31** (figure 3.12) where the tetrahalocuprates are in a similar orientation, the differences in the packing can easily be seen. In **3.31** the plane of the pyridine rings are nearly parallel to the b axis (figure 3.12) but in **3.37** they are nearly parallel to the ac-plane, (figure 3.16). As can be seen by the halide···halide contacts in table 3.4, the compounds **3.31** and **3.34-3.37** (50-100% Br) are unlikely to have any significant magnetic properties, as they all have relatively long lengths halide···halide contacts (well over 4.5Å). This may be due to a combination of the steric distribution about the cation and/or the size difference of bromine compared to chlorine.

After seeing the structural changes occuring in the 25-50% bromine compounds a further four compounds were synthesised to try and get a more accurate idea as to where the structural transition occurs. The four compounds were made at intervals at 5% intervals between 30 and 45% Br.

As with the rest of this series, differences in the trans angle pairings is a representative indicator of structural changes. Looking at the trans angles in table 2.7 it can be seen that the structural change occurs between 35% and 40% Br. The large increase of the unit cell volume between the same two compounds also shows where the change occurs.

Table 3.7 Structural features of the tetrahalocuprate anions

Compound (Br %)	Br % of halides		Trans Angles (°)		Unit cell volume (Å^3)
	X1	X2 *			
3.38 (30)	84.8	50.4	133.07(3)	138.46(3)	1904.87(10)
3.39 (35)	86.5	53.2	133.00(3)	138.38(3)	1909.03(14)
3.3.10 (40)	100	100	123.51(3)	135.76(3)	1989.38(18)
3.3.11 (45)	100	100	123.57(4)	135.76(5)	1993.68(19)

* X1 and X2 are the two different halogen atoms present in the asymmetric unit of the crystal structures. The other two halogens of the tetrahalocuprates are related by symmetry so therefore the same as X1 and X2

Table 2.8 Shortest interlayer and intralayer through space halide...halide distances between anion halogen atoms

Compound (Br %)	Intralayer contact (Å)	Interlayer Contact (Å)
3.38 (30)	4.0597(7)	4.4669(6)
3.39 (35)	4.0638(7)	4.4695(6)
3.3.10 (40)	6.0732(7)	5.1459(5)
3.3.11 (45)	6.0895(8)	5.1459(5)

The halide...halide contacts show a clear change in structure between compounds **3.38**, **3.39** and **3.3.10**, **3.3.11**, due to the same discussed structural differences between compounds **3.31** and **3.34**. Only compounds **3.38** and **3.39** have contacts shorter than 4.5Å, giving them a possibility of magnetic exchange through a similar pathway to figure **3.13** which will be discussed in the magnetic exchange section of this chapter (section 3.5).

3.4 3,4-dimethylpyridinium tetrahalocuprates

Reaction of 3,4-dimethylpyridine with HX and CuX_2 (X=Cl and/or Br) in aqueous solution gave $(3,4\text{-dmpyH})_2CuX_4$ salts. Crystals suitable for single crystal x-ray diffraction were grown by slow evaporation of an aqueous solution of each salt. Seven complexes were made with ratios of 0, 5, 25, 50, 75, 95 and 100% of X = Br to Cl, where the ratio applied to the CuX_2 salt and its corresponding acid, as shown in scheme 3.1. All complexes crystallised in the triclinic spacegroup P-1. Comparison of structural features of interest are shown in tables **3.1** and **3.2.**

Table 3.9 Selection of crystal structure features which are indicative of structural changes between the compounds

Compound (Br ratio)	Cell Volume (Å^3)	Anion trans angles (^{o})		Average Cu-X length (Å)
3.41 (0)	916.37(6)	139.78(3)	142.59(3)	2.2526(8)
3.42 (5)	926.75(4)	139.60(4)	141.17(4)	2.2770(10)
3.43 (25)	944.83(6)	139.29(2)	139.725(13)	2.3291(5)
3.44 (50)	944.81(6)	132.099(17)	134.060(18)	2.384(1)
3.45 (75)	949.24(7)	132.22(4)	134.16(4)	2.3858(9)
3.46 (95)	968.47(9)	134.87(4)	138.24(4)	2.384(1)
3.47 (100)	975.72(6)	134.69(2)	138.13(2)	2.3878(6)

Table 3.10 Bromine% of halides of 3,4 dmpy tetrahalocuprates, where X1-4 are the four halogens present in the tetrahalocuprates. All four are different as none are related by symmetry, and they are all present in the asymmetric unit for each compound.

Compound (Br %)	X1	X2	X3	X4
3.41 (0)	0	0	0	0
3.42 (5)	4.6	5.3	10.9	27.1
3.43 (25)	23.3	30.2	51.6	76.8
3.44 (50)	86.9	88.8	89.4	90.1
3.45 (75)	97.7	98.1	98.2	99.8
3.46 (95)	100	100	100	100
3.47 (100)	100	100	100	100

As with the previous dimethylpyridine analogues, within each series compounds which have very similar anion trans angles also have similar crystal packing. A change in trans angles between two subsequent compounds in the series is a good indicator of a change in the crystal packing, similarly to the 2,4 and 3,5 analogues. In this case, i.e the 3,4 dmpy, there are three different structures within the series; (1) **3.41**, **3.42** and **3.43**,(2) **3.44**, **3.45** and(3) **3.46** , **3.47**. The pairings of the anion trans angles is an simple yet representative predictor of where in this series the different structural motifs occur. One compound of each of the three different structural types will be described in more detail. The compounds without mixed Br/Cl anions will be compared as they do not have the additional factor of the mixed halides, however still show similar crystal structures. The molecular units of all the compounds of this series are similar. The extent of the structural differences of the compounds can be seen after comparing the crystal packing of the three compounds.

3.41 Crystal structure of 3.41

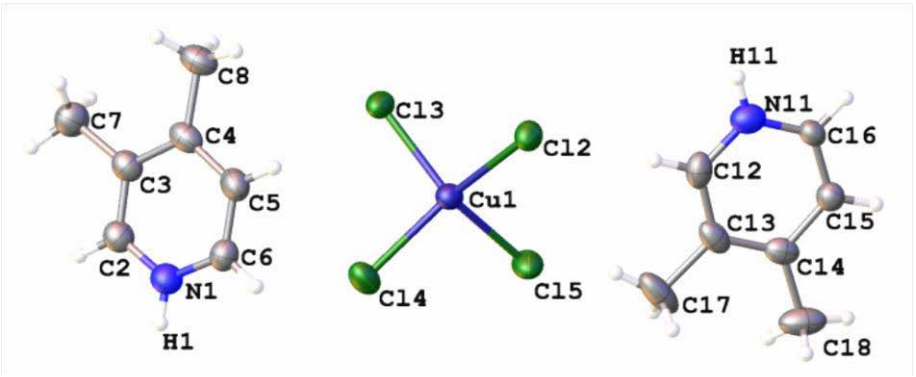

Figure 3.18 Molecular unit of compound **3.41**. The labelled hydrogen atoms are involved in hydrogen bonding interactions. **50%** probability thermal ellipsoids are shown

The molecular unit of compound **3.41,** the first structural type, contains two pyridinium ions, and a single tetrachlorocuprate anion. The anion trans angles are 139.778(3)° and 142.59(3)°. The average Cu-Cl bond length is 2.2522(8)Å which is comparable to both the 2,4 and 3,5

analogues. The angle between the mean planes of the pyridine rings in the molecular unit is 48.62(9)°.

Hydrogen bonding is a major contributor to the structure, with a hydrogen bonding interaction to each halogen of the tetrachlorocuprate. Details of the hydrogen bonding can be seen in table 3.11. The image of the hydrogen bonding in figure 3.19 shows the bifurcated hydrogen bonding between the hydrogen on the pyridine nitrogen and two halogens of an individual anion. Each anion has two different cations hydrogen bonded to it.

Table 3.11 Representative table of hydrogen bonding for compound **3.41**

D-H...A	d(H...A)	d(D...A)	<(DHA)	Symm. Op
N1-H1...Cl1	2.5852(6)	3.279(3)	138.45(15)	[x, y+1, z]
N1-H1...Cl2	2.4483(6)	3.148(2)	139.00(15)	[x, y+1, z]
N11-H11...Cl3	2.4639(8)	3.288(3)	160.65(17)	[x, y-1, z]
N11-H11...Cl4	2.8641(7)	3.380(3)	120.24(18)	[x, y-1, z]

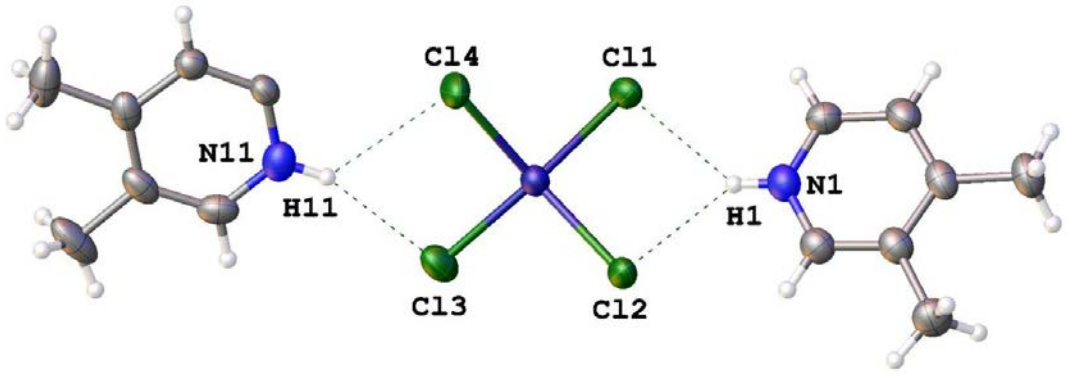

Figure 3.19 Hydrogen bonding interactions present in 3.41 shown with 50% probability thermal ellipsoids. The interactions are represented by the dashed lines. Details of the interactions are shown in table 3.11 above.

Crystals of **3.41** pack into single isolated layers of anions and cations, in an ABAC type arrangement (figure 3.20). Within each cation layer the orientation of the dmpy rings alternates with a rotation of nearly 180° relative to the nitrogens. The orientation between layers also alternates with the angle of 48.62(9)° between the plane of the rings of each layer.

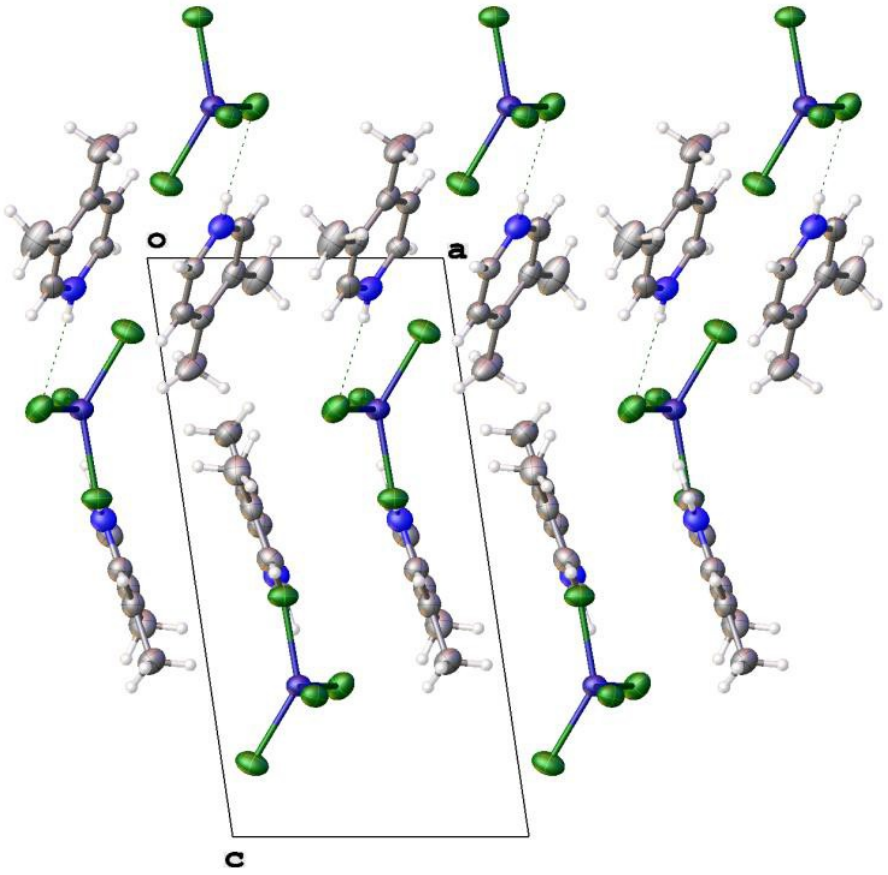

Figure 3.20 Packing diagram of the *ac*-plane of **3.41** shows π-stacking interactions, and the difference in orientation between different cation layer.

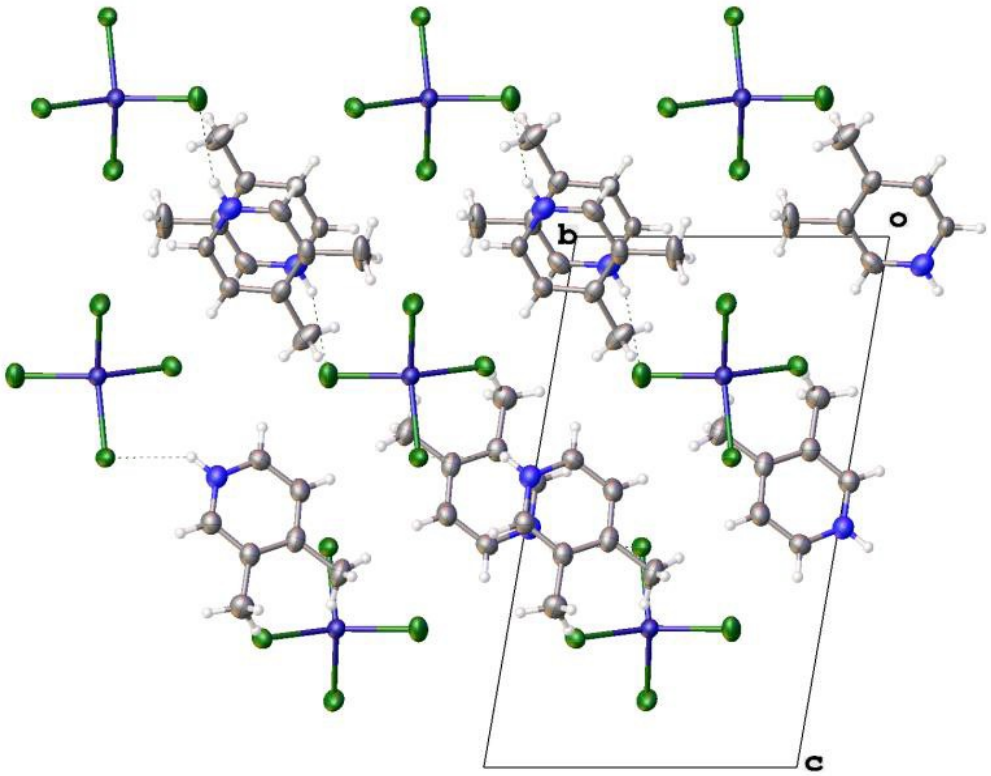

Figure 3.21 packing of the *bc*-pane shows the intralayer rotation of the cations. A possible ladder type magnetic exchange pathway can be seen with the closeness and orientation of the halogen atoms of the tetrachlorocuprates

An alternative packing view of **3.41** (figure 3.21) shows the alternating pyridine orientation both within a single cation layer, and between adjacent cation layers.

π-stacking interactions are also a likely contributor to structure stability. Figure 3.22 shows the π-stacking present in **3.41**. For the interaction between the N11 rings the centroid to centroid distance is 3.529(2)Å, with a ring shift of 0.842(4)Å. The rings are parallel with an angle of 0^{o} between them. The other interaction involving the N1 rings has a centroid-centroid distance of 3.300(3)Å and a shift of 1.842(5)Å between rings. The angle between the rings is also 0^{o} as they are symmetry related.

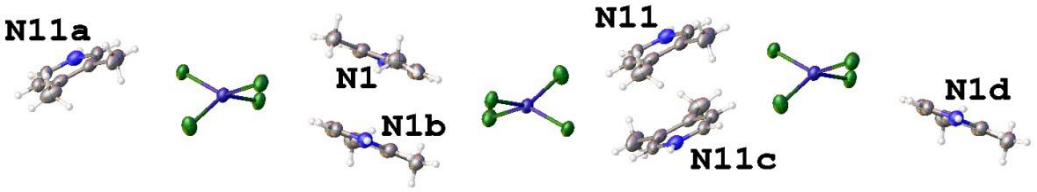

Figure 3.22 Diagram showing the different π-stacking interactions of the different cation layers.

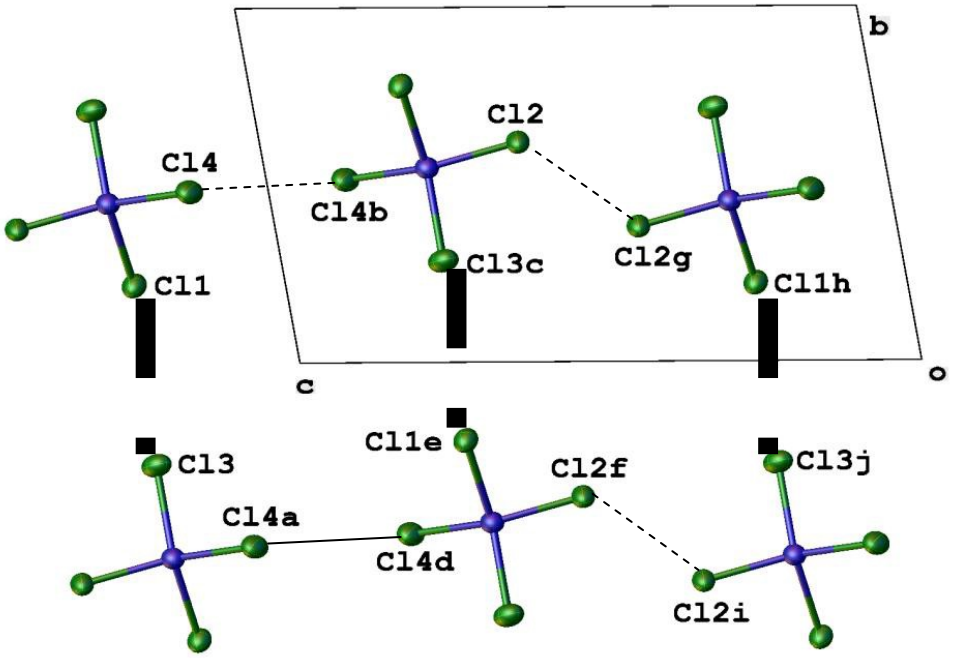

Figure 3.23 Possible magnetic exchange pathway. Dashed lines represent through space halide...halide contacts. Cations are omitted for clarity.

A proposed ladder structured magnetic pathway can be seen in figure 3.23. The chloride...chloride through space interactions are represented by the dashed lines. All three contacts are under 5Å, making them a possible magnetic pathway. The interaction distances (Å) are as follows; Cl1···Cl3 4.6705(10), Cl2···Cl2g 4.0214(13) and Cl4···Cl4b 3.7588(14). These contacts will be discussed further in the magnetic section (3.5) of this chapter.

3.42 Crystal structure of 3.44

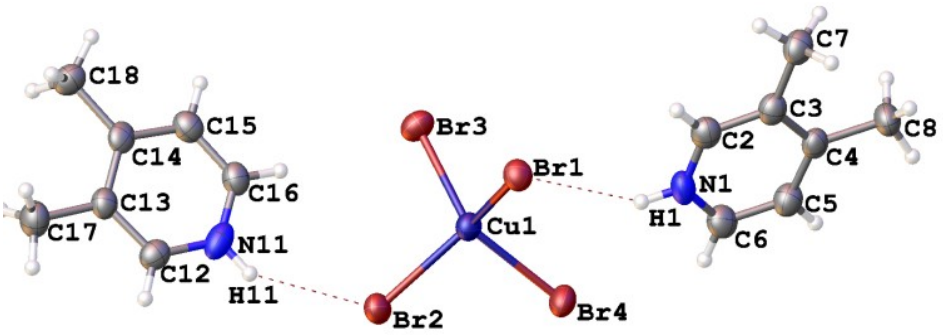

Figure 3.24 Molecular unit of compound **3.44**. The dashed lines represent hydrogen bonding interactions. 50% probability thermal ellipsoids are shown.

The molecular unit of **3.44 (**type two) has the same contents as **3.41**, except in a visibly different orientation. In **3.41** the pyridine nitrogens are facing more towards the copper of the tetrahalocuprate (figure 3.24) compared to **3.44** where they are beginning to angle away from the copper. The angle between the plane of the rings is also larger at 55.7(2)°, which is nearly a 15% increase compared to the angle in **3.41.** The average Cu-Br bond length is 2.3858(9)Å, which is consistent with other dmpy tetrabromocuprates. The anion trans angles are 132.22(4) Å and 134.16(4)Å which are both significantly smaller that in **3.41** moving the geometry slightly closer towards a tetrahedron.

The crystal packing of **3.44** is similar to that of **3.41** in the sense that it forms isolated layers of cations and anions. There are two different anion layers, with nearly 180° rotation of the anions, with respect to the anions in adjacent anion layers. The cations pack into two different layers. Within each individual layer there is a 180° rotation between alternate cations. As with the type one and three compounds the cations of adjacent layers are nearly orthogonal to each other. The greater angle between the alternating cation layers can be seen in figure 3.25, compared to figure 3.21 showing the same view of compound **3.41**.

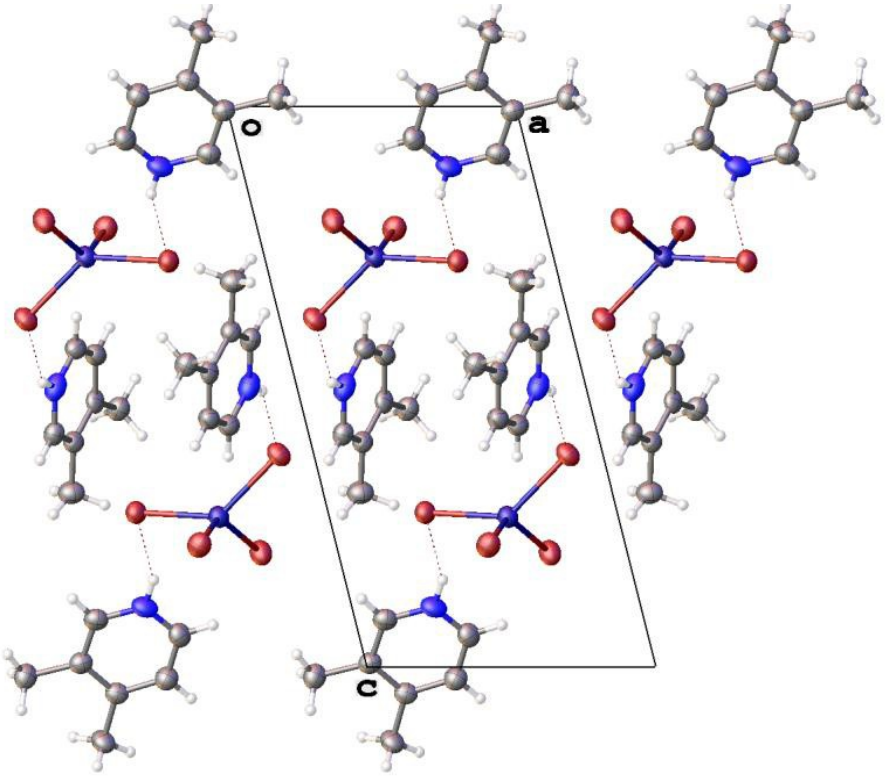

Figure 3.25 Packing view of the *ac*-plane shows the separated anion and cation layer, but also how the cations alternate between the different cation layer.

π-stacking interactions also contribute to the stability of the structure (figure 3.26). As in **3.41**, π-stacking interactions are only present in every second cation layer, compared to **3.41,** where they are present in every cation layer. This emphasises the greater isolation of the cations within every second layer due to the size increase from moving from chloride to bromide containing anions. The centroid to centroid distance of the interaction is 3.627(2)Å with a shift of 1.199(5)Å.

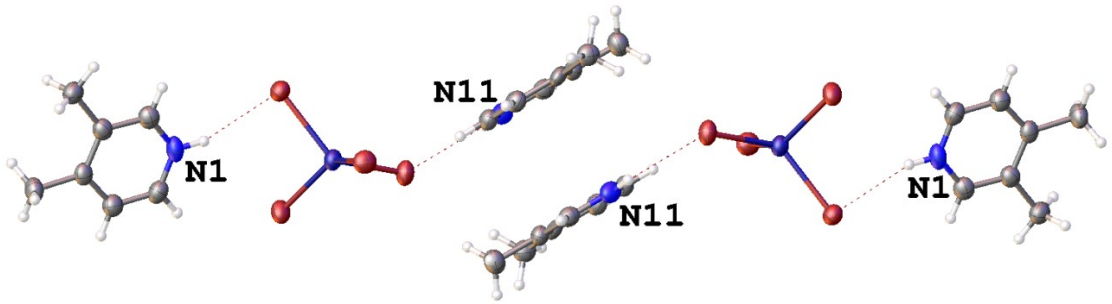

Figure 3.26 π-stacking interaction in compound **3.44**. Only the N11 containing pyridines are involved in these interactions, whereas in **3.41** the N1 containing rings are also involved in π-stacking interactions.

An alternative view of the packing of **3.44** (figure 3.27) is a good summary of the structural features showing the π stacking interactions and the alternating orientations of both the anion and cation layers.

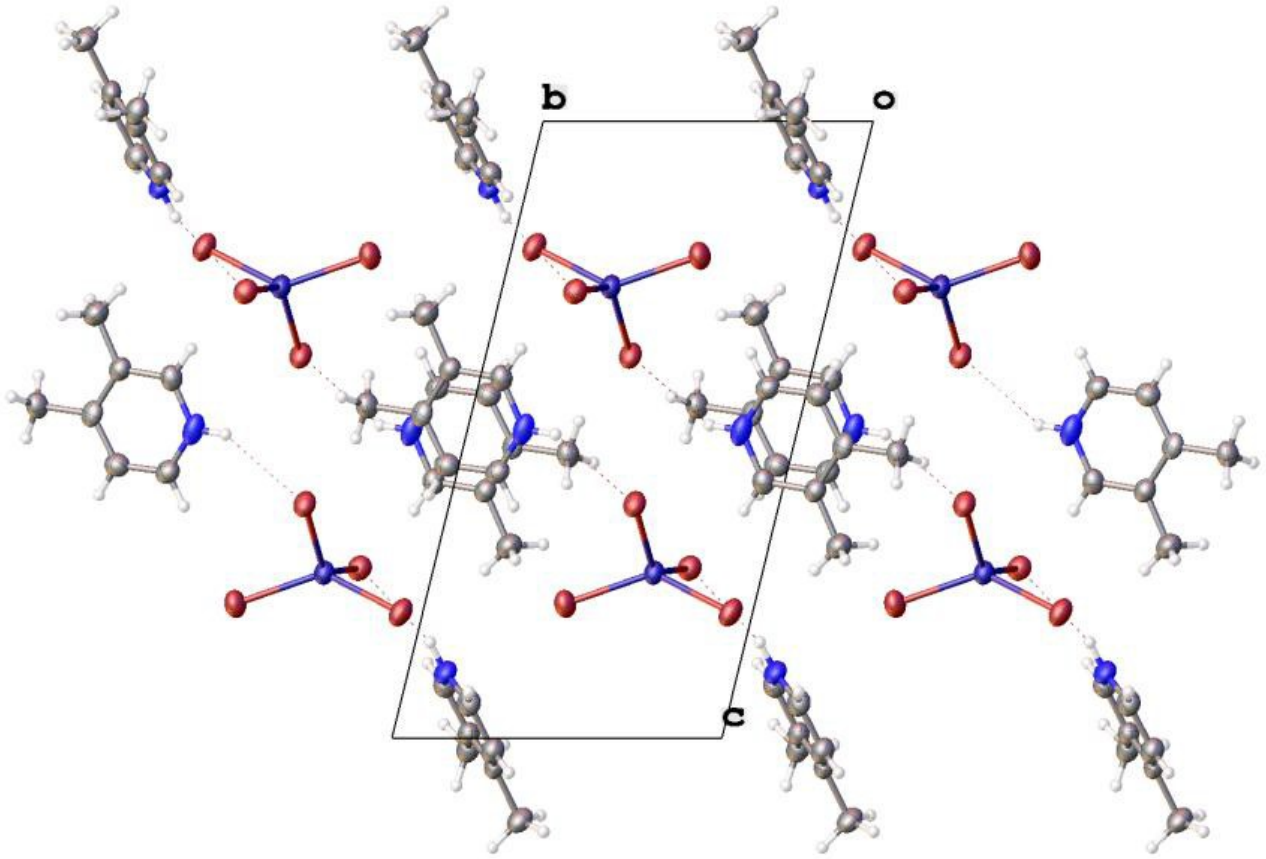

Figure 3.27 The angles between the cations of different layers can be seen by in the packing diagram of the *bc*-plane.

Table 3.12 Hydrogen bonding interactions of compound 3.44

D-H···A	d(H···A)	d(D···A)	<(DHA)	Symm. Op
N1-H1...Br1	2.5484(6)	3.317(5)	149.3(4)	
N1-H1...Br4	3.0673(6)	3.629(5)	124.9(4)	
N11-H11...Br3	2.6256(6)	3.376(5)	146.5(4)	
N11-H11...Br3	3.0107(6)	3.626(6)	130.2(4)	[-x+2, -y+1, -z+1]

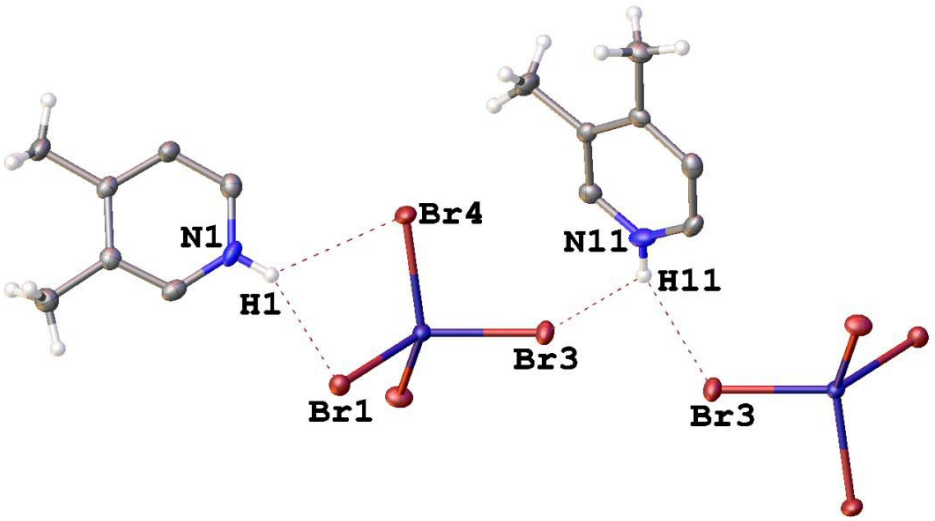

Figure 3.28 Diagram of the hydrogen bonding interactions of **3.44**, shown with 50% probability thermal ellipsoids. Detals of the interactions represented by the dashed lines are in table 3.12 above. The non hydrogen bonding hydrogens have been omitted for clarity.

The difference in the orientation of the cations with respect to the anions between **3.41** and **3.44** can be seen in figure 3.28 of the hydrogen bonding interactions present in **3.44**. In **3.41** there are two bifurcated hydrogen bonds to an individual anion (figure 3.19) compared to **3.44** which has N1-H1 forming a bifurcated hydrogen bond to two halogens of a single anion, however the second cation forms a bifurcated hydrogen bond between two different anions.

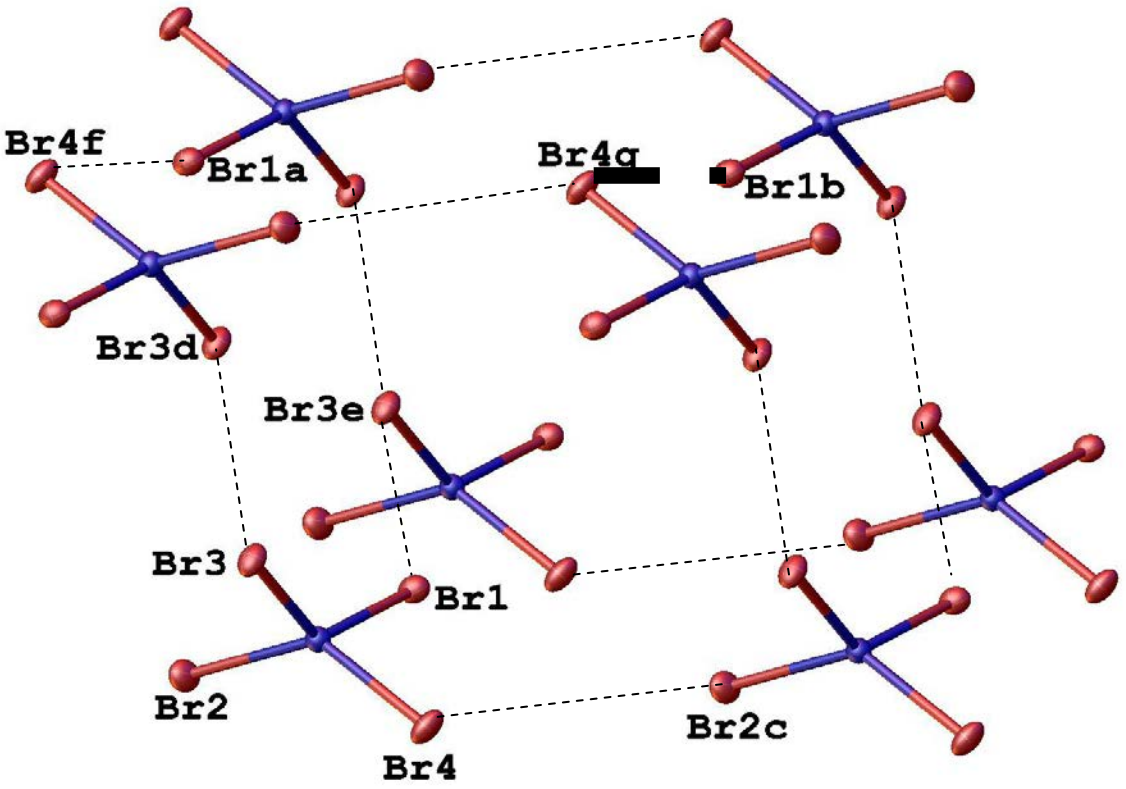

Figure 3.29 Illustration of the possible 3D magnetic exchange pathway in **3.44**. The cations are omitted for clarity. The dashed lines represent the halide halide interasctions described below.

There is a possible 3D magnetic exchange pathway present in **3.44**. There are halide...halide through space interactions of less than 5Å between anions in all three dimensions making the proposed 3D exchange pathway possible. The interactions that may form this pathway are shown in figure 3.29. The interactions are Br1···Br3e (4.4009(5)Å), Br4···Br2c (4.4287(5)Å, Br3···Br3d (3.7329(6)Å) and Br4f···Br1a (4.6442(5)Å)

3.43 Crystal structure of 3.47

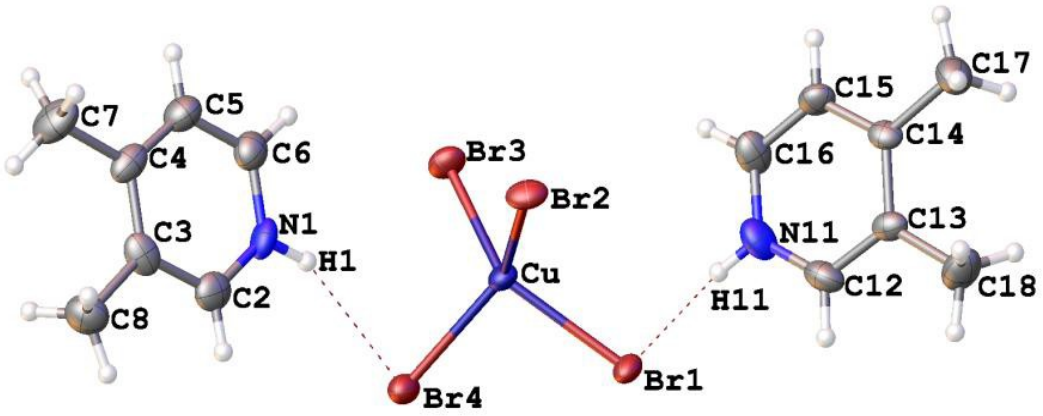

Figure 3.30 Molecular unit of 3.47. The labelled hydrogen atoms are those involved in hydrogen bonding.

The difference between the molecular units of **3.44** and **3.47** is not as large as between **3.41** and **3.44**, however there are still notable changes. The angle between the planes of the pyridine rings has increased nearly 15% from those in **3.44** with an angle of $63.04(12)^0$. The average Cu-Br bond length remains similar to **3.44** being 2.3878(6)Å, however the trans angles have increased slightly to $134.69(2)^0$ and $138.13(2)^0$.. The π-stacking interaction is similar to compound **3.44**, as only the N1 containing rings are involved. Figure 3.31 shows this interaction. The same figure also shows the change in angles between the pyridine layers.

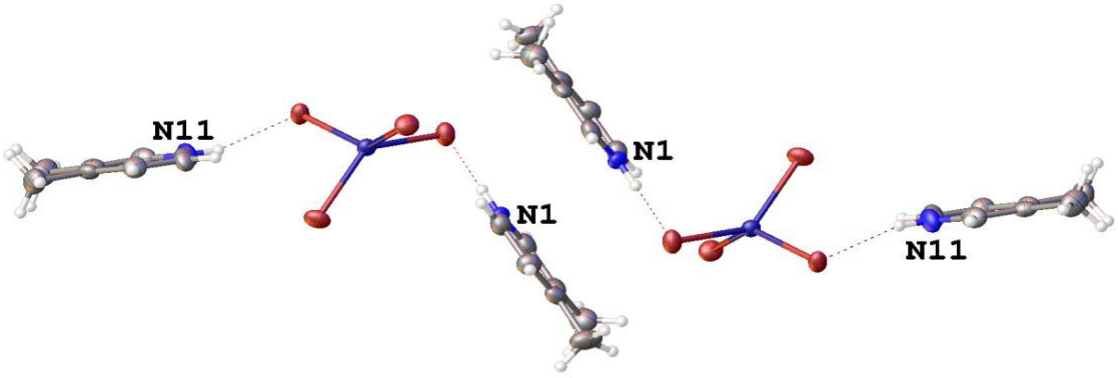

Figure 3.31 **π** stacking interaction present in mpound **3.47**. When compared to figure 3.25 the different pyridinium orientations can be seen between the two compounds. 50% probability thermal ellipsoids are shown. The centroid to centroid distance of the N1 rings is 3.911(3)Å with a shift of 2.090(6)Å.

The crystal packing (figure3.32) of the type three compounds is similar to the type one and two compounds. There are two alternating anion layers, and two different cation layers. There is almost 180° rotation between anions of adjacent layers. Both cation layers contain cations in two alternating orientations, with a nearly 180° rotation between the cations within each layer.

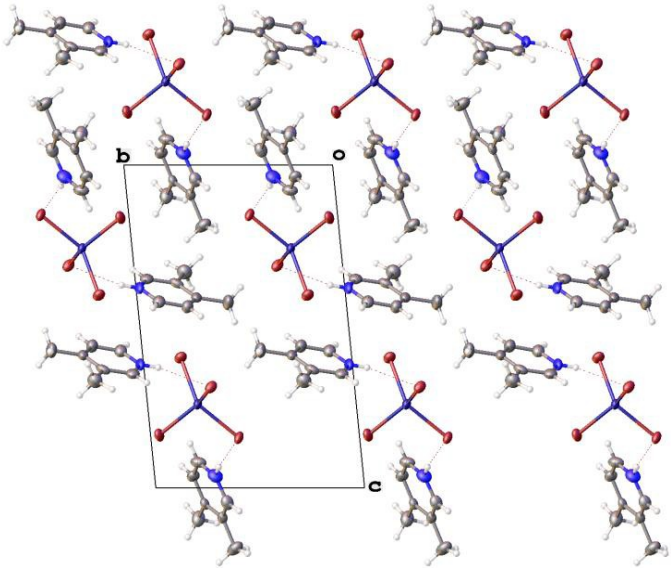

Figure 3.32 Packing diagram of the bc plane of compound **3.47**, shown with 50% probability thermal ellipsoids. The alternating anion layers can be clearly seen., as well as the alternating pyridine orientations between and within individual cation layers.

The hydrogen bonding interactions are also similar to **3.44** except at larger angles. Details can be seen in figure 3.33 and table 3.13.

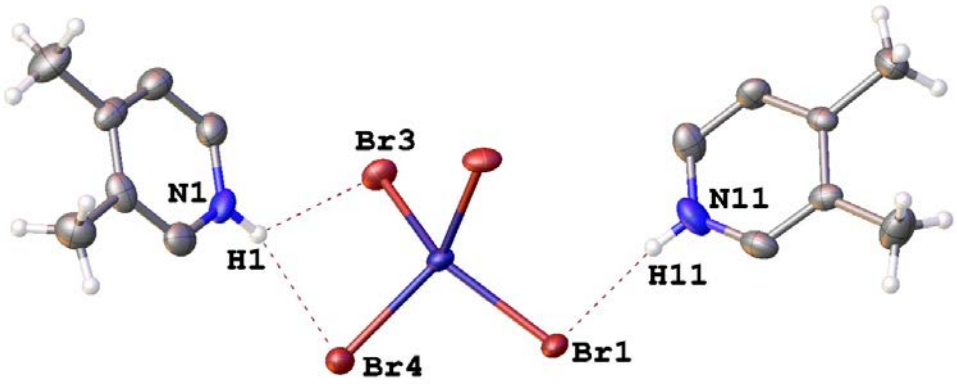

Figure 3.33 Diagram showing the hydrogen bonding interactions in compound **3.47**, shown with 50% probability thermal ellipsoids. Details of the interactions represented by the dashed lines can be found above in table 3.13. The pyridine ring hydrogen atoms not involved in hydrogen bonding were omitted for clarity.

Table 3.13 Representative table of hydrogen bonding for compound **3.47**

D-H···A	d(H···A)	d(D···A)	<(DHA)	Symm. Op
N1-H1...Br3	2.9865(4)	3.564(3)	126.3(2)	
N1-H1...Br4	2.5437(4)	3.335(3)	153.4(2)	
N11-H11...Br1	2.4362(4)	3.276(4)	165.6(2)	

There is a possible ladder structured 2D magnetic exchange pathway in the compound. The magnetic exchange is likely to be relatively weak due to the halide halide contacts being close to 5Å. The contacts which form the possible ladder type pathway are Br1···Br1b (4.8900(6)Å), Br3···Br3e (5.0366(9)Å) and Br3e···Br4f (4.5890(9)Å). Figure 3.34 illustrates the proposed pathway with dashed lines representing the halide...halide through space interactions.

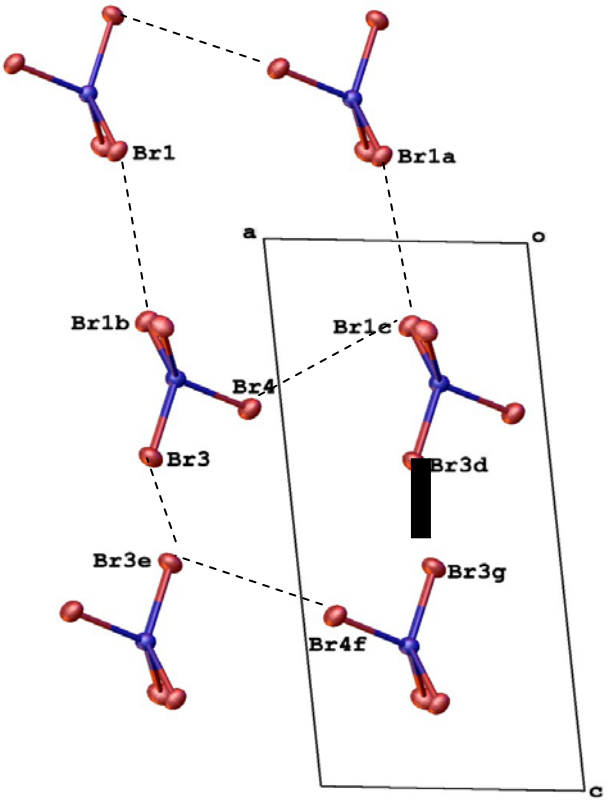

Figure 3.34 Packing diagram of the ac-plane of compound **3.47**, shown with 50% probability thermal ellipsoids. The labelled atoms are involved in the proposed magnetic exchange pathway. The cations have been omitted for clarity.

3.5 Magnetic exchange

Recall the magnetic exchange pathway of interest is the double halide bridge, as previously seen in chapter 1. (figure 3.35).

d – The distance between the Br atoms

θ_1 – The angle Cu_1-Br_1….Br_2

θ_2 – The angle Cu_2-Br_2….Br_1

τ – The dihedral angle Cu_1–Br_1 ….Br_2–Cu_2

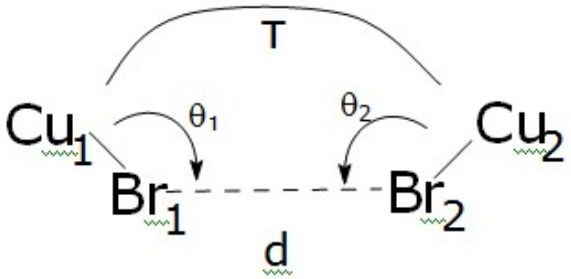

Figure 3.35 Example of the double halide bridge topology used to describe halide···halide interactions. Br is the halide in this example.

From what is known about the double halide bridge exchange interactions, as it currently stands the strongest magnetism comes from a short d value, and where the τ angle is 180^0.

The compounds which we have magnetic data for will be described and compared in terms of the double halide bridge topology. The Curie constant and magnetic exchange value, J, will also be used to describe the magnetic interactions. The Curie constant is typically around 0.4 for compounds with no, or very weak antiferromagnetic exchange, and higher for compounds which have antiferromagnetic exchange.

Unfortunately due to technical difficulties, despite valiant efforts by Mark Turnbull and his colleagues at Clark University, no magnetic data for the 3,5-dimethylpyridine compounds was able to be obtained.

Compounds **3.41**-**3.43** have been shown to have very similar crystal structures, with very similar possible magnetic exchange pathways (figure 3.37). The same pathway applies to all three compounds, with the values appropriate to the individual compounds.

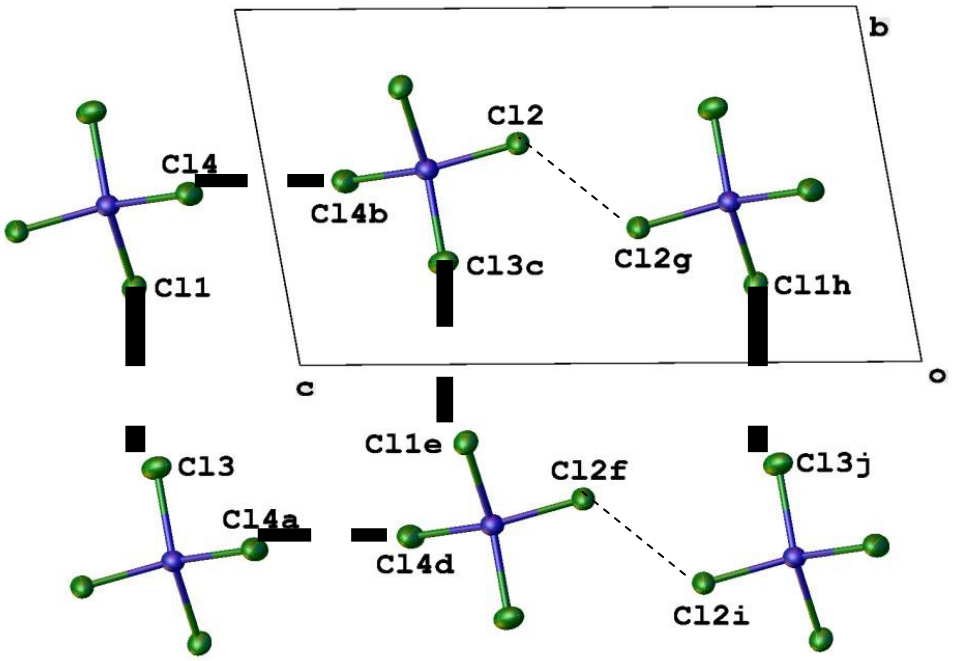

Figure 3.37 Possible magnetic exchange pathway for compounds **3.41**-**3.43**. Dashed lines represent through space halide...halide contacts. Cations are omitted for clarity.

compound 3.41 100:0 Cl:Br

Table 3.14 Geometric features of the halide···halide contacts in **3.41**.

contact	D (Å)	Θ1 (^{0})	Θ2(^{0})	T (^{0})	Inter/intra
Cl1...Cl3	4.6707(9)	145.48(3)	170.10(2)	-80.33(10)	intra
Cl2...Cl2g	4.0211(13)	117.20(3)	117.20(3)	180.00(4)	inter
Cl4...Cl4b	3.7596(14)	161.98(5)	161.98(5)	180.00(4)	inter

Compound **3.41** is well fit by a 2D-Heisenberg model, although the exchange is so weak it could also be fit using other models[40]. The fitting of **3.41** gave a Curie constant of 0.45, and J = -1.82K. The fitting and more accurate values can be seen in figure 3.38.

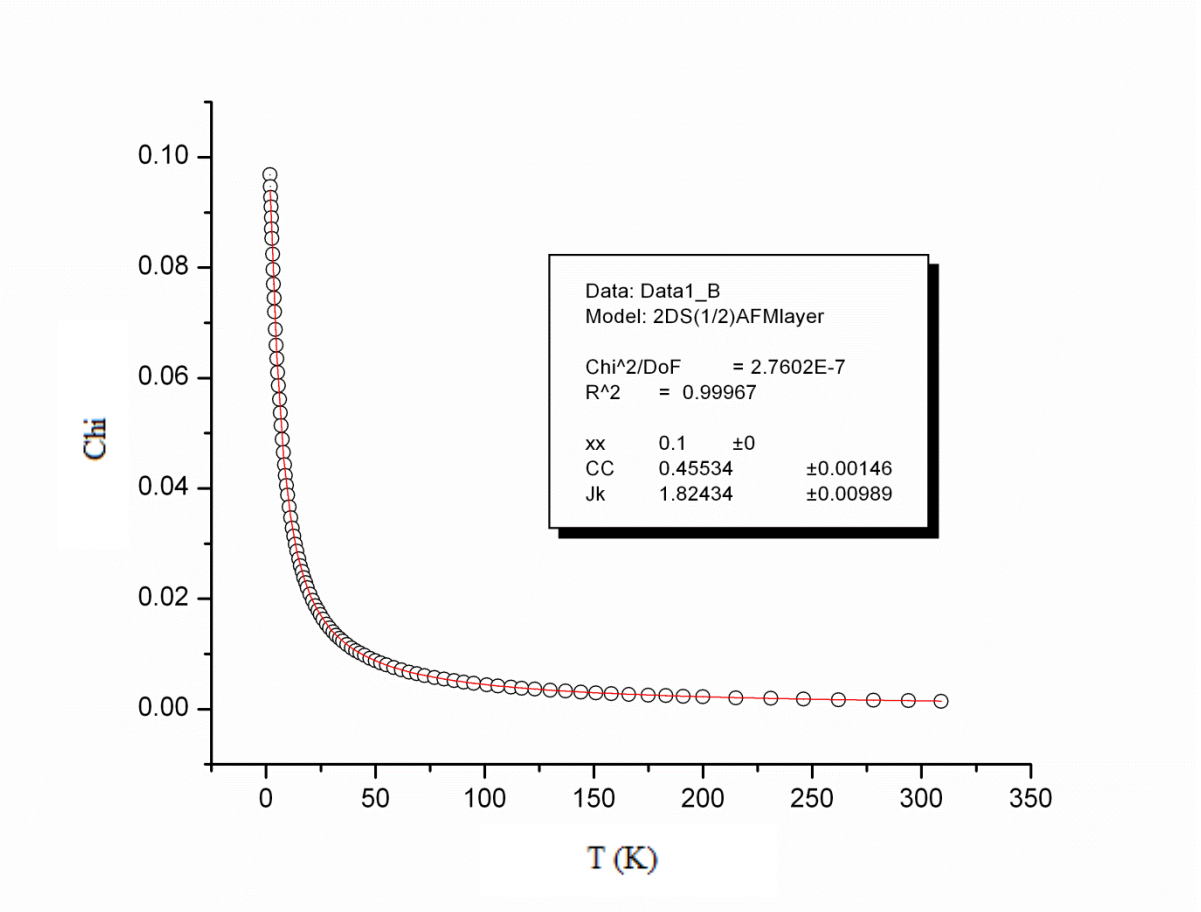

Figure 3.38 Plot and fitting of Chi V T for compound **3.41**

Compound 3.42 95:5 Cl:Br

Table 3.15 Geometric features of the halide···halide contacts in **3.42.**

contact	D (Å)	Θ1	Θ2	τ	Inter/intra
Cl1....Cl3	4.6311(6)	144.30(2)	169.59(2)	-79.34(12)	Intra
Cl2...Cl2	3.7727(11)	163.07(4)	163.07(4)	180.00(11)	Inter
Cl4...Cl4	4.0210(12)	117.493(7)	117.493(7)	180.00(4)	inter

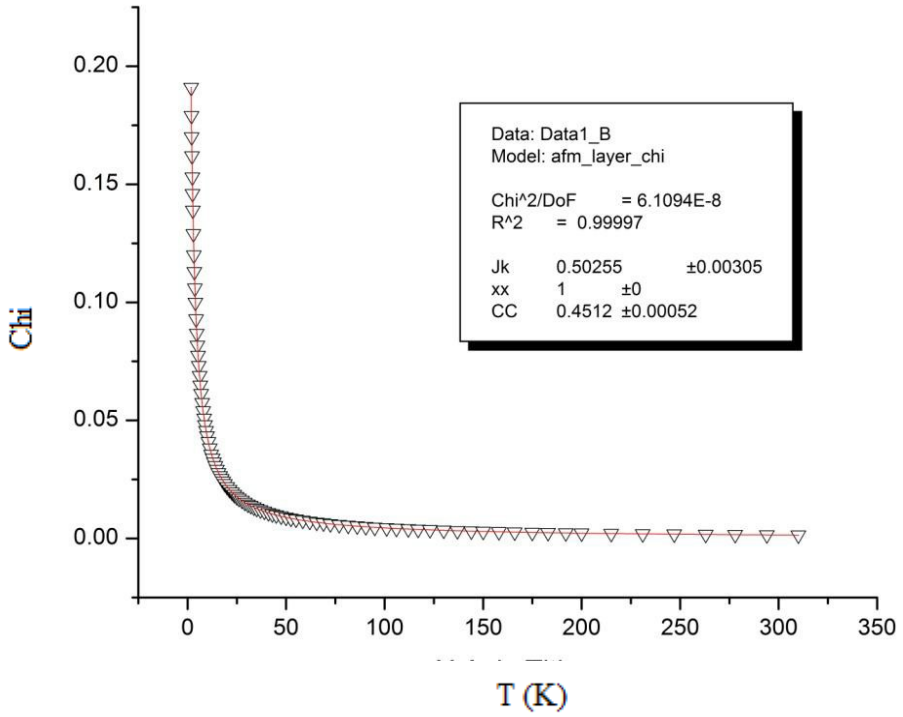

Figure 3.39 Plot and fitting of Chi V T for compound **3.42.**

Compound 3.42 showed very similar, very weak antiferromagnetic exchange to compound **3.41**. It was fit using the same 2D-Heisenberg model giving a Curie constant of 0.45, and J = -0.50K.

Compound 3.43 75:25 Cl:Br

Table 3.16 Geometric features of the halide···halide contacts in **3.43.**

contact	D(Å)	Θ1	Θ2	τ	Inter/intra
Cl1...Cl3	4.5775(7)	144.336(19)	168.433(19)	-73.70(7)	Intra
Cl2...Cl2	3.9507(13)	116.83(2)	116.83(2)	180.00(4)	Inter
Cl4...Cl4	3.7646(11)	165.04(4)	165.04(4)	180.00(6)	inter

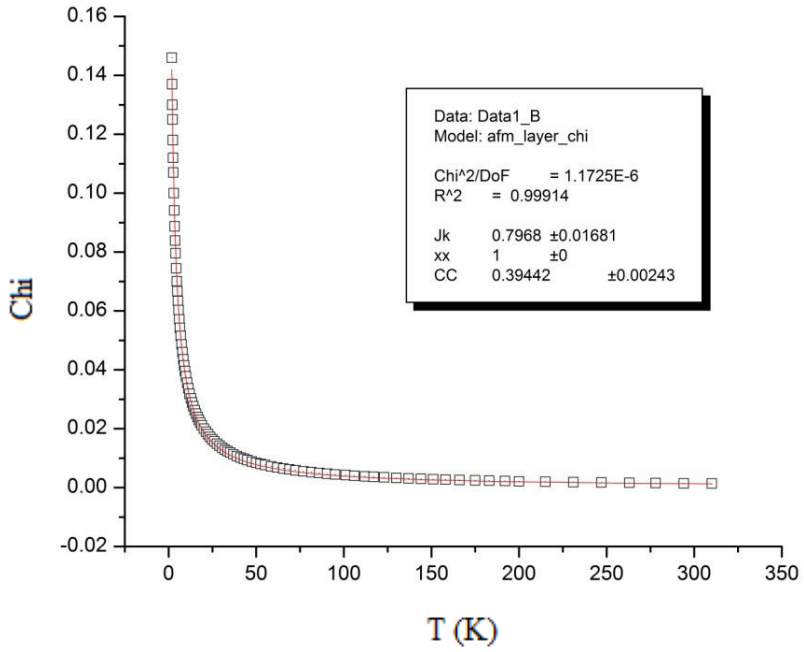

Figure 3.40 Plot and fitting of Chi V T for compound **3.43.**

Again this compound gave similar magnetic data to the pure tetrachlorocuprate complex, with very weak antiferromagnetic exchange fit again using the same model with a curie constant of 0.39, and J = -0.80K.

Compounds **3.45-3.47** have a ladder arrangement of the anions. They are "strong-rung" systems with the "rung" interactions being stronger than the "rails". The data suggests that the rail interactions may be ferromagnetic which is interesting and slightly unusual[40].

Compound 3.45 25:75 Cl:Br

Although compound 3.45 shows similar magnetic exchange to compounds **3.46** and **3.47**, it has a slightly different exchange pathway (figure 3.41).

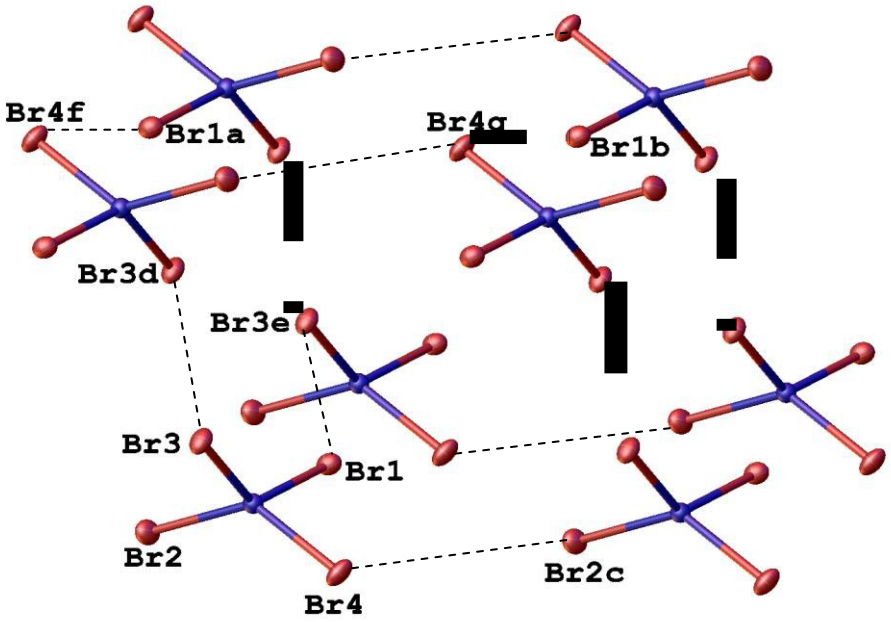

Figure 3.41 Possible magnetic exchange pathway for compound **3.45**. Dashed lines represent through space halide...halide contacts. Cations are omitted for clarity.

Table 3.17 Geometric features of the halide···halide contacts in **3.45**.

contact	D (Å)	Θ1 (^{0})	Θ2(^{0})	T (^{0})	Inter/intra
Br1...Br3e	4.4074(10)	106.65(3)	136.46(3)	134.56(6)	intra
Br3...Br3d	3.7524(15)	149.56(4)	149.56(4)	180.00(11)	inter
Br2c...Br4	4.4241(10)	122.18(3)	141.98(3)	122.14(6)	intra
Br4f···Br1a	4.6442(5)Å	99.38(3)	161.71(3)	-89.46(10)	inter

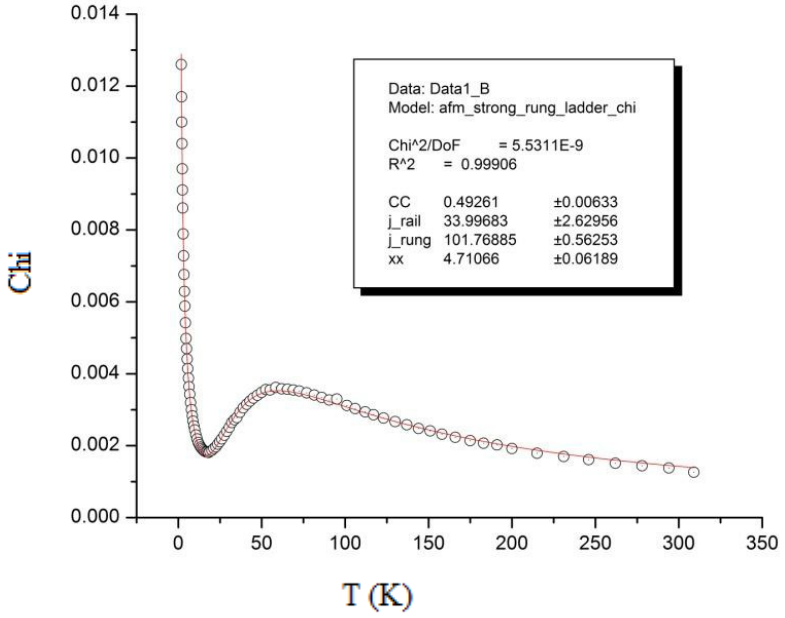

Figure 3.42 Plot and fitting of Chi V T for compound **3.45.**

The ladder fitting of compound **3.45** gives a Curie constant of 0.49. The rail interactions have J = -33K, and rung interaction of J = -101K. The Br2···Br2 interaction is likely to be the rung interaction as it has a τ angle of 180° which has been shown to lead to the strongest double halide bridge interactions.

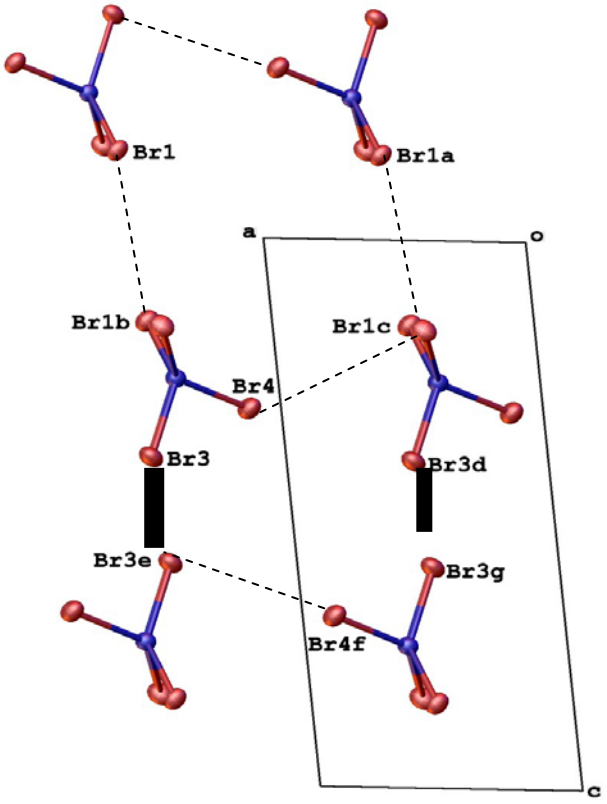

Figure 3.43 Possible magnetic exchange pathway for compound **3.47**. Dashed lines represent through space halide...halide contacts. Cations are omitted for clarity.

The magnetic pathway for compounds **3.46** and **3.47** is shown in figure 3.43. Unfortunately magnetic data for compound **3.46** was not able to be obtained, but it is safe to speculate that it is likely to show similar magnetic exchange to compound **3.47**, as they have very very similar structures.

Compound 3.47 0:100 Cl:Br

Table 3.18 Geometric features of the halide···halide contacts in **3.47.**

contact	D (Å)	Θ1 (^{0})	Θ2(^{0})	T (^{0})	Inter/intra
Br1...Br1b	4.8900(6)	152.181(17)	152.181(17)	180.00(4)	inter
Br3...Br3e	4.6278(7)	144.252(18)	144.252(18)	180.00(4)	inter
Br3c...Br4	4.5888(5)	88.332(15)	148.178(16)	-105.92(4)	intra

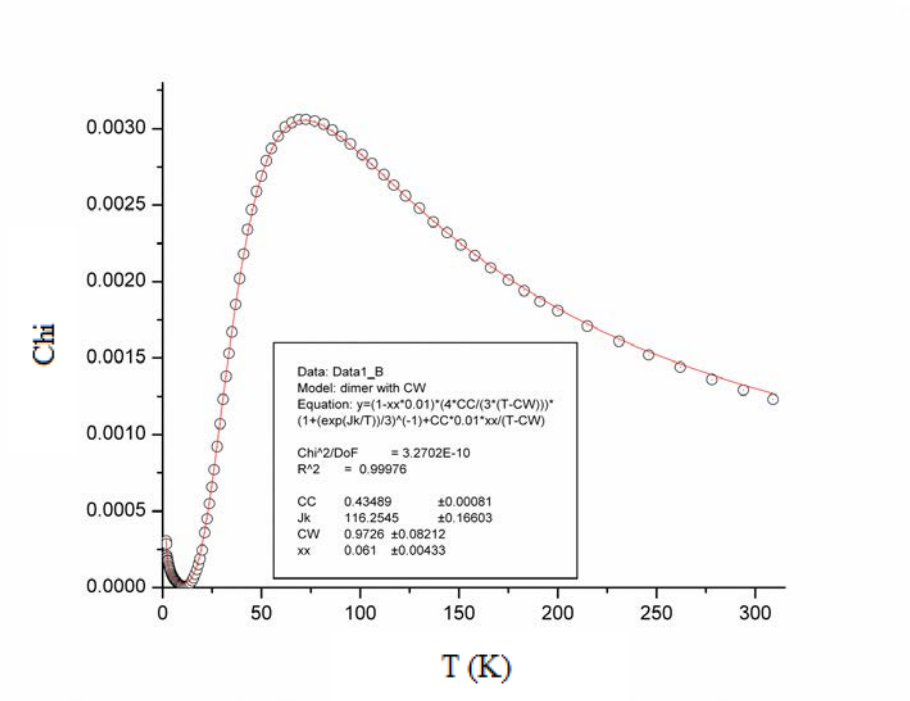

Figure 3.44 Plot and fitting of Chi V T for compound **3.47**

The data for compound **3.47** is also fitted to a strong rung model (figure 3.44) with a Curie constant of 0.43 and J= 116K. Either of the contacts with a τ angle of 180° could be the strong rung interaction.

3.6 Conclusions

A combination of the differing anion trans angles and the anion halide ratios have been shown to be an indicator of different crystal structures within a series of an individual DMPY isomer. Even though there is a significant amount of error in the halide ratio determination of the compounds, which require further analysis for more accurate values, they have been shown to still be valid in showing general trends within a series. Throughout the series bromine is dominant over chlorine in the halide ratio of the anions. This was the case for all isomers with the anions halides being mostly bromine when the experimental solution contained 25% or more bromine.

The 2,4 isomer series has shown that having a methyl group adjacent to the hydrogen bonding pyridine nitrogen gives long halide...halide contacts caused by the methyl group protruding into the anion layers, forcing the anions apart. These results suggest the 2,3, 2,5, and 2,6 DMPY isomers would likely give a similar result as the hydrogen bonding interactions play an important role in the structural stability of these compounds. The 2,6 isomer may have even greater anion separation due to methyl groups on both positions adjacent to the nitrogen.

For both the 3,4 and 3,5 isomers the geometry of the cations did not have as large an effect on the anion separation compared to the 2,4 isomer, as they did not have a methyl group adjacent the the hydrogen bonding nitrogen to protrude into the anion layer. The main factor affecting the halide...halide contact distances was the anions Cl:Br ratio.

The 3,5 isomer compounds with 35% or less bromine in the initial solution were the only 3,5 compounds with short enough halide···halide compounds for possible magnetic exchange. Although no magnetic data was able to be obtained, following the trends of the 3,4 isomer it

is unlikely the compounds are likely to show any significant antiferromagnetic interactions due to being mostly chloride anions.

The 3,4 isomer compounds showed a range of magnetic results. Compounds 3.41-3.43 all showed very weak antiferromagnetic exchange, which is not unexpected being mostly chloride containing anions.

Compounds 3.45-3.47 showed particularly interesting magnetic properties. All of the compounds were fit to a strong rung model, and on initial inspection appear to have ferromagnetic rails which has rarely been seen before.[42]

Chapter 4

Imidazolium tetrahalocuprates

4.1 Introduction

As there are no imidazolium tetrahalocuprates reported in the literature, it was proposed to synthesise a range of ions with varying R groups (figure 4.1).

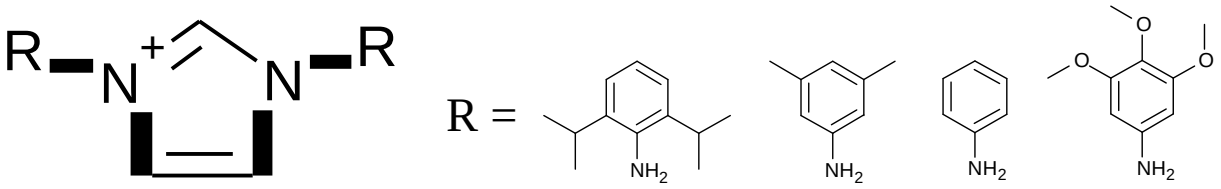

Figure 4.1 General structure of proposed imidazolium ions to try and form tetrahalocuprates

To briefly recap the potential benefits of using imidazolium ions in the formation of tetrahalocuprate over the conventional methods; they are often synthesised as Cl^- or Br^- salts, they are synthesised as cations so do not require acid protonation, and there is a large range of R substituents that may be used. The preparations of these imidazolium ions is based on literature procedures (figure 4.2).

1)

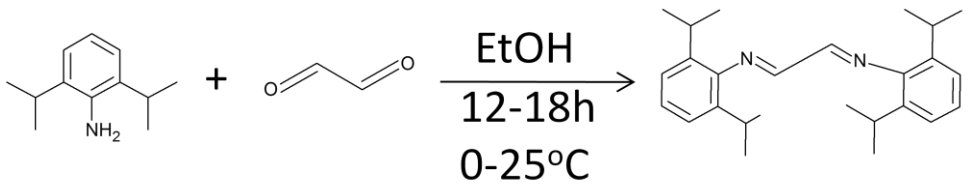

2)

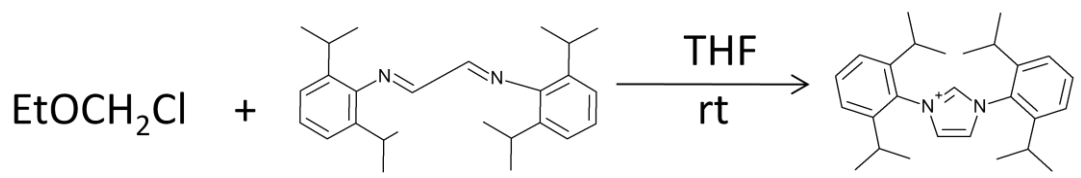

Figure 4.2 Reactions scheme for the formation of imidazolium ions, using 2,6-diisopropylaniline as an example

Early results using the 2,6-diisopropylaniline imidazolium ion suggested that having substituted phenyl R groups lead to the ions having too much steric bulk to give tetrahalocuprates with close enough anion interactions to have possible magnetic exchange pathways. There were no halide···halide distances between anions of less than 9Å. From this result it was decided that smaller R groups were needed, such as tert-butyl, ethyl and methyl. Although the imidazolium salts were easy to synthesise, tetrahalocuprate formation due to solubility issues, proved to be more challenging, resulting in few crystallising in the available time. Although it was proposed that using imidazolium ions would remove the need for acid protonation, in some cases e.g. the ethyl substituted imidazolium ion, acid was needed to solubilise both the imidazolium ion and copper salt in the same solution.

4.2 1,3 bis-(2,6-diisopropylphenyl)imidazolium

Reaction of copper(II) chloride with 2 equivalents of 1,3 bis-(2,6-diisopropylphenyl)imidazolium chloride in isopropanol gave 1,3-Bis(2,6-di-isopropylphenyl)imidazole.Cu_2Cl_6, (compound **4.2**). Single crystals suitable for X-ray diffraction were obtained by slow evaporation. Crystals of this compound form in the triclinic space group P -1.

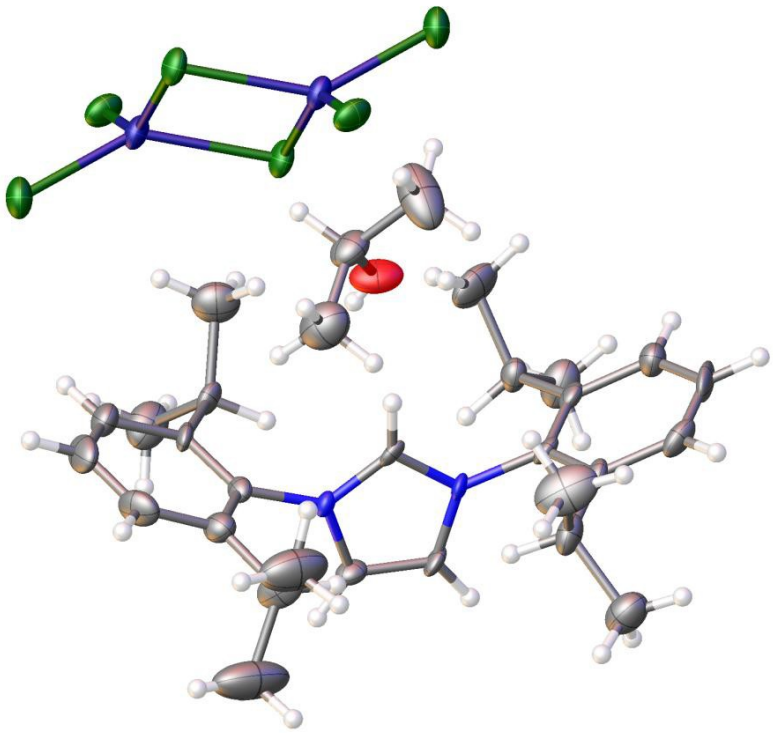

Figure 4.3 Molecular unit of compound **4.1** showing Cu_2Cl_6 moiety with a single imidazolium cation and one isopropanol solvent molecule.

The molecular unit of compound **4.2** contains a imidazolium ion, an isopropyl solvent molecule and a $CuCl_3$ ion, which is half of the di-copper unit seen in figure 4.3. The largest Cl-Cu-Cl angles about each copper(II) atom are 144.48(5)° and 140.52(5)° giving each copper a geometry between square planar and tetrahedral. The average Cu-Cl bond length is normal at 2.243(1)Å.

The isopropylphenyl groups are angled towards each other with respect to the imidazole, with fold angles of 123.73° and 124.43°.

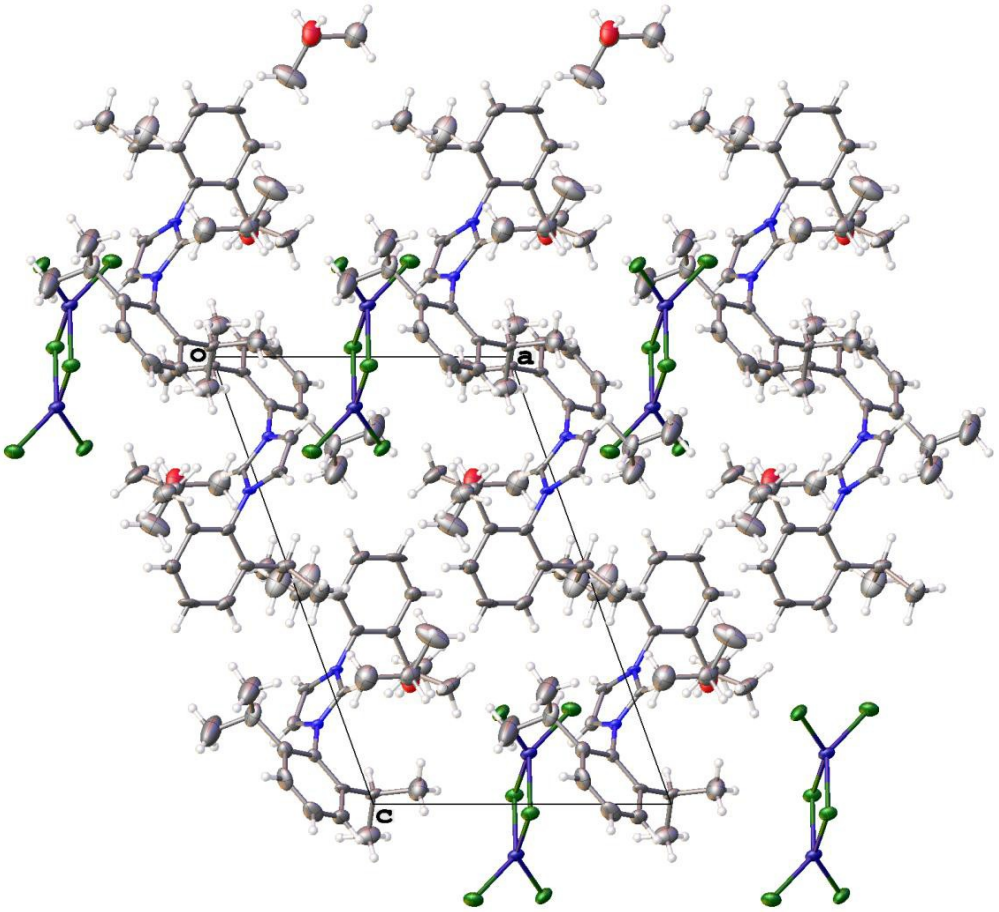

Figure 4.4 Packing diagram of the ac-plane of compound **4.2**.

Crystals of compound **4.2** form two dimensional layers (figure 4.4) with non bonded chains of imidazolium ions. The copper anions sit between the chains with the non-bridging chlorides sitting near the central imidazole part of the cations. The diisopropylphenyl substituents sit between the di-copper anions, and due to their size separate the anions to such an extent that there are no halide···halide contacts anywhere near short enough to have possible magnetic exchange interactions.

4.3 N,N-di-*tert*-butyl imidazolium

Reaction of N,N-di-*tert*-butyl imidazolium chloride with copper(II) chloride in conc HCl resulted in a green solution which crystalised into two different polymorphs within the same vial; one in the form of red block shaped crystals (compound **4.3a**) and the other green needle like crystals (compound **4.3b**). Although the aim of using imidazolium cations was to remove the requirement of acid, in this case it was needed due to solubility issues. Single crystals suitable for x-ray diffraction were obtained for both polymorphs.

4.3a Red crystals

The red crystals (**4.3a**) crystallise in the monoclinic spacegroup P21/c.

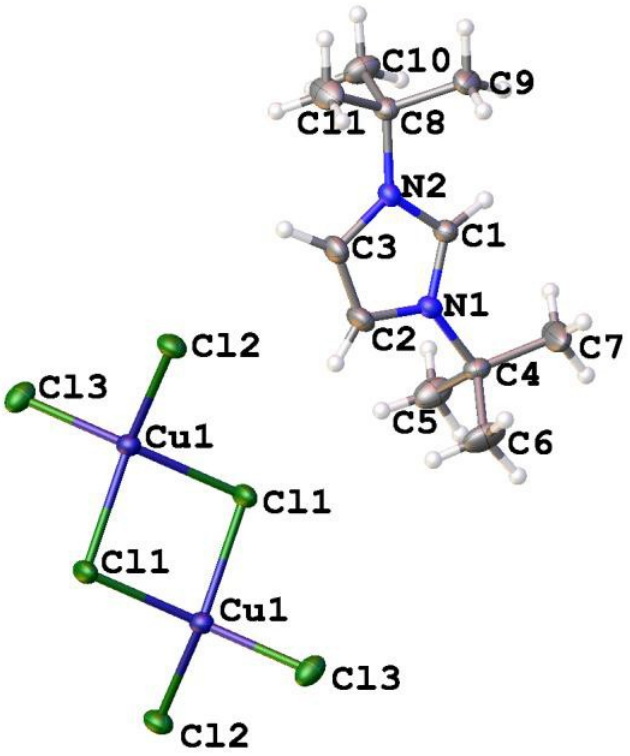

Figure 4.4 molecular unit of **4.2** showing di-copper (II) moiety with a single imidalolium ion

The Molecular unit contains a single imidazolium cation, and half of the di-copper(II) moiety shown in figure 4.1. The angles Cl3-Cu1-Cl1 and Cl2-Cu1-Cl1 are both approximately 139°, therefore the geometry about each copper(II) is nearly half way between square planar and tetrahedral geometry. The Cu1-Cl3 and Cu1-Cl2 are similar, with an average of 2.20Å. The bridging Cu1-Cl1 bonds are slightly longer at 2.3290(4) Å.

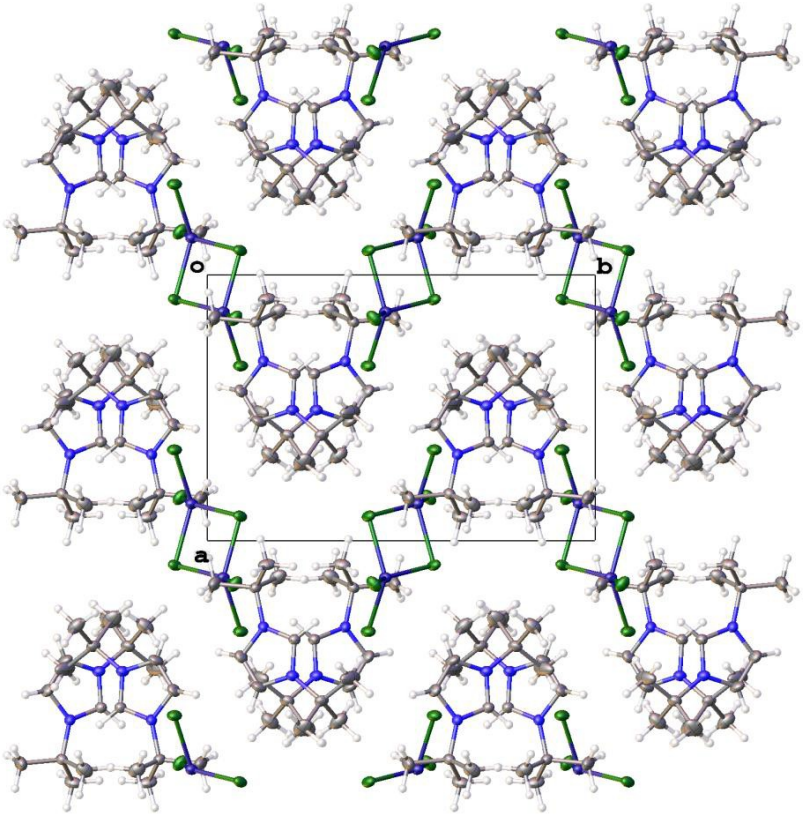

Figure 4.5 packing diagram of the ab plane of compound **4.3a**

The crystals pack into isolated layers of anions and cations (Figure 4.2). The imidazolium ions alternate orientation between each layer, as would be expected, to allow for the bulky tertiary-butanol group packing. There are no halide...halide contacts short enough so any magnetic pathways are unlikely.

4.3b Green crystals

Unfortunately the crystal structure of the green crystals is still only partially solved and still remains a bit of a mystery. They were also late results in the project and there was insufficient time to repeat the experiment, so the following is a very tentative result.

From the current solution of the crystal structure (figure 4.6) there appears to be a 1:1 ratio of imidazloium ions to tetrachlorocuprate anions, which in itself cannot be fully correct as this leads to a charge inbalance. But after multiple attempts at solving the structure, all attempts included tetrachlorocuprate anions to a fair degree of certainty, which suggests a possible tetrachlorocuprate intermediate to the formation of the di-copper structure.

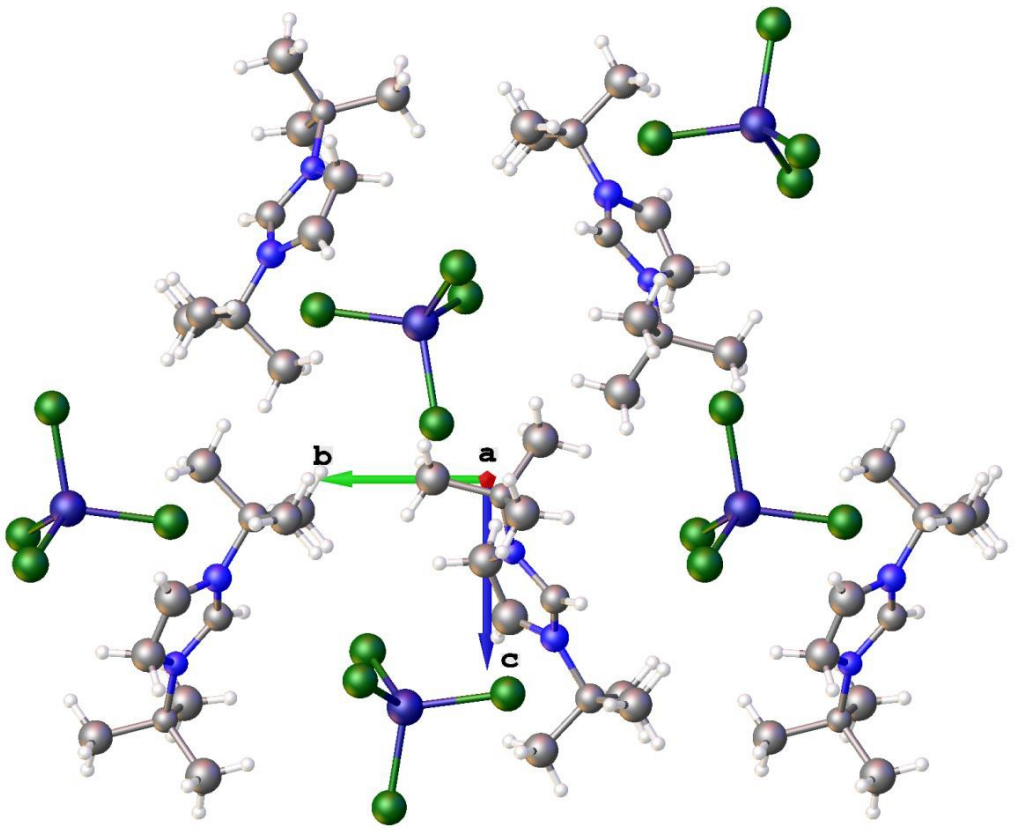

Figure 4.6 Tentative crystal structure of compound **4.3b** showing likely tetrachlorocuprate anions

4.4 Conclusions

From the complexes discussed in this chapter, although few in number, it is strongly suggested that the imidazolium ions were too large to give compounds with possible magnetic exchange interactions. Work on synthesising a number of other NN-di-substituded phenyl-imidazolium ions was undertaken but none successfully isolated. In hindsight they were unlikely to have formed copperhalide complexes with possible magnetic exchange as the substitution of the phenyl rings would have been just as sterically hindering as compound **4.2.** Some work using NN-diethylimidazolium was undertaken to see if the smaller N substituents lead to short enough halide···halide contacts to have possible magnetic exchange, but none crystallised in time for analysis. To further this work it would be worth investigating the diethyl imidazolium further as well as NN-dimethylimidazolium.

Chapter 5

Conclusion

This thesis has described the formation of three series of tetrahalocuprate complexes using different organic cations. The cations used in each series are; (1) 5-amino-2-substituted-pyridines, (2) different dimethypyridine isomers, (3) imidazolium salts. The structure of these complexes was investigated using X-ray crystallography.

The 5-amino-2-substituted-pyridine series was compared to previously reported, analogous 2-amino-5-substituted-pyridine complexes. The study of the 5-amino series showed there was a large effect on the compounds by only swapping the amino and substituent groups positions, resulting in four different structure types; (1) the common two isolated cations to a single anion motif, (2) extra bromine substitution in the 6 position in the tetrabromocuprates, (3) substituted Cu_3 chains and (4) water bridged copper chloride chains in the iodo substituted complex. Where magnetic studies were carried out, results showed all of the complexes analysed either had very very weak, or no magnetic exchange at all. As hydrogen bonding has been shown to be such a large contributor to the structure of these compounds future work could be to use di-amino pyridines, as they have the additional hydrogen bonding substituent.

In the dimethylpyridine series the (2,4), (3,5), and (3,4) isomers were used in the preparation of mixed halide tetrahalocuprates. It was found that bromine was dominant over chlorine in the anions with the anions being nearly 100% bromine when over 20% Br was used in the experimental solution. The 2,4 isomer showed no magnetic exchange due to the methyl group adjacent to the hydrogen bonding protonated pyridine nitrogen. Magnetic studies of the 3,5 and 3,4 isomers showed these compounds showed similar trends to the known literature

compounds with the mostly bromide anion complexes having greater magnetic exchange than the complexes which contained mostly chloride anions. Having mixed halide anions has been shown to have structural effects on the compounds, but little effect on the magnetic properties of these compounds as the mixed halide compounds had very similar magnetic results to the compounds with pure chloride or pure bromide anions.

A number of different imidazolium salts were used in attempts to make tetrahalocuprate complexes. The investigation of imidazolium salts, in this study showed them to be unsuitable for preparing tetrahalocuprate complexes with magnetic exchange due to the size of the imidazolium salts used. Although the imidazolium salts were used beause they did not require the use of concentrated acid for protonation, it was found in some cases, when synthesising the tetrahalocuprate complexes, acid was needed due to solubility issues. It is unlikely that imidazoloium ions will form tetrahalocuprate complexes with significant magnetic exchange, however smaller imidazolium ions may show some positive results.

5 Experimental

5.1 General experimental

Melting points were determined using an Electrothermal melting point apparatus and are uncorrected. The Campbell microanalytical laboratory, University of Otago, Dunedin performed elemental analyses.

Magnetic data were collected using a Quantum Design MPMS-XL SQUID magnetometer. Crystals of the samples were powdered and packed into a #3 gelatin capsule. The magnetization of the sample as a function of applied field was collected from 0 to 50 kOe at 1.8 K. Several data points were collected as the field was reduced to zero to check for hysteresis; none was observed. Susceptibility data were taken on samples cooled in zero field over the temperature range from 1.8 to 310 K in an applied field of 1 kOe.

Unless otherwise stated, reagents were obtained from commercial sources and used as received.

The following compounds were prepared using literature procedures: 1,3-di-τ-butylimidazolium chloride[45], 1,3-Bis(2,6-di-isopropylphenyl)imidazolium chloride[46]

Where yields are low compared to similar compounds, it is the yield from the first harvest only and the remaining sample was lost in one of many large earthquakes.

5.2 5-amino-2-substituent tetrahalocuprates

Bis 5-amino-2-methylpyridinium tetrachlorocuprate **2.2a**

5-amino-2-methylpyridine (2mmol, 0.216g) was slurried in 2mL of distilled water. 1mL of conc. HCl was added to the slurry. $CuCl_2.2H_2O$ (1mmol, 0.171g) was then added and stirred until dissolved. The resulting yellow solution was filtered with filter paper and then left in a 10mL beaker for slow evaporation. After approximately one month yellowy brown crystals were harvested by vacuum filtration and washed with a little *tert*-butanol. Yield 0.344g (76%). M.p. 159^0C. I.R. (KBr) 3434(s), 3339(s), 3045(m), 2977(m), 1955(w), 1828(w), 1643(m), 1616(m), 1564(s), 1467(m), 1392(w), 1333(m), 1304(m), 1245(w), 1152(m), 1046(w), 980(w), 915(w), 829(s), 757(m), 694(m), 521(s)

Bis 5-amino-6-bromo-2-methylpyridinium tetrabromorocuprate **2.2b**

5-amino-2-methylpyridine (1mmol, 0.108g) and $CuBr_2$ (0.5mmol, 0.086g) was dissolved in 2 mL of 48% HBr. The resulting purple solution was filtered with filter paper and then left in a 10 mL beaker for slow evaporation. After approximately six months purple/brown crystals were harvested by vacuum filtration and washed with a little *tert*-butanol. Yield 0.082g (39.4%). M.p. 146^0C. I.R. (KBr) 3444(s), 3339(s), 3206(w), 2895(sb), 1937(w), 1751(w), 1638(m), 1611(s), 1580(s), 1554(s), 1451(w), 1359(m), 1335(s), 1299(s), 1113(m), 971(w), 878(m), 840(s), 778(w), 566(m)

Bis -5-amino-2-chloropydridinium tetrachlorocuprate **2.3**

5-amino-2-chloropyridine (2mmol, 0.256g) and $CuCl_2.2H_2O$ (1mmol, 0.171g) were dissolved in conc. HCl (5mL excess) with stirring and gentle heating. The resulting yellow solution was filtered with filter paper and then left in a 10mL beaker for slow evaporation. After approximately 3 month yellowy green crystals were harvested and washed with a little *tert*-butanol. Yield 0.2g (21.6%). M.p. 135^0C. Anal. Found: C, 24.24 H, 2.62 N, 11.09 Calc. for: $C_{10}H_{12}N_4Cl_{6.8}Cu_{1.3}$ C, 23.46 ; H, 2.36 ; N, 10.94 . I.R. (KBr) 3582(m), 3449(m), 2828(sb), 2568(s), 1609(m), 1541(w), 1465(s), 1123(m), 856(m), 834(m), 725(m), 644(m), 514(m)

Bis -5-amino-2-bromopydridinium tetrachlorocuprate **2.4**

5-amino-2-chloropyridine (2mmol, 0.256g) and $CuCl_2.2H_2O$ (1mmol, 0.171g) were dissolved in conc. HCl(5mL excess) with stirring and gentle heating. The resulting yellow solution was filtered with filter paper and then left in a 10mL beaker for slow evaporation. After approximately 3 months yellowy green crystals were harvested and washed with a little *tert*-butanol. Yield 0.305g (27.6%). Other than a crystal structure, no other analysis was carried out as the sample was lost in a large magnitude earthquake. After a number of attempts no further crystals were able to be made in the available time.

Bis 5-amino-2-iodopyridinium tetrachlorocuprate **2.5**

5-amino-2-iodopyridine (2mmol, 0.216g) was slurried in 2mL of distilled water. 1mL of conc. HCl was added to the slurry. $CuCl_2.2H_2O$ (1mmol, 0.171g) was then added and stirred until dissolved. The resulting yellow solution was filtered with filter paper and then left in a 10mL beaker for slow evaporation. After approximately one month yellowy brown crystals were harvested by vacuum filtration and washed with a little *tert*-butanol. Yield 0.1g (15.8%). M.p. 102^0C. Anal. Found: C, 17.89 H, 2.38 N, 8.19 Calc. for: $C_{10}H_{12}N_4O_2Cl_4Cu_{1.27}I_2$ C, 17.2 ; H, 1.73 ; N, 8.02 . I.R. (KBr) 3444(s), 3339(s), 2900(mb), 1940(w), 1900(w), 1621(s), 1589(s), 1540(s), 1445(s), 1380(m), 1336(m), 1303(s), 1144(m), 836(s), 682(w), 645(m), 585(m), 510(s)

5.3 Dimethylpyridine tetrahalocuprates

2,4 dimethylpyridine, 100% Cl, **3.21**

$CuCl_2.2H_2O$ (1.504g, 8.82mmol) was dissolved in 30mL H_2O. In a separate flask 2,4-dimethylpyridine (2mL, 17.64mmol) was mixed with conc. HCl, 37% (10mL excess). The acid solution was added dropwise to the $CuCl_2$ solution with constant magnetic stirring. The combined solution was then filtered through filter paper and left to slow evaporate in a 90mm round crystallizing dish. Yellow crystals formed on standing for approximately 1 month. The crystals were filtered under vacuum and washed with warm *tert*-butanol. Yield 3.13g (82%). M.p. 111^0C. Anal. Found: C, 39.63 H, 4.56 N, 6.61 Calc. for $C_{14}H_{20}N_2Cl_4Cu$: C, 39.88; H, 4.78; N, 6.64. I.R. (KBr) 3253(m), 3010(s), 2919(s), 2891(s), 1991(w), 1920(w), 1844(w), 1636(s), 1618(s), 1521(m), 1292(m), 1036(m), 815(s), 520(m), 487(m)

2,4 dimethylpyridine, 95% Cl, 5% Br **3.22**

$CuCl_2.2H_2O$ (1.429g, 8.379mmol) and $CuBr_2$ (0.099g, 0.441mmol) was dissolved in 30mL H_2O. In a separate flask 2,4-dimethylpyridine (2mL, 17.64mmol) was mixed with conc. HCl, 37% (9.5mL excess) and conc. HBr, 48% (0.4mL excess). The acid solution was added dropwise to the Cu(II) solution with constant magnetic stirring. The combined solution was then filtered through filter paper and left to slow evaporate in a 90mm round crystallizing dish. Orange crystals formed on standing for approximately 1 month. The crystals were filtered under vacuum and washed with warm *tert*-butanol. Yield 2.93g (77.6%). M.p. 93^0C.

Anal. Found: C, 37.60 H, 4.60 N, 6.30 Calc. for $C_{14}H_{20}N_2Cl_{3.39}CuBr_{0.6}$: C, 37.5; H, 4.5; N, 6.25. I.R. (KBr) 3240(w), 2962(s), 2885(s), 1991(w), 1919(w), 1841(w), 1634(s), 1616(s), 1522(m), 1291(m), 1036(m), 815(s), 520(m), 488(m)

2,4 dimethylpyridine, 75% Cl, 25% Br **3.23**

$CuCl_2.2H_2O$ (1.128g, 6.615mmol) and $CuBr_2$ (0.493g, 2.205mmol) was dissolved in 30mL H_2O. In a separate flask 2,4-dimethylpyridine (2mL, 17.64mmol) was mixed with conc. HCl, 37% (7.5mL excess) and conc. HBr, 48% (2mL excess). The acid solution was added dropwise to the Cu(II) solution with constant magnetic stirring. The combined solution was then filtered through filter paper and left to slow evaporate in a 90mm round crystallizing dish. Red crystals formed on standing for approximately 1 month. The crystals were filtered under vacuum and washed with warm *tert*-butanol. Yield 1.95g (51.1%). M.p. 114^0C. Anal. Found: C, 31.73 H, 3.86 N, 5.39 Calc. for $C_{14}H_{20}N_2Cl_{1.66}CuBr_{2.34}$: C, 31.99; H, 3.83; N, 5.33. I.R. (KBr) 3236(w), 2929(s), 2885(s), 1982(w), 1913(w), 1841(w), 1714(w), 1629(s), 1616(s), 1523(m) 1486(m), 1291(m), 1233(m), 1036(m), 813(s), 520(m)

2,4 dimethylpyridine, 50% Cl, 50% Br **3.24**

$CuCl_2.2H_2O$ (0.725g, 4.41mmol) and $CuBr_2$ (0.985g, 4.41 mmol) was dissolved in 30mL H_2O. In a separate flask 2,4-dimethylpyridine (2mL, 17.64mmol) was mixed with conc. HCl, 37% (5mL excess) and conc. HBr, 48% (4mL excess). The acid solution was added dropwise to the Cu(II) solution with constant magnetic stirring. The combined solution was then

filtered through filter paper and left to slow evaporate in a 90mm round crystallizing dish. Red crystals formed on standing for approximately 1 month. The crystals were filtered under vacuum and washed with warm *tert*-butanol. Yield 3.65g (95.6%). M.p. 112^0C. Anal. Found: C, 32.15 H, 4.07 N, 5.40 Calc. for $C_{14}H_{20}N_2Cl_{1.60}CuBr_{2.40}$: C, 31.82; H, 3.82; N, 5.30. I.R. (KBr) 3236(w), 2928(s), 2889(s), 1984(w), 1909(w), 1820(w), 1718(w), 1634(s), 1616(s), 1523(m), 1291(m), 1234(m), 1035(m), 812(s), 520(m)

2,4 dimethylpyridine, 25% Cl, 75% Br **3.25**

$CuCl_2.2H_2O$ (0.376g, 2.205mmol) and $CuBr_2$ (1.478g, 6.615mmol) was dissolved in 30mL H_2O. In a separate flask 2,4-dimethylpyridine (2mL, 17.64mmol) was mixed with conc. HCl, 37% (2.5mL excess) and conc. HBr, 48% (6mL excess). The acid solution was added dropwise to the Cu(II) solution with constant magnetic stirring. The combined solution was then filtered through filter paper and left to slow evaporate in a 90mm round crystallizing dish. Yellow crystals formed on standing for approximately 1 month. The crystals were filtered under vacuum and washed with warm *tert*-butanol. Yield 2.10g (55%). M.p. 115^0C. Anal. Found: C, 28.57 H, 3.47 N, 4.75 Calc. for $C_{14}H_{20}N_2CuBr_4$: C, 28.05; H, 3.36; N, 4.67. I.R. (KBr) 3235(w), 2928(s), 2889(s), 1978(w), 1894(w), 1807(w), 1712(w), 1633(s), 1617(s), 1527(m), 1369(m), 1290(m), 1233(m), 1035(m), 807(s), 520(m)

2,4 dimethylpyridine, 5% Cl, 95% Br **3.26**

$CuCl_2.2H_2O$ (0.076 g, 0.441mmol) and $CuBr_2$ (1.872g, 8.379mmol) was dissolved in 30mL H_2O. In a separate flask 2,4-dimethylpyridine (2mL, 17.64mmol) was mixed with conc. HCl, 37% (0.5mL excess) and conc. HBr, 48% (7.6mL excess). The acid solution was added dropwise to the Cu(II) solution with constant magnetic stirring. The combined solution was then filtered through filter paper and left to slow evaporate in a 90mm round crystallizing dish. Yellow crystals formed on standing for approximately 1 month. The crystals were filtered under vacuum and washed with warm *tert*-butanol. Yield 1.64g (43%). M.p. 118^0C. Anal. Found: C, 28.42 H, 3.36 N, 4.87 Calc. for $C_{14}H_{20}N_2CuBr_4$: C, 28.05; H, 3.36; N, 4.67. I.R. (KBr) 3240(w), 3071(s), 2924(s), 1976(w), 1896(w), 1796(w), 1716(w), 1633(s), 1617(s), 1520(m), 1369(m), 1290(m), 1233(m), 1034(m), 807(s), 520(m)

2,4 dimethylpyridine 100% Br **3.27**

$CuBr_2$ (1.97g, 8.82mmol) was dissolved in 30mL H_2O. In a separate flask 2,4-dimethylpyridine (2mL, 17.64mmol) was mixed with conc. HBr, 48% (8mL excess). The acid solution was added dropwise to the $CuBr_2$ solution with constant magnetic stirring. The combined solution was then filtered through filter paper and left to slow evaporate in a 90mm round crystallizing dish. Yellow crystals formed on standing for approximately 1 month. The crystals were filtered under vacuum and washed with warm *tert*-butanol. Yield 1.52g (39.8%). M.p. 121^0C. Anal. Found: C, 28.1 H, 3.36 N, 4.64 Calc. for $C_{14}H_{20}N_2CuBr_4$: C,

28.05; H, 3.36; N, 4.67. I.R. (KBr) 3067(s), 2928(s), 1980(w), 1889(w), 1796(w), 1634(s), 1617(s), 1525(m), 1398(m), 1292(m), 1233(m), 1034(m), 807(s), 456(m)

3,5 dimethylpyridine, 100% Cl, **3.31**

$CuCl_2.2H_2O$ (1.504g, 8.82mmol) was dissolved in 30mL H_2O. In a separate flask 3,5-dimethylpyridine (2mL, 17.64mmol) was mixed with conc. HCl, 37% (10mL excess). The acid solution was added dropwise to the $CuCl_2$ solution with constant magnetic stirring. The combined solution was then filtered through filter paper and left to slow evaporate in a 90mm round crystallizing dish. Yellow crystals formed on standing for approximately 1 month. The crystals were filtered under vacuum and washed with warm *tert*-butanol. Yield 2.92g (76.5%). M.p. 123^0C. Anal. Found: C, 39.63 H, 4.81 N, 6.64 Calc. for $C_{14}H_{20}N_2Cl_4Cu$: C, 39.88; H, 4.78; N, 6.64. I.R. (KBr) 3175(s), 3068(s), 1901(w), 1836(w), 1624(w), 1547(s), 1458(m), 1251(s), 1138(m), 931(m), 811(s), 679(s), 509(w)

3,5 dimethylpyridine, 95% Cl, 5% Br **3.32**

$CuCl_2.2H_2O$ (1.429g, 8.379mmol) and $CuBr_2$ (0.099g, 0.441mmol) was dissolved in 30mL H_2O. In a separate flask 3,5-dimethylpyridine (2mL, 17.64mmol) was mixed with conc. HCl, 37% (9.5mL excess) and conc. HBr, 48% (0.4mL excess). The acid solution was added dropwise to the Cu(II) solution with constant magnetic stirring. The combined solution was then filtered through filter paper and left to slow evaporate in a 90mm round crystallizing dish. Orange crystals formed on standing for approximately 1 month. The crystals were

filtered under vacuum and washed with warm *tert*-butanol. Yield 2.93g (77.6%). M.p. 118^0C. Anal. Found: C, 38.09 H, 4.64 N, 6.43 Calc. for $C_{14}H_{20}N_2Cl_4Cu$: C, 39.88; H, 4.78; N, 6.64. I.R. (KBr) 3175(s), 3071(s), 1900(w), 1625(m), 1545(s), 1456(m), 1251(s), 1138(m), 981(m), 930(m), 810(s), 679(s)

3,5 dimethylpyridine, 75% Cl, 25% Br **3.33**

$CuCl_2.2H_2O$ (1.128g, 6.615mmol) and $CuBr_2$ (0.493g, 2.205 mmol) was dissolved in 30mL H_2O. In a separate flask 3,5-dimethylpyridine (2mL, 17.64mmol) was mixed with conc. HCl, 37% (7.5mL excess) and conc. HBr, 48% (2mL excess). The acid solution was added dropwise to the Cu(II) solution with constant magnetic stirring. The combined solution was then filtered through filter paper and left to slow evaporate in a 90mm round crystallizing dish. Red crystals formed on standing for approximately 1 month. The crystals were filtered under vacuum and washed with warm *tert*-butanol. Yield 3.51g (91.9%). M.p. 105^0C. Anal. Found: C, 32.36 H, 3.89 N, 5.46 Calc. for $C_{14}H_{20}N_2Cl_{1.57}CuBr_{2.43}$: C, 31.74; H, 3.81; N, 5.29. I.R. (KBr) 3175(s), 3071(s), 1896(w), 1831(w), 1623(m), 1545(s), 1457(m), 1251(s), 1137(m), 1049(w), 926(m), 807(s), 678(s), 508(w)

3,5 dimethylpyridine, 50% Cl, 50% Br **3.34**

$CuCl_2.2H_2O$ (0.725g, 4.41mmol) and $CuBr_2$ (0.985g, 4.41mmol) was dissolved in 30mL H_2O. In a separate flask 3,5-dimethylpyridine (2mL, 17.64mmol) was mixed with conc. HCl, 37% (5mL excess) and conc. HBr, 48% (4mL excess). The acid solution was added dropwise

to the Cu(II) solution with constant magnetic stirring. The combined solution was then filtered through filter paper and left to slow evaporate in a 90mm round crystallizing dish. Red crystals formed on standing for approximately 1 month. The crystals were filtered under vacuum and washed with warm *tert*-butanol. Yield 3.11g (81.5%). M.p. 103^0C. Anal. Found: C, 28.81 H, 3.50 N, 4.87 Calc. for $C_{14}H_{20}N_2Cl_{0.33}Cu\ Br_{3.67}$: C, 28.75; H, 3.45; N, 4.79. I.R. (KBr) 3041(s), 1976(w), 1911(w), 1831(w), 1751(w), 1623(w), 1568(m), 1465(w), 1268(m), 1043(w), 986(w), 829(m), 675(m)

3,5 dimethylpyridine, 25% Cl, 75% Br **3.35**

$CuCl_2.2H_2O$ (0.376 g, 2.205mmol) and $CuBr_2$ (1.478g, 6.615 mmol) was dissolved in 30mL H_2O. In a separate flask 3,5-dimethylpyridine (2mL, 17.64mmol) was mixed with conc. HCl, 37% (2.5mL excess) and conc. HBr, 48% (6mL excess). The acid solution was added dropwise to the Cu(II) solution with constant magnetic stirring. The combined solution was then filtered through filter paper and left to slow evaporate in a 90mm round crystallizing dish. Yellow crystals formed on standing for approximately 1 month. The crystals were filtered under vacuum and washed with warm *tert*-butanol. Yield 3.28g (86%). M.p. 100^0C. Anal. Found: C, 28.34 H, 3.31 N, 4.73 Calc. for $C_{14}H_{20}N_2CuBr_4$: C, 28.05; H, 3.36; N, 4.67. I.R. (KBr) 3175(s), 3069(s), 1896(w), 1832(w), 1623(m), 1545(s), 1458(s), 1251(s), 1137(m), 1048(m), 978(m), 926(m), 806(s), 677(s), 508(w)

3,5 dimethylpyridine, 5% Cl, 95% Br **3.36**

$CuCl_2.2H_2O$ (0.076g, 0.441mmol) and $CuBr_2$ (1.872g, 8.379mmol) was dissolved in 30mL H_2O. In a separate flask 3,5-dimethylpyridine (2mL, 17.64mmol) was mixed with conc. HCl, 37% (0.5mL excess) and conc. HBr, 48% (7.6mL excess). The acid solution was added dropwise to the Cu(II) solution with constant magnetic stirring. The combined solution was then filtered through filter paper and left to slow evaporate in a 90mm round crystallizing dish. Yellow crystals formed on standing for approximately 1 month. The crystals were filtered under vacuum and washed with warm *tert*-butanol. Yield 2.17g (56.9%). M.p. 94^0C. Anal. Found: C, 28.25 H, 3.38 N, 4.71 Calc. for $C_{14}H_{20}N_2CuBr_4$: C, 28.05; H, 3.36; N, 4.67. I.R. (KBr) 3045(s), 2895(s), 1976(m), 1906(m), 18319w), 1748(w) 1625(w), 1564(s), 1460(m), 1268(s), 1042(m), 991(m), 919(w), 827(s), 727(m), 675(s), 536(w)

3,5 dimethylpyridine 100% Br **3.37**

$CuBr_2$ (1.97g, 8.82mmol) was dissolved in 30mL H_2O. In a separate flask 3,5-dimethylpyridine (2mL, 17.64mmol) was mixed with conc. HBr, 48% (8mL excess). The acid solution was added dropwise to the $CuBr_2$ solution with constant magnetic stirring. The combined solution was then filtered through filter paper and left to slow evaporate in a 90mm round crystallizing dish. Yellow crystals formed on standing for approximately 1 month. The crystals were filtered under vacuum and washed with warm *tert*-butanol. Yield 2.19g (57.4%). M.p. 105^0C. Anal. Found: C, 28.19 H, 3.36 N, 4.73 Calc. for $C_{14}H_{20}N_2CuBr_4$: C,

28.05; H, 3.36; N, 4.67. I.R. (KBr) 3030(s), 2893(s), 1976(m), 1908(m), 1833(w), 1751(w), 1628(m), 1564(s), 1467(m), 1268(s), 1042(m), 923(w), 828(s), 727(m), 675(s), 536(w)

3,5 dimethylpyridine, 70% Cl, 30% Br **3.38**

$CuCl_2.2H_2O$ (1.053g, 6.174mmol) and $CuBr_2$ (0.59g, 2.646mmol) was dissolved in 30mL H_2O. In a separate flask 3,5-dimethylpyridine (2mL, 17.64mmol) was mixed with conc. HCl, 37% (7 mL excess) and conc. HBr, 48% (2.4mL excess). The acid solution was added dropwise to the Cu(II) solution with constant magnetic stirring. The combined solution was then filtered through filter paper and left to slow evaporate in a 90mm round crystallizing dish. Red crystals formed on standing for approximately 1 week. The crystals were filtered under vacuum and washed with warm *tert*-butanol. Yield 3.41g (71.4%). M.p. 105^0C. Anal. Found: C, 30.09 H, 3.65 N, 5.00 Calc. for $C_{14}H_{20}N_2Cl_{1.30}CuBr_{2.70}$: C, 31.04; H, 3.72; N, 5.17. I.R. (KBr) 3175(s), 3069(s), 1896(w), 1832(w), 1623(m), 1545(s), 1458(m), 1251(s), 1137(m), 1048(m), 978(m), 926(m), 806(s), 725(w), 677(s), 530(w)

3,5 dimethylpyridine, 65% Cl, 35% Br **3.39**

$CuCl_2.2H_2O$ (0.977g, 5.733mmol) and $CuBr_2$ (0.69g, 3.087mmol) was dissolved in 30mL H_2O. In a separate flask 3,5-dimethylpyridine (2mL, 17.64mmol) was mixed with conc. HCl, 37% (6.5mL excess) and conc. HBr, 48% (2.8mL excess). The acid solution was added dropwise to the Cu(II) solution with constant magnetic stirring. The combined solution was

then filtered through filter paper and left to slow evaporate in a 90mm round crystallizing dish. Red crystals formed on standing for approximately 1 week. The crystals were filtered under vacuum and washed with warm *tert*-butanol. Yield 3.66g (76.6%). M.p. 103^0C. Anal. Found: C, 29.54 H, 3.55 N, 4.84 Calc. for $C_{14}H_{20}N_2Cl_{1.22}CuBr_{2.78}$: C, 30.79; H, 3.69; N, 5.13. I.R. (KBr) 3058(s), 1893(w), 1831(w), 16239(m), 1547(s), 1458(m), 1315(w), 1251(m), 1137(m), 1048(w), 925(w), 805(s), 676(s)

3,5 dimethylpyridine, 60% Cl, 40% Br **3.310**

$CuCl_2.2H_2O$ (0.902g, 5.292mmol) and $CuBr_2$ (0.788g, 3.528 mmol) was dissolved in 30mL H_2O. In a separate flask 3,5-dimethylpyridine (2mL, 17.64mmol) was mixed with conc. HCl, 37% (6mL excess) and conc. HBr, 48% (3.2mL excess). The acid solution was added dropwise to the Cu(II) solution with constant magnetic stirring. The combined solution was then filtered through filter paper and left to slow evaporate in a 90mm round crystallizing dish. Red crystals formed on standing for approximately 1 week. The crystals were filtered under vacuum and washed with warm *tert*-butanol. Yield 3.60g (68.1%). M.p. 103^0C. Anal. Found: C, 29.37 H, 3.56 N, 4.86 Calc. for $C_{14}H_{20}N_2CuBr_4$: C, 28.05; H, 3.36; N, 4.67. I.R. (KBr) 3041(s), 2893(s), 1976(w), 1908(w), 1833(w), 1751(w), 1628(m), 1568(s), 1463(w), 1320(w), 1268(m), 1141(w), 1042(w), 828(s), 727(m), 675(s)

3,5 dimethylpyridine, 55% Cl, 45% Br **3.311**

$CuCl_2.2H_2O$ (0.827g, 4.851mmol) and $CuBr_2$ (0.887g, 3.969mmol) was dissolved in 30mL H_2O. In a separate flask 3,5-dimethylpyridine (2mL, 17.64mmol) was mixed with conc. HCl, 37% (5.5mL excess) and conc. HBr, 48% (3.6mL excess). The acid solution was added dropwise to the Cu(II) solution with constant magnetic stirring. The combined solution was then filtered through filter paper and left to slow evaporate in a 90mm round crystallizing dish. Red crystals formed on standing for approximately 1 week. The crystals were filtered under vacuum and washed with warm *tert*-butanol. Yield 3.19g (60.3%). M.p. 102^0C. Anal. Found: C, 29.30 H, 3.54 N, 4.87 Calc. for $C_{14}H_{20}N_2CuBr_4$: C, 28.05; H, 3.36; N, 4.67. I.R. (KBr) 3045(s), 2893(s), 1977(w), 1909(w), 1832(w), 1750(w), 1628(m), 1568(s), 1465(m), 1347(w), 1320(w), 1268(s), 1141(w), 1041(m), 991(m), 924(w), 828(s), 727(m), 675(s), 536(w)

3,4 dimethylpyridine, 100% Cl, **3.41**

$CuCl_2.2H_2O$ (1.504g, 8.82mmol) was dissolved in 30mL H_2O. In a separate flask 3,4-dimethylpyridine (2mL, 17.64mmol) was mixed with conc. HCl, 37% (10mL excess). The acid solution was added dropwise to the $CuCl_2$ solution with constant magnetic stirring. The combined solution was then filtered through filter paper and left to slow evaporate in a 90mm round crystallizing dish. Yellow crystals formed on standing for approximately 1 month. The crystals were filtered under vacuum and washed with warm *tert*-butanol. Yield 1.78g (46.6%).

M.p. 136^{0}C. Anal. Found: C, 40.04 H, 4.80 N, 6.67 Calc. for $C_{14}H_{20}N_2Cl_4Cu$: C, 39.88; H, 4.78; N, 6.64. I.R. (KBr) 3045(s), 2902(s), 2031(w), 1974(w), 1916(w), 1795(w), 1729(w), 1633(s), 1589(s), 1520(s), 1484(s), 1229(m), 1160(s), 832(s), 704(m)

3,4 dimethylpyridine, 95% Cl, 5% Br **3.42**

$CuCl_2.2H_2O$ (1.429g, 8.379mmol) and $CuBr_2$ (0.099g, 0.441mmol) was dissolved in 30mL H_2O. In a separate flask 3,4-dimethylpyridine (2mL, 17.64mmol) was mixed with conc. HCl, 37% (9.5mL excess) and conc. HBr, 48% (0.4mL excess). The acid solution was added dropwise to the Cu(II) solution with constant magnetic stirring. The combined solution was then filtered through filter paper and left to slow evaporate in a 90mm round crystallizing dish. Orange crystals formed on standing for approximately 1 month. The crystals were filtered under vacuum and washed with warm *tert*-butanol. Yield 1.38g (36.2%). M.p. 133^{0}C. Anal. Found: C, 38.28 H, 4.62 N, 6.37 Calc. for $C_{14}H_{20}N_2Cl_{3.52}CuBr_{0.48}$: C, 37.88; H, 4.54; N, 6.31. I.R. (KBr) 3054(s), 2906(s), 2028(w), 1972(w), 1913(w), 1794(w), 1727(w), 1633(s), 1589(s), 1520(s), 1484(s), 1230(m), 1160(s), 832(s), 704(m)

3,4 dimethylpyridine, 75% Cl, 25% Br **3.43**

$CuCl_2.2H_2O$ (1.128g, 6.615mmol) and $CuBr_2$ (0.493g, 2.205 mmol) was dissolved in 30mL H_2O. In a separate flask 2,4-dimethylpyridine (2mL, 17.64mmol) was mixed with conc. HCl, 37% (7.5mL excess) and conc. HBr, 48% (2mL excess). The acid solution was added dropwise to the Cu(II) solution with constant magnetic stirring. The combined solution was

then filtered through filter paper and left to slow evaporate in a 90mm round crystallizing dish. Red crystals formed on standing for approximately 1 month. The crystals were filtered under vacuum and washed with warm *tert*-butanol. Yield 2.40g (62.9%). M.p. 116^0C. Anal. Found: C, 33.24 H, 3.93 N, 5.50 Calc. for $C_{14}H_{20}N_2Cl_{2.18}CuBr_{1.82}$: C, 33.52; H, 4.02; N, 5.58. I.R. (KBr) 3054(s), 2906(s), 2004(w), 1958(w), 1902(w), 1774(w), 1718(w), 1633(s), 1592(s), 1522(s), 1482(s), 1159(m), 819(s), 704(m)

3,4 dimethylpyridine, 50% Cl, 50% Br **3.44**

$CuCl_2.2H_2O$ (0.725g, 4.41mmol) and $CuBr_2$ (0.985g, 4.41mmol) was dissolved in 30mL H_2O. In a separate flask 3,4-dimethylpyridine (2mL, 17.64mmol) was mixed with conc. HCl, 37% (5 mL excess) and conc. HBr, 48% (4mL excess). The acid solution was added dropwise to the Cu(II) solution with constant magnetic stirring. The combined solution was then filtered through filter paper and left to slow evaporate in a 90mm round crystallizing dish. Red crystals formed on standing for approximately 1 month. The crystals were filtered under vacuum and washed with warm *tert*-butanol. Yield 3.10g (81.2%). M.p. 112^0C. Anal. Found: C, 29.53 H, 3.46 N, 4.92 Calc. for $C_{14}H_{20}N_2Cl_{1.60}CuBr_{2.40}$: C, 31.82; H, 3.82; N, 5.30. I.R. (KBr) 3057(s), 2902(s), 2004(w), 1954(w), 1896(w), 1770(w), 1712(w), 1633(s), 1591(m), 1524(s), 1482(s), 1159(m), 815(s), 703(m)

3,4 dimethylpyridine, 25% Cl, 75% Br **3.45**

$CuCl_2.2H_2O$ (0.376g, 2.205mmol) and $CuBr_2$ (1.478g, 6.615mmol) was dissolved in 30mL H_2O. In a separate flask 3,4-dimethylpyridine (2mL, 17.64mmol) was mixed with conc. HCl, 37% (2.5 mL excess) and conc. HBr, 48% (6mL excess). The acid solution was added dropwise to the Cu(II) solution with constant magnetic stirring. The combined solution was then filtered through filter paper and left to slow evaporate in a 90mm round crystallizing dish. Yellow crystals formed on standing for approximately 1 month. The crystals were filtered under vacuum and washed with warm *tert*-butanol. Yield 3.41g (89.4%). M.p. 112^0C. Anal. Found: C, 28.85 H, 3.42 N, 4.82 Calc. for $C_{14}H_{20}N_2CuBr_4$: C, 28.05; H, 3.36; N, 4.67. I.R. (KBr) 3041(s), 2902(s), 2004(w), 1897(w), 1764(w), 1709(w), 1634(s), 1590(m), 1523(s), 1485(s), 1237(m), 1198(m), 1165(m), 1023(m), 952(m), 896(m), 819(s), 704(m)

3,4 dimethylpyridine, 5% Cl, 95% Br **3.46**

$CuCl_2.2H_2O$ (0.076g, 0.441mmol) and $CuBr_2$ (1.872g, 8.379mmol) was dissolved in 30mL H_2O. In a separate flask 3,4-dimethylpyridine (2mL, 17.64mmol) was mixed with conc. HCl, 37% (0.5 mL excess) and conc. HBr, 48% (7.6mL excess). The acid solution was added dropwise to the Cu(II) solution with constant magnetic stirring. The combined solution was then filtered through filter paper and left to slow evaporate in a 90mm round crystallizing dish. Orange crystals formed on standing for approximately 1 month. The crystals were filtered under vacuum and washed with warm *tert*-butanol. Yield 2.50g (65.5%). M.p. 113^0C.

Anal. Found: C, 28.25 H, 3.38 N, 4.71 Calc. for $C_{14}H_{20}N_2CuBr_4$: C, 28.05; H, 3.36; N, 4.67. I.R. (KBr) 3056(s), 2906(s), 2005(w), 1897(w), 1766(w), 1709(w), 1634(s), 1590(m), 1525(s), 1485(s), 1237(m), 1198(m), 1165(m), 1023(m), 952(m), 896(m), 818(s), 704(m)

3,4 dimethylpyridine 100% Br **3.47**

$CuBr_2$ (1.97g, 8.82mmol) was dissolved in 30mL H_2O. In a separate flask 3,4-dimethylpyridine (2mL, 17.64mmol) was mixed with conc. HBr, 48% (8mL excess). The acid solution was added dropwise to the $CuBr_2$ solution with constant magnetic stirring. The combined solution was then filtered through filter paper and left to slow evaporate in a 90mm round crystallizing dish. Yellow crystals formed on standing for approximately 1 month. The crystals were filtered under vacuum and washed with warm *tert*-butanol. Yield 2.38g (62.4%). M.p. 121^{0}C. Anal. Found: C, 28.22 H, 3.38 N, 4.71 Calc. for $C_{14}H_{20}N_2CuBr_4$: C, 28.05; H, 3.36; N, 4.67. I.R. (KBr) 3045(s), 2906(s), 2004(w), 1893(w), 1764(w), 1709(w), 1634(s), 1590(m), 1524(s), 1485(s), 1237(m), 1198(m), 1164(m), 1024(m), 951(w), 896(m), 811(s), 704(m)

1,3-di-τ-butylimidazoliumchloride tetrachloropuprate **4.3**

$CuCl_2.2H_2O$ (0.086g, 0.5mmol) and imidazolium chloride (0.216g, 1mmol) were dissolved in MeoH (2mL) and conc. HCl (1mL). The resulting green solution was filtered using filter paper and left in a 10mL beaker for slow evaporation. Both red and green crystals formed after approximately 1 month. A single crystal of each suitable for x-ray diffraction was taken from the solution. Unfortunately the remaining solution and crystals were lost in a large magnitude earthquake so no further analysis was done.

1,3-Bis(2,6-di-isopropylphenyl)imidazolium chloride + $CuCl_2.2H_20$ **4.2**

$CuCl_2.2H_2O$ (0.022g, 0.125mmol) and imidazolium chloride (0.25g, 0.25mmol) were dissolved in isopropanol (10mL) and gently heated for 10-15 minutes. The resulting pale yellow solution was left to slow evaporate in a 10mL beaker. A single crystal suitable for x-ray diffraction was removed. The remaining compound was lost in a large magnitude earthquake so no further analysis was done

Crystallography

Tables **C1 – C6** list crystal data and X-ray experimental details for the thirty crystal structures discussed in this thesis. Selected bond lengths and angles are listed in the discussion of the structures, and the remaining distances and angles, as well as atom coordinates, anisotropic displacement parameters and hydrogen atom coordinates are available from the Chemistry Department, University of Canterbury.

All measurements were made with a Siemens CCD area detector using graphite monochromised Mo Kα (λ = 0.71073 Å) radiation at the temperature indicated in the following tables. The data reduction was performed using SAINT[46]. Intensities were corrected for Lorentz and polaraisation effects and for absorption using SADABS[47]. Space groups were determined from systematic absences and checked for higher symmetry. The structures were solved by direct methods, and refined on F^2 using all data by full-matrix least-squares procedures with OLEX-2[48]. All non-hydrogen atoms were refined with anisotropic displacement parameters. Hydrogen atoms not found were included in calculated positions with isotropic displacement parameters 1.3 times the isotropic equivalent of their carrier carbons. In all cases, final Fourier synthesis showed no significant residual electron density in chemically sensible positions.

Table C1 – Crystal data and X-ray experimental details for **2.2a, 2.2b, 2.3, 2.4 and 2.5**

Compound	**2.2a**	**2.2b**	**2.3**	**2.4**	**2.5**
Empirical formula	$C_{12}H_{18}N_4Cl_4Cu$	$C_{12.02}H_{15.70}N_4Br_{5.98}Cu$	$C_{10}H_{12}Cl_{6.77223}Cu_{1.25}N_4$	$C_{20}H_{24}Br_4Cl_{9.69}Cu_{2.63}N_8$	$C_{10}H_{15.4}Cl_4CuI_2N_4O_2$
Formula weight	423.64	757.89	1015.48	1205.80	679.38
Temperature (K)	113	113	113	113	113
Crystal system	monoclinic	orthorhombic	triclinic	orthorhombic	triclinic
Space group	C2/c	Pbcn	P-1	Cmca	P-1
Unit cell dimensions: a (Å)	12.7406(6)	16.3748(7)	8.1022(4)	14.5660(4)	8.1232(3)
b (Å)	8.0648(6)	8.5967(4)	8.1886(4)	7.9171(2)	8.9577(4)
c (Å)	16.5544(10)	14.9706(8)	14.9984(9)	31.1672(9)	13.9151(7)
α (°)	90.00	90.00	96.869(3)	90.00	79.998(2)
β (°)	90.051(4)	90.00	92.031(3)	90.00	78.4190(10)
γ (°)	90.00	90.00	117.979(2)	90.00	85.351(2)
Volume ($Å^3$)	1700.97(18)	2107.40(17)	867.70(8)	3594.22(17)	975.73(7)
Z	4	4	1	4	2
Density (calculated) (Mg/m^3)	1.654	2.389	1.943	2.228	2.312
Absorption coefficient (mm^{-1})	1.909	12.384	2.597	6.741	4.841
F(000)	860.0	1417.0	502.0	2322.0	638.0
Crystal size (mm)	0.6 × 0.34 × 0.14	0.35 × 0.25 × 0.10	0.28 × 0.28 × 0.04	0.15 × 0.1 × 0.03	0.58 × 0.28 × 0.13
2Theta range for data collection (°)	4.92 to 55°	5.44 to 50.34°	5.5 to 50.5°	5.22 to 55.04°	5.44 to 56.56°
Reflections collected	18268	36190	16720	37960	29067
Independent reflections [R(int)]	1950[0.1537]	1888[0.1046]	3135[0.0940]	2154[0.0859]	4839[0.0260]
Observed reflections [I>2σ(I)]	1780	1338	2559	1730	4369
Data / restraints / parameters	1950/0/97	1888/0/108	3135/0/208	2154/4/124	4839/12/225
Goodness-of-fit on F^2	1.080	0.561	0.890	1.113	1.161
R_1 [I>2sigma(I)	0.0551	0.0258	0.0462	0.0361	0.0247
wR_2 (all data)	0.1445	0.0875	0.1282	0.0843	0.0551

Table C2 – Crystal data and X-ray experimental details for **3.21, 3.22, 3.23, 3.24 and 3.25**

Compound	**3.21**	**3.22**	**3.23**	**3.24**	**3.25**
Empirical formula	$C_{14}H_{20}N_2Cl_4Cu$	$C_{14}H_{20}N_2Cl_{3.39}CuBr_{0.61}$	$C_{14}H_{20}N_2Cl_{1.66}CuBr_{2.34}$	$C_{14}H_{20}N_2Cl_{1.60}CuBr_{2.40}$	$C_{14}H_{20}N_2Cu\ Br_4$
Formula weight	421.66	448.65	262.99	264.20	599.50
Temperature (K)	113	113	113	113	113
Crystal system	monoclinic	monoclinic	monoclinic	monoclinic	monoclinic
Space group	C2/c	C2/c	C2/c	C2/c	C2/c
Unit cell dimensions: a (Å)	19.075(3)	19.1499(8)	19.4225(9)	19.4362(7)	19.7765(7)
b (Å)	7.3083(13)	7.3316(3)	7.4055(3)	7.3971(3)	7.4195(3)
c (Å)	16.116(3)	16.1543(10)	16.2277(11)	16.2149(9)	16.2246(9)
α (°)	90.00	90.00	90.00	90.00	90.00
β (°)	124.877(7)	124.689(2)	124.113(2)	124.0350(10)	123.588(2)
γ (°)	90.00	90.00	90.00	90.00	90.00
Volume ($Å^3$)	1843.2(6)	1864.91(16)	1932.46(18)	1931.89(15)	1983.18(15)
Z	4	4	4	4	4
Density (calculated) (Mg/m^3)	1.520	1.598	1.808	1.817	2.008
Absorption coefficient (mm^{-1})	1.759	2.952	6.205	6.312	9.156
F(000)	860	904.0	1029	1032.8	1148
Crystal size (mm)	0.7 × 0.5 × 0.4	0.7 × 0.25 × 0.25	0.7 × 0.5 × 0.2	0.7 × 0.4 × 0.25	0.5 × 0.4 × 0.3
2Theta range for data collection (°)	5.2 to 69.46°	5.18 to 54.98°	5.06 to 55°	6.06 to 55°	4.94 to 55°
Reflections collected	25925	20325	21025	20486	22010
Independent reflections [R(int)]	3511[0.0331]	2148[0.0290]	2223[0.0506]	2217[0.0481]	2286[0.0503]
Observed reflections [I>2σ(I)]	3183	1943	1973	1973	2039
Data / restraints / parameters	3511/0/98	2148/0/100	2223/0/100	2217/0/100	2286/0/98
Goodness-of-fit on F^2	0.901	1.062	1.089	1.063	1.072
R_1 [I>2sigma(I)	0.0246	0.0184	0.0234	0.0206	0.0194
wR_2 (all data)	0.1055	0.0536	0.0614	0.0538	0.0497

Table C3 – Crystal data and X-ray experimental details for **3.26, 3.27, 3.31, 3.32 and 3.33**

Compound	**3.26**	**3.27**	**3.31**	**3.32**	**3.33**
Empirical formula	$C_{14}H_{20}N_2CuBr_4$	$C_{14}H_{20}N_2CuBr_4$	$C_{14}H_{20}N_2Cl_4Cu$	$C_{14}H_{20}N_2Cl_4Cu$	$C_{14}H_{20}N_2Cl_{1.57}CuBr_{2.43}$
Formula weight	634.95	599.50	421.66	421.66	529.77
Temperature (K)	113	113	113	113	113
Crystal system	monoclinic	monoclinic	monoclinic	monoclinic	monoclinic
Space group	C2/c	C2/c	C2/c	C2/c	C2/c
Unit cell dimensions: a (Å)	19.8274(7)	19.8408(6)	9.9901(6)	10.0438(3)	10.2403(3)
b (Å)	19.8274(7)	7.4493(2)	15.1632(9)	15.1534(5)	15.2308(5)
c (Å)	19.8274(7)	16.2691(8)	12.3405(6)	12.3661(4)	12.5572(5)
α (°)	90.00	90.00	90.00	90.00	90.00
β (°)	123.580(2)	123.6410(10)	102.874(3)	103.225(2)	103.8710(10)
γ (°)	90.00	90.00	90.00	90.00	90.00
Volume ($Å^3$)	1994.79(15)	2001.87(13)	1822.37(18)	1832.18(10)	1901.41(11)
Z	4	4	4	4	4
Density (calculated) (Mg/m^3)	2.114	1.989	1.537	1.529	1.852
Absorption coefficient (mm^{-1})	9.238	9.070	1.779	1.769	6.496
F(000)	1216	1148	860	860	1036
Crystal size (mm)	0.4 × 0.25 × 0.1	0.32 × 0.26 × 0.06	0.6 × 0.15 × 0.11	0.64 × 0.3 × 0.23	0.45 × 0.37 × 0.24
2Theta range for data collection (°)	4.94 to 60.98°	4.94 to 54.98°	5.38 to 55°	5.38 to 55°	4.9 to 65.94°
Reflections collected	26387	21984	20374	19491	28166
Independent reflections [R(int)]	3037[0.0520]	2308[0.1144]	2097[0.0367]	2109[0.0332]	3461[0.0422]
Observed reflections [I>2σ(I)]	2414	1931	1933	1886	2710
Data / restraints / parameters	3037/0/98	2308/0/98	2097/0/98	2109/0/98	3461/0/100
Goodness-of-fit on F^2	0.989	0.998	1.037	1.086	0.991
R_1 [I>2sigma(I)	0.0246	0.0367	0.0206	0.0481	0.0243
wR_2 (all data)	0.0542	0.0931	0.0620	0.1617	0.0594

Table C4 – Crystal data and X-ray experimental details for **3.34, 3.35, 3.36, 3.37 and 3.38**

Compound	**3.34**	**3.35**	**3.36**	**3.37**	**3.38**
Empirical formula	$C_{14}H_{20}N_2Cl_{0.33}Cu\ Br_{3.67}$	$C_{14}H_{20}N_2CuBr_4$	$C_{14}H_{20}N_2CuBr_4$	$C_{14}H_{20}\ N_2CuBr_4$	$C_{14}H_{20}N_2Cl_{1.30}CuBr_{2.70}$
Formula weight	584.92	599.47	599.47	599.50	541.86
Temperature (K)	113	113	113	113	113
Crystal system	monoclinic	monoclinic	monoclinic	monoclinic	monoclinic
Space group	C2/c	C2/c	C2/c	C2/c	C2/c
Unit cell dimensions: a (Å)	19.9348(7)	19.9825(7)	20.0454(10)	20.0474(6)	10.2478(3)
b (Å)	7.2442(3)	7.2389(2)	7.2736(4)	7.2802(2)	15.2584(5)
c (Å)	16.1240(5)	7.2389(2)	16.1475(9)	16.1616(5)	12.5585(4)
α (°)	90.00	90.00	90.00	90.00	90.00
β (°)	121.535(2)	121.473(2)	121.527(2)	121.5570(10)	104.061(2)
γ (°)	90.00	90.00	90.00	90.00	90.00
Volume ($Å^3$)	1984.62(12)	1986.50(11)	2006.82(19)	2009.95(10)	1904.87(10)
Z	4	4	4	4	4
Density (calculated) (Mg/m^3)	1.958	2.005	1.978	1.981	1.889
Absorption coefficient (mm^{-1})	8.533	9.140	8.997	9.034	6.994
F(000)	1124.6	1148.0	1144.0	1148.0	1055.0
Crystal size (mm)	0.5 × 0.4 × 0.2	0.75 × 0.65 × 0.5	0.34 × 0.31 × 0.1	0.36 × 0.20 × 0.05	0.55 × 0.3 × 0.27
2Theta range for data collection (°)	5.32 to 54.98°	5.34 to 59.92°	5.32 to 55°	5.32 to 55°	5.34 to 55°
Reflections collected	21482	24663	22045	21548	20879
Independent reflections [R(int)]	2277[0.0394]	2882[0.0721]	2303[0.1428]	2308[0.0786]	2186[0.0363]
Observed reflections [I>2σ(I)]	1981	2184	1937	2112	1883
Data / restraints / parameters	2277/0/100	2882/0/98	2303/0/98	2308/0/98	2186/0/100
Goodness-of-fit on F^2	1.076	0.965	0.978	1.042	1.108
R_1 [I>2sigma(I)	0.0180	0.0260	0.0459	0.0341	0.0179
wR_2 (all data)	0.0477	0.0533	0.1198	0.0943	0.0489

Table C5 – Crystal data and X-ray experimental details for **3.39, 3.310, 3.311, 3.41 and, 3.42**

Compound	**3.39**	**3.310**	**3.311**	**3.41**	**3.42**
Empirical formula	$C_{14}H_{20}N_2Cl_{1.22}CuBr_{2.78}$	$C_{14}H_{20}N_2CuBr_4$	$C_{14}H_{20}N_2CuBr_4$	$C_{14}H_{20}N_2Cl_4Cu$	$C_{14}H_{20}N_2Cl_{3.52}Cu\ Br_{0.48}$
Formula weight	545.17	599.50	599.50	421.66	443.00
Temperature (K)	113	113	113	113	113
Crystal system	monoclinic	monoclinic	monoclinic	triclinic	triclinic
Space group	C2/c	C2/c	C2/c	P-1	P-1
Unit cell dimensions: a (Å)	10.2539(4)	19.9237(10)	19.9647(11)	7.5372(3)	7.6034(2)
b (Å)	15.2741(6)	7.2627(4)	7.2568(4)	8.8537(3)	8.8646(2)
c (Å)	12.5656(6)	16.1431(8)	16.1421(9)	14.8186(6)	14.8617(4)
α (°)	90.00	90.00	90.00	77.378(2)	77.2290(10)
β (°)	104.063(2)	121.608(2)	121.517(3)	78.648(2)	78.6790(10)
γ (°)	90.00	90.00	90.00	73.681(2)	73.4230(10)
Volume ($Å^3$)	1909.03(14)	1989.38(18)	1993.68(19)	916.37(6)	926.75(4)
Z	4	4	4	2	2
Density (calculated) (Mg/m^3)	1.897	2.002	1.997	1.528	1.588
Absorption coefficient (mm^{-1})	7.124	9.127	9.107	1.769	2.715
F(000)	1060.0	1148.0	1148.0	430.0	447.0
Crystal size (mm)	0.7 × 0.5 × 0.4	0.7 × 0.5 × 0.3	0.6 × 0.4 × 0.27	0.7 × 0.34 × 0.18	0.47 × 0.45 × 0.11
2Theta range for data collection (°)	5.32 to 54.98°	5.32 to 54.98°	5.32 to 53.26°	4.86 to 55°	4.88 to 55°
Reflections collected	20608	20925	18116	21183	21180
Independent reflections [R(int)]	2190[0.0655]	2281[0.0638]	2086[0.0686]	4215[0.0930]	4257[0.0850]
Observed reflections [I>2σ(I)]	1942	1926	1619	3644	3657
Data / restraints / parameters	2190/0/100	2281/0/98	2086/0/98	4215/0/194	4257/300/198
Goodness-of-fit on F^2	1.112	1.083	0.996	1.054	1.075
R_1 [I>2sigma(I)	0.0213	0.0236	0.0327	0.0468	0.0396
wR_2 (all data)	0.0543	0.0648	0.0835	0.1371	0.1141

Table C6 – Crystal data and X-ray experimental details for **3.43, 3.44, 3.45, 3.46 and 3.47**

Compound	**3.43**	**3.44**	**3.45**	**3.46**	**3.47**
Empirical formula	$C_{14}H_{20}N_2Cl_{2.18}CuBr_{1.82}$	$C_{14}H_{20}Br_{3.95304}Cl_{0.04696}CuN_2$	$C_{14}H_{20}N_2Cl_{0.09}Br_{3.91}Cu$	$C_{14}H_{20}CuN_2Br_4$	$C_{14}H_{20}N_2CuBr_4$
Formula weight	502.75	597.41	595.56	599.47	599.50
Temperature (K)	113	113	113	113	113
Crystal system	triclinic	triclinic	triclinic	triclinic	triclinic
Space group	P-1	P-1	P-1	P-1	P-1
Unit cell dimensions: a (Å)	7.7120(3)	7.7241(3)	7.7365(3)	7.1806(4)	7.1974(3)
b (Å)	8.9100(3)	8.1505(3)	8.1611(3)	9.6503(5)	9.6705(3)
c (Å)	14.9129(5)	15.9285(6)	15.9598(8)	14.5687(7)	14.6076(5)
α (°)	76.998(2)	76.208(2)	76.167(3)	94.161(3)	94.055(2)
β (°)	79.020(2)	76.131(2)	76.138(3)	95.841(3)	95.762(2)
γ (°)	72.698(2)	88.761(2)	88.812(3)	104.233(3)	104.234(2)
Volume ($Å^3$)	944.83(6)	944.81(6)	949.24(7)	968.47(9)	975.72(6)
Z	2	2	4	2	2
Density (calculated) (Mg/m^3)	1.767	2.100	2.594	2.711	2.041
Absorption coefficient (mm^{-1})	5.315	9.516	6.758	6.638	9.304
F(000)	496.0	572.0	570.4	796.0	574.0
Crystal size (mm)	0.8 × 0.72 × 0.3	0.6 × 0.33 × 0.14	0.28 × 0.20 × 0.05	4.0 × 0.6 × 0.45	0.7 × 0.65 × 0.32
2Theta range for data collection (°)	4.86 to 55°	5.14 to 54.98°	2.7 to 53.12°	2.82 to 46.18°	4.96 to 55°
Reflections collected	21577	20746	20042	14164	21914
Independent reflections [R(int)]	4329[0.0981]	4331[0.0352]	3916[0.1267]	2697[0.0753]	4483[0.0494]
Observed reflections [I>2σ(I)]	3886	3793	2640	2276	3787
Data / restraints / parameters	4329/0/198	4331/0/193	3916/0/197	2697/0/194	4483/0/194
Goodness-of-fit on F^2	1.043	1.284	0.715	1.137	1.052
R_1 [I>2sigma(I)	0.0440	0.0245	0.0469	0.0363	0.0299
wR_2 (all data)	0.1217	0.0580	0.1265	0.1021	0.0785

REFERENCES

1. Pelissetto, A. and E. Vicari, *Critical phenomena and renormalization-group theory.* Phys. Rep., 2002. **368**(6): p. 549-727.
2. Dagotto, E. and T.M. Rice, *Surprises on the way from one- to two-dimensional quantum magnets: the ladder materials.* Science (Washington, D. C.), 1996. **271**(5249): p. 618-23.
3. Anderson, P.W., et al., *Resonating-valence-bond theory of phase transitions and superconductivity in lanthanum copper oxide (La2CuO4)-based compounds.* Phys. Rev. Lett., 1987. **58**(26): p. 2790-3.
4. Sokol, A. and D. Pines, *Toward a unified magnetic phase diagram of the cuprate superconductors.* Phys. Rev. Lett., 1993. **71**(17): p. 2813-16.
5. Carlin, R.L., et al., *Magnetochemistry of copper(II): exchange interactions in catenated acetatodiamminebromocopper.* Inorg. Chem., 1986. **25**(11): p. 1786-9.
6. Woodward, F.M., et al., *Structure and magnetic properties of (5BAP)2CuBr4: magneto-structural correlations of layered S = 1/2 Heisenberg antiferromagnets.* Inorg. Chim. Acta, 2001. **324**(1,2): p. 324-330.
7. Hatfield, W.E. and J.H. Helms, *From the magnetic susceptibility of clusters to the magnetic susceptibility of chains with novel structures.* Mater. Sci., 1992. **17**(2): p. 21-31.
8. Ueda, K., et al., *Theoretical study and comparison with experiments for atacamite, Cu2Cl(OH)3.* Mol. Cryst. Liq. Cryst. Sci. Technol., Sect. A, 1997. **306**: p. 33-40.
9. Matsumoto, T., et al., *Heat Capacities of the S = 1/2 Two-Dimensional Heisenberg Antiferromagnet Bis(2-amino-5-chloro-pyridinium) Tetrabromocuprate(II) [(5CAP)2CuBr4] and Its Diamagnetic Analogue [(5CAP)2ZnBr4]*. J. Phys. Chem. B, 2000. **104**(43): p. 9993-10000.

10. Turnbull, M.M., et al., *Synthesis, structure and magnetic susceptibility of two 5-nitro-2-aminopyridinium cuprates: (5-NAP)2CuCl4 and the quantum magnetic ladder (5-NAP)2CuBr4.H2O.* Mol. Cryst. Liq. Cryst. Sci. Technol., Sect. A, 2002. **376**: p. 469-476.

11. Halvorson, K. and R.D. Willett, *Structures of ethylenediammonium tetrabromocuprate(II) and propylenediammonium tetrabromocuprate(II).* Acta Crystallogr., Sect. C Cryst. Struct. Commun., 1988. **C44**(12): p. 2071-6.

12. Turnbull, M.M., C.P. Landee, and B.M. Wells, *Magnetic exchange interactions in tetrabromocuprate compounds.* Coord. Chem. Rev., 2005. **249**(23): p. 2567-2576.

13. Minguez Espallargas, G., et al., *Reversible Extrusion and Uptake of HCl Molecules by Crystalline Solids Involving Coordination Bond Cleavage and Formation.* J. Am. Chem. Soc., 2006. **128**(30): p. 9584-9585.

14. Jasiewicz, B., et al., *Crystal structure, spectroscopy and magnetism of selected (-)sparteine and alpha -isosparteine tetrahalocuprate salts.* J. Mol. Struct., 2006. **794**(1-3): p. 311-319.

15. Awwadi, F.F., R.D. Willett, and B. Twamley, *The Aryl Chlorine-Halide Ion Synthon and Its Role in the Control of the Crystal Structures of Tetrahalocuprate(II) Ions.* Cryst. Growth Des., 2007. **7**(4): p. 624-632.

16. Turnbull, M.M., et al., *Synthesis, structure and magnetic behavior of bis(2-amino-5-fluoropyridinium) tetrachlorocuprate: A magnetic ladder.* Abstracts of Papers, 234th ACS National Meeting, Boston, MA, United States, August 19-23, 2007, 2007: p. INOR-874.

17. Zhong, C., et al., *Syntheses, structures, and properties of a series of metal ion-containing dialkylimidazolium ionic liquids.* Bull. Chem. Soc. Jpn., 2007. **80**(12): p. 2365-2374.

18. Staniland, S.S., et al., *Structural and Magnetic Properties of [BDTA]2[MCl4] [M = Cu (1), Co (2), and Mn (3)], Revealing an S = 1/2 Square-Lattice Antiferromagnet with Weak Magnetic Exchange.* Inorg. Chem., 2006. **45**(15): p. 5767-5773.

19. Shapiro, A., et al., *Synthesis, Structure, and Magnetic Properties of an Antiferromagnetic Spin-Ladder Complex: Bis(2,3-dimethylpyridinium) Tetrabromocuprate.* J. Am. Chem. Soc., 2007. **129**(4): p. 952-959.

20. Haddad, S.F. and R.H. Al-Far, *Crystal Structure of Three Isomorphous Compounds of 2,5-Dibromopyridine with Tetrahalometalate(II) Ions.* J. Chem. Crystallogr., 2008. **38**(9): p. 663-669.

21. Adams, C.J., et al., *Solid state synthesis of coordination compounds from basic metal salts.* CrystEngComm, 2008. **10**(12): p. 1790-1795.

22. Bai, J., et al., *Theoretical study of crystal structures and intermolecular interactions in isomorphous adducts [2-ClPyH]+2[MCl2-4](M = Co, Cu, Ni).* Gaodeng Xuexiao Huaxue Xuebao, 2007. **28**(6): p. 1113-1116.

23. Tremelling, G.W., et al., *Transition metal complexes of 2-amino-3,5-dihalopyridines: Syntheses, structures and magnetic properties of (3,5-diCAPH)2CuX4 and (3,5-diBAPH)2CuX4.* Dalton Trans., 2009(47): p. 10518-10526.

24. Snively, L.O., et al., *Magnetic susceptibility of 1,2-ethanediammonium tetrachlorocuprate: a layered structure with strong interlayer magnetic coupling.* Phys. Rev. B Condens. Matter, 1979. **20**(5): p. 2101-4.

25. De Jongh, L.J. and A.R. Miedema, *Simple magnetic model systems.* Advan. Phys., 1974. **23**(1): p. 1-260.

26. Snively, L.O., G.F. Tuthill, and J.E. Drumheller, *Measurement and calculation of the superexchange interaction through the two-halide bridge in the eclipsed layered*

compounds [NH3(CH2)nNH3]CuX for n = 2-5 and X = Cl4 and Cl2Br2. Phys. Rev. B Condens. Matter, 1981. **24**(9): p. 5349-55.

27. Van Kalkeren, G., W.W. Schmidt, and R. Block, *Superexchange in insulators: comparison of different methods.* Physica B+C (Amsterdam), 1979. **97**(4): p. 315-37.
28. Giantsidis, J., et al., *S = 1/2 quantum Heisenberg antiferromagnet ladders.* Synth. Met., 2001. **122**(3): p. 517-522.
29. Li, L., et al., *Synthesis, structure, and magnetic behavior of bis(2-amino-5-fluoropyridinium) tetrachlorocuprate(II).* Inorg. Chem. (Washington, DC, U. S.), 2007. **46**(26): p. 11254-11265.
30. Woodward, F.M., et al., *Two-dimensional S = 1/2 Heisenberg antiferromagnets: Synthesis, structure, and magnetic properties.* Phys. Rev. B Condens. Matter Mater. Phys., 2002. **65**(14): p. 144412/1-144412/13.
31. Place, H. and R.D. Willett, *Structure of bis(2-amino-5-methylpyridinium) tetrachlorocuprate(II) and bis(2-amino-5-methylpyridinium) tetrabromocuprate(II).* Acta Crystallogr., Sect. C Cryst. Struct. Commun., 1987. **C43**(6): p. 1050-3.
32. Hammer, P.R., et al., *Magnetic studies of the two-dimensional, S = 1/2 Heisenberg antiferromagnets (5CAP)2CuCl4 and (5MAP)2CuCl4.* J. Appl. Phys., 1997. **81**(8, Pt. 2A): p. 4615-4617.
33. Satyanarayana, D. and B.K. Mohapatra, *Lutidinium tetrahalocuprates(II).* Chem. Zvesti, 1974. **28**(6): p. 753-6.
34. Ali, B.F., R. Al-Far, and S.F. Haddad, *Hydrogen Bonded, pi...pi Stacked and X...pi Framework Structures in Bis(2,6-Lutidinium) Tetrahalocuprate(II) Complexes.* J. Chem. Crystallogr., 2010. **40**(8): p. 696-701.

35. Marcotrigiano, G., L. Menabue, and G.C. Pellacani, *Tetrahalo- and (mixed-tetrahalo)cuprates of the piperazinium dication. Coordination geometry changes in some CuX42- anions.* Inorg. Chem., 1976. **15**(10): p. 2333-6.

36. Haddad, S.F., M.A. AlDamen, and R.D. Willett, *The role of non-classical supramolecular interactions in the structures of 2-amino-4,6-dimethylpyridinium tetrahalocuprate (II) salts.* Inorg. Chim. Acta, 2006. **359**(2): p. 424-432.

37. Wikaira, J.L., et al., *Transition metal complexes of 2-amino-3-chloro-5-trifluoromethylpyridine: syntheses, structures, and magnetic properties of [(TMCAPH)2CuBr4] and [(TMCAPH)2CuCl4]*. J. Coord. Chem., 2010. **63**(17): p. 2949-2964.

38. Steiner, T., *The Hydrogen Bond in the Solid State.* Angewandte Chemie International Edition, 2002. **41**(1): p. 48-76.

39. Janiak, C., *A critical account on [small pi]-[small pi] stacking in metal complexes with aromatic nitrogen-containing ligands.* Journal of the Chemical Society, Dalton Transactions, 2000(21): p. 3885-3896.

40. Patyal, B.R., B.L. Scott, and R.D. Willett, *Crystal-structure, magnetic-susceptibility, and EPR studies of bis(piperidinium) tetrabromocuprate(II): a novel monomer system showing spin diffusion.* Phys. Rev. B Condens. Matter, 1990. **41**(3): p. 1657-63.

41. Zhou, P., et al., *Novel low-dimensional spin 1/2 antiferromagnets: two-halide exchange pathways in A2CuBr4 salts.* J. Appl. Phys., 1991. **69**(8, Pt. 2B): p. 5804-6.

42. *Private communication*, Prof Mark M. Turnbull, Carlson School of Chemistry and Biochemistry, Clark University, 950 Main St., Worcester, MA 01610, 508-793-7167

43 F. H. Allen, *The Cambridge Structural Database: a quarter of a million crystal structures and rising, Acta Cryst.*, B**58**, 380-388, 2002

44. *Private communication*, Firas Awwadi, Jordan University

45. Chu, Y., H. Deng, and J.-P. Cheng, *An Acidity Scale of 1,3-Dialkylimidazolium Salts in Dimethyl Sulfoxide Solution.* The Journal of Organic Chemistry, 2007. **72**(20): p. 7790-7793.

46. Thomson, J.E., et al., *Probing the Efficiency of N-Heterocyclic Carbene Promoted O- to C-Carboxyl Transfer of Oxazolyl Carbonates.* The Journal of Organic Chemistry, 2008. **73**(7): p. 2784-2791.

47. Bruker-AXS, SAINT+, 1997-1999

48. G. M. Sheldrick, SADABS, University of Gottingen, 1998.

49. O. V. Dolomanov, L. J. Bourhis, R. J. Gildea, J. A. K. Howard and H. Puschmann, OLEX2: a complete structure solution, refinement and analysis program, J. Appl. Cryst. (2009). **42**, 339-341